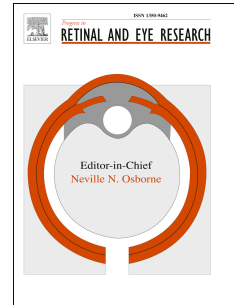# Journal Pre-proof

Optical coherence tomography diagnostic signs in posterior uveitis

Francesco Pichi, Alessandro Invernizzi, William R. Tucker, Marion R. Munk

Please cite this article as: Pichi, F., Invernizzi, A., Tucker, W.R., Munk, M.R., Optical coherence tomography diagnostic signs in posterior uveitis, *Progress in Retinal and Eye Research* (2019), doi: https://doi.org/10.1016/j.preteyeres.2019.100797.

OPTICAL COHERENCE TOMOGRAPHY DIAGNOSTIC SIGNS IN POSTERIOR UVEITIS

Francesco Pichi MD[1,2], Alessandro Invernizzi MD[3,4], William R Tucker[5], Marion R Munk[6,7,8]

[1]Eye Institute, Cleveland Clinic Abu Dhabi, Abu Dhabi, United Arab Emirates.

[2]Cleveland Clinic Lerner College of Medicine, Case Western Reserve University, Cleveland, Ohio, USA

[3]Eye Clinic, Department of Biomedical and Clinical Science 'Luigi Sacco', Luigi Sacco Hospital, University of Milan, Milan, Italy

[4]Save Sight Institute, University of Sydney, Sydney, New South Wales, Australia

[5]Moorfields Eye Hospital NHS Foundation Trust, London, United Kingdom

[6]Department of Ophthalmology, Inselspital, Bern University Hospital and University of Bern, Switzerland

[7]BPRC, Bern Photographic Reading Center, University of Bern, Switzerland

[8]Feinberg School of Medicine, Northwestern University Chicago, Chicago, Illinois

Corresponding Author

Francesco Pichi MD

Eye Institute

Cleveland Clinic Abu Dhabi

Al Maryah Island – Abu Dhabi (UAE)

PO Box 112412

Tel: +971(0)559176234

Email: ilmiticopicchio@gmail.com

Declaration of Interests

Funding source

OPTICAL COHERENCE TOMOGRAPHY BIOMARKERS IN POSTERIOR UVEITIS

A diagnostic sign refers to a quantifiable biological parameter that is measured and evaluated as an indicator of normal biological, pathogenic, or pharmacologic responses to a therapeutic intervention. When used in translational research discussions, the term itself often alludes to a signs used to accelerate or aid in diagnosis or monitoring and provide insight into "personalized" medicine. Many new diagnostic signs are being developed that involve imaging technology. Optical coherence tomography is an imaging technique that provides in vivo quasi-histological images of the ocular tissues and as such it's able to capture the structural and functional modifications that accompany inflammation and infection of the posterior part of the eye. From the hyperreflective inflammatory cells and deposits in the vitreous and on the hialoid, to the swollen photoreceptors bodies in multiple evanescent white dots syndrome, and from optical difference of the subretinal fluid compartments in Vogt-Koyanagi-Harada disease to the hyporeflective granulomas in the choroid, these tomographical signs can be validate to reach the status of biomarkers. Non-invasive imaging diagnostic signs of inflammation can be very useful to clinicians seeking to make a diagnosis and can represent a dataset for machine learning to offer a more empirical approach to the detection of posterior uveitis.

OPTICAL COHERENCE TOMOGRAPHY DIAGNOSTIC SIGNS IN POSTERIOR UVEITIS

Keywords

Optical coherence tomography; diagnostic signs; posterior uveitis; infectious uveitis

Table of Contents

INTRODUCTION

In recent years the health sciences have been experiencing a shift from population-based approaches to individual personalized practice. The success of these efforts will largely depend on the continued identification of diagnostic signs that reflect the individual's health status and risk at key time points, and the subsequent successful integration of these signs into medical practice. These diagnostic signs can be inferred from imaging methods: imaging signs have many advantages since they are usually noninvasive, they yield both qualitative and quantitative data and they are relatively comfortable for patients.

Optical coherence tomography (OCT) is an imaging technique that provides in vivo quasi-histological images of the ocular tissues with a resolution beyond that of any other non-invasive technology. Since the introduction of OCT into clinical practice two decades ago, it has dramatically changed the understanding and the management of many ocular conditions, including those resulting from inflammation.

Inflammation is a response of the body to harmful stimuli. The inflammatory process promotes changes to the blood supply, the cellular components and the chemical environment of the involved area. These structural and functional modifications can result in transient and/or permanent changes to the tissues, we believe in ocular tissue many of these can be detected with OCT and act as imaging diagnostic signs of ocular inflammation (uveitis).

The present review will assess those OCT changes in posterior uveitis, that is inflammation affecting the vitreous, retina, retinal vessels, choroid and sclera that can be used by the clinicians as diagnostic signs of inflammation and, combined with other sources of information, can be used for diagnosis (Table 1). Most importantly

4

we believe these OCT signs of posterior uveitis can produce a dataset that machine learning and neural networks may be able to employ in the future to spot anomalies on OCTs that a human observer would miss.

1. VITREOUS OCT SIGNS IN POSTERIOR UVEITIS

1.1 Vitritis

Inflammation affecting the posterior segment of the eye leads to inflammatory cells infiltrating the vitreous body and a protein-rich inflammatory exudate into the vitreous resulting in haze (Forrester, 1991). The resolution of current OCT scanners cannot distinguish nanoscale single cells but clumps of cells with inflammatory exudate are visible on OCT B scans as punctate spots floating in the posterior vitreous (Saito M et al, 2013) (Figure 1). Although the presence of these spots in the vitreous is a useful indicator of the presence of vitritis, they can persist long term and therefore are not a reliable diagnostic sign for recurrence or response to treatment (Nussenblatt et al, 1985).

Vitreous haze, however, has been accepted as a surrogate measure of posterior segment uveitis activity making its reduction a key primary outcome for clinical trials of new uveitis therapies as decrease of vitreous haze is accompanied by visual acuity improvement. (Kimura et al, 1959; Kempen et al 2015; Lowder et al, 2011). The percent of patients reaching a vitreous haze of 0 is accepted as single efficacy endpoint of the FDA for treatments in non-infectious uveitis (UCLA/AUS society workshop March 22-23 2019 UCLA Stein Eye institute). Unlike anterior chamber 'cells' which can be physically counted by the clinician (Jabs et al 2005) an assessment of vitreous haze currently requires comparison against published haze

scales, the National Eye Institute (NEI) vitreous haze grading scale being the most commonly used (Nussenblatt et al, 1985; Davis et al 2010).

These stepwise scales are reliant on human assessors making a subjective comparison to published standardized photographs and there is poor interobserver agreement (Hornbeak et al, 2014). Also, on the six step NEI scale most uveitis patients in clinical practice cluster around the lowest steps in the scale, making monitoring change more difficult (Davis et al, 2010).

Keane et al describe one solution using OCT technology, to measure the OCT signal intensity of the posterior vitreous, effectively the signal noise coming from this part of the B-scan image relative to the RPE intensity; this correlates to a vitreous haze score (Keane et al, 2014). High decimal scores suggest increased scatter from the protein exudate and lower scores signifying a clearer vitreous. By using a ratio of vitreous signal intensity to the signal intensity from the RPE they can control for overall noise in the image from other sources e.g. cataract. This VRI (Vitreous/RPE Relative Intensity) Score can now be measured in an automated fashion and has been shown to correlate with disease activity and resolution (Keane et al, 2014; Keane et al, 2015). The approach was also presented and suggested at the UCLA/AUS workshop 2019 on objective measures of intraocular inflammation for use in clinical trials. Further work to pass the stringent requirements of regulatory authorities may allow such an objective measure to be incorporated into uveitis clinical trials as an outcome.

1.2 Posterior Hyaloid face precipitates (ARN/Toxo)

While vitritis appears on OCT images as diffuse increased reflectivity (proteins) of the vitreous and distinct hyperreflective punctate dots (cells) spread over a darker

6

background regardless of the underlying disease, peculiar patterns of OCT signs may characterize the posterior vitreous and the vitreo-retinal interface in some specific etiologies. (Invernizzi et al, 2019)

In 1996, at the dawn of the OCT era, Nakao and Ohba described peculiar perivascular deposits lying on the retinal surface in patients affected by Human T cell Lymphotropic Virus type 1 (HLTV-1). (Nakao and Ohba, 1996) These findings were postulated to be clots of T lymphocytes migrated from the retinal vasculature and proliferating on the inner retinal surface. Similar deposits were then reported by the same authors in a patient with acute retinal necrosis. (Nakao et al, 1998) In 2007 these preretinal deposits were described for the first time on time domain OCT in a patient with toxoplasmic chorioretinitis. (Guagnini et al, 2007) The OCT scans showed the exact location of the deposits and then followed their progressive resolution in response to treatment.

Hyper-reflective preretinal oval deposits were reported on spectral domain OCT (SD-OCT) images in a series of patients with active toxoplasmic chorioretinitis. (Goldenberg et al, 2013) These deposits were located both adjacent and far away from active lesions and were present in five eyes of five patients. Such a high prevalence of the new finding was likely related to the higher resolution of the SD-OCT compared to that of other imaging techniques previously available. SD-OCT allowed the authors to follow the evolution of these alterations in response to treatment. The deposits became smaller, entered the retina and disappeared with time until complete resolution leaving no scar (Figure 2A). (Goldenberg et al, 2013)

In a recent paper comparing distinctive feature of necrotizing retinitis of different etiology, the same deposits were found in 6 eyes (60%) with active toxoplasmic

7

chorioretinitis and in 1 eye (8%) with viral retinitis. (Invernizzi et al, 2018a) The oval deposits were located not only on the surface of the retina but also along the detached posterior hyaloid (Figure 2B). Preretinal round-shaped oval deposits on SD-OCT were then proposed as a possible suggestive sign for toxoplasmic etiology in case of necrotizing retinitis of unknown cause, although Varicella Zoster Virus (VZV) and syphilis (section 1.3) remain among the differentials.

Up till now the nature of these preretinal oval deposits is still to be determined. The available literature (Guagnini et al, 2007; Invernizzi et al, 2018a) suggests these deposits to be clots of inflammatory cells, likely T lymphocytes, representing a specific inflammatory response to different stimuli in most of the cases represented by the toxoplasmic infection, but occasionally triggered by other entities. The role of HLTV-1 virus in the development of these peculiar formations is still unclear.

1.3 Syphilitic superficial retinal precipitates

There are 2 main forms of syphilitic retinochoroiditis: confluent and placoid (Cunningham et al, 2014). OCT diagnostic signs of the placoid form are presented in section 4.7. The confluent form presents with large, triangular areas with a "ground-glass" appearance distinct from the typical white, necrotizing retinitis seen with herpetic retinitis. (Figure 3A, Figure 3B) Areas of confluent syphilitic retinochoroiditis are often associated with vasculitis, hyperfluorescence of the margins in fluorescein angiography (FA), they tend to heal with minimal disruption of the retinal pigment epithelium and they may be associated with superficial pre-retinal precipitates.

This punctuate retinitis with inner retinal and preretinal small, creamy white precipitates is an unusual feature of ocular syphilis rarely reported to date (Reddy et

al 2006, Wickremasinghe et al 2009) but its OCT detection is of a distinctive clinical pattern that may assist rapid diagnosis. (Figure 3C) The precipitates can subsequently migrate over the inflamed retina during the evolution of the infection and its treatment. As such, these superficial retinal precipitates appear tomographically and behave similarly to the pre-retinal oval deposits seen in toxoplasmosis and viral necrotizing retinitis; however, syphilitic preretinal deposits detected on OCT are usually overlying an area of retinitis with a clinical "ground-glass" appearance while in toxoplasmosis or ARN the OCT dots overlay an area of dense, white retinitis.

The presence of confluent retinitis associated with multiple preretinal/inner retinal dots has a high diagnostic predictive value, increasing the pre-test probability of syphilis significantly.

1.4. Candida preretinal lesions

Fungi can penetrate the eye from the outside world through a surgical or traumatic wound (exogenous route) or from inside the body following hematogenous spreading (endogenous route). Once they entered the eye, fungal elements proliferate in colonies in search for the most suitable environment to grow. This may differ according to the specific needs of the microorganism. (Wykoff et al, 2008; Lingappan et al, 2012)

Candida albicans is a common member of the human gut flora and a commensal organism, but it can become pathogenic under a variety of conditions, especially in immunocompromised patients. This yeast, along with other species of the same genus, is responsible for most of the cases of endogenous fungal endophthalmitis

(Sallam et al, 2006). Once in the bloodstream Candida spp can enter the eye from the choroid (commonest penetration route) or from the retinal circulation. Regardless of the access site, the Candida elements direct towards the vitreous cavity as here they find the perfect environment to grow. (Rao and Hidayat, 2001)

As the Candida penetrates the eye from either the retinal or choroidal vasculature, retinal alterations always accompany the vitreous lesions. Once reached the vitreous cavity the colonies grow from the retinal surface towards the core of the vitreous chamber. For this reason, they are initially packed between the retinal surface and the posterior hyaloid (Figure 4A) and only later they extend into the proper vitreous body (Figure 4B). (Invernizzi et al, 2017c) The fungi can stimulate the proliferation of new vessels on the retinal surface. These usually grow towards the colonies likely following the inflammatory cytokines gradient and can be visualized on OCT. (Invernizzi et al, 2018b)

Candida colonies in the vitreous appear on SD-OCT as preretinal round-shaped hyper-reflective aggregates of various size, characterized by a homogeneous internal pattern. A peculiar finding seems to be an almost complete obscuration of the retinal layers underneath the lesions (Figure 4A). This pattern, resembling a white cloud (preretinal hyper-reflective aggregate) accompanied by the underlying shower (shadow cone), was named "rain-cloud" sign by the authors that described it first. (Invernizzi et al, 2017c)

Not all the fungi are characterized by a pre-retinal growth. *Aspergillus species* for example tend to grow underneath the retina as they found the most favorable environment at this level. (Rao and Hidayat, 2001) The SD-OCT images will consequently show fungal material accumulated into the subretinal space in the form

10

of an abscess. (Adam and Sigler, 2014) However, these OCT signs cannot be considered diagnostic for Aspergillus endogenous endophthalmitis.

2. PERIPAPILLARY OCT SIGNS IN POSTERIOR UVEITIS

2.1 Peripapillary changes secondary to inflamed/swollen optic nerve

Inflammatory swelling of the optic nerve head is termed papillitis and occurs with anterior uveitis, intermediate uveitis and posterior/panuveitis (Jones, 2013) (Figure 5A). The exact mechanism is unknown, but it is proposed that pro-inflammatory cytokines spread towards the optic nerve head leading to swelling and vasodilation (Cho HJ et al. 2014). The cytokines may arrive by diffusing through the vitreous in a vitritis or spread directly from local peripapillary inflammatory chorioretinal lesions in toxoplasmosis (Smith et al 2002) or sarcoidosis (Eckstein et al 2012). OCT provides the opportunity to quantify and delineate the character of the papillitis. Cho et al (2014) used a standard peripapillary retinal nerve fiber layer (RNFL) circular scan combined with a volumetric cube to show increased RNFL and total retinal thickness during periods of active uveitis in 22 eyes of 14 patients. Philiponnet et al (2017) also found a significant increase in RNFL thickness and peripapillary total retinal thickness between 17 active posterior uveitis eyes and a control group. Most importantly when considering papillitis as a sign of uveitis activity, Cho et al (2014) also showed the thickening and papillitis resolving as uveitis activity decreased. However, while in 10 of 14 patients this resolution was simultaneous with uveitis, in 4 patients the papillitis thickening lagged behind by 2 months up to 1 year. Further peripapillary thickening

visible on the retinal thickness maps correlates with peripheral capillary leakage on angiography and is discussed further in section 3.2 (Tian et al, 2018).

2.2 Optic nerve granulomas

Optic nerve head granuloma is most commonly associated with sarcoidosis, a chronic idiopathic multisystem disorder characterized by inflammatory granuloma with non-caseating histology (Blain et al, 1965; Jabs and Johns, 1986). Tuberculosis leading to a tuberculoma of the optic nerve head and granulomas related to toxoplasma, toxocara or cryptococcus should be excluded, particularly in immunocompromised patients (Sivadasan et al, 2013). Direct granulomatous infiltration of the optic nerve head is one of several possible sarcoid optic nerve presentations alongside papillitis and papilledema secondary to raised intracranial pressure from neurosarcoidosis (Ingestad and Stigmar, 1971). Ex-vivo histological examination of these optic nerves has shown a non-caseating granulomatous reaction within the optic nerve head (Figure 5D). (Gass and Olson, 1976)

In contrast to papillitis, described previously, the OCT characteristics of these infiltrative lesions can be more severe with very swollen, hemorrhagic optic discs revealing peripapillary intraretinal fluid, subretinal fluid, retinal thickening with hyper-reflective dots suggesting an inflammatory cellular infiltrate (Figure 5D, Figure 5E) (Hickman et al, 2016) and choroidal thickening (Goldberg et al, 2015). The granulomatous tissue is highly reflective on OCT and can be nodular (Figure 5F). (Goldberg et al, 2015) Both Hickman et al (2016) and Goldberg et al (2015) report resolution of the granulomas and OCT signs with standard corticosteroid treatment, however there can be some long standing inner retinal atrophy where the

12

peripapillary changes were most severe, and residual gliosis on the nerve head. The core of larger granulomatous lesions of the optic nerve may become hypoxic leading to the production of pro-angiogenic factors promoting the growth of new vessels feeding the granuloma. These vascularized lesions can be successfully treated adding anti-VEGF injections to the underlying therapy and OCT can follow the lesion regression (Invernizzi et al, 2015a).

3. INNER RETINAL OCT SIGNS IN POSTERIOR UVEITIS

3.1 Retinal nerve fiber layer thickening

When there is active uveitis in an eye and pro-inflammatory cytokines are present leading to macula edema and papillitis it is also common to see more diffuse retinal thickening that correlates with disease activity (Castellano et al, 2009). Yamamoto et al (2011) first reported, in 12 eyes with Vogt-Koyanagi-Harada (VKH), that there was RNFL thickening in all quadrants of the peri-foveal area but thickest nasally. They showed this thickening was significantly greater than in control patients and showed a reduction in the convalescent phase. They found no corresponding leak on fluorescein angiogram.

Din et al (2014) found a thicker RNFL in 309 eyes with active uveitis and a trend to the thickness correlating to activity with thinning as overall activity decreased. Moore et al (2015) examined 211 eyes with heterogeneous anterior, intermediate and posterior uveitic entities. They found a mean global RNFL thickness of 140 microns in uveitis patients compared to a mean of 95 microns reported in normative databases in the literature. They therefore suggested macular edema secondary to uveitis, even

when subtle, can cause artifactual RNFL thickening confounding measurement and follow-up for glaucomatous patients.

3.2 Perivascular thickening

Retinal vasculitis can be a primary uveitic entity or secondary to another underlying disease (Abu El-Asrar et al, 2005). While periphlebitis, haemorrhages and sheathing are important indicators of activity in retinal vasculitis, there may also be a simple leak from posterior pole vessels, particularly in conditions such as birdshot chorioretinopathy or sarcoidosis (Karampelas et al. 2015). Preclinical studies on inflamed murine retinal vessels show enlargement with thickening and distortion of the surrounding paravascular retina. This perivascular thickening corresponded to extravasation of immune cells on histology (Chu CJ et al, 2013). OCT machines used in eye clinics around the world may be able to match these most advanced research imaging techniques. (Wojtkowski et al, 2005; Dolz-Marco et al, 2014).

Knickelbein et al (2018) describe a simple multi-view OCT technique using existing hardware, image acquisition and processing to create wider field topographic maps that can be followed up over time. The scan locations were fovea centered, optic disc centered and two further scans centered on the inferotemporal and superotemporal arcades. They found perivascular thickening which increased with disease activity, decreased with treatment and stayed stable during remission.

Tian et al (2018) used montaged enface widefield OCT to also prove an association between peripheral capillary angiographic leakage and the presence of perivascular, macular and generalized thickening on topographic maps. The included 88 patients had intermediate uveitis, broadening the application and further unpublished data

14

from the authors (Munk M) suggests this could offer a possible surrogate marker that can be used to guide treatment, detect disease recrudescence and guide the need for more invasive angiography in patients where these procedures are not part of regular routine follow-up (Figure 6A-C).

3.3 Dengue foveolitis

Dengue fever is a mosquito-transmitted viral disease that affects humans. There are 4 viral serotypes (DEN-1, DEN2, DEN-3, and DEN-4) of the genus Flavivirus (Flaviviridae family) commonly found in tropical and subtropical regions.

Ocular involvement in dengue fever is a relatively rare occurrence, with reported incidence varying from 7.9% to 40.3%. The posterior segment is most commonly affected, and sight threatening complications can occur in 5%–8% of cases. The main fundus changes are macula and retinal hemorrhages, peripapillary hemorrhage, Roth's spot, diffuse retinal edema, vitreous cells, blurring of the optic disc margin, serous retinal detachment, choroidal effusions, and nonspecific maculopathy (Figure 7A). It has been reported that approximately 10% of all dengue fever patients suffer from maculopathy with central vision loss. (Mehkri et al, 2015; Akanda et al, 2018)

Teoh et al (2010) used time-domain OCT to classify three types of dengue maculopathy: Type 1 with diffuse retinal thickening centered around the fovea, Type 2 with cystoid macular edema occurring within the retina and disrupting the photoreceptor layers, and Type 3 with foveolitis characterized by a yellow orange characteristic lesion at the fovea that was later identified as an acute macular neuroretinopathy (AMN) lesion. (Li et al, 2015; Munk et al, 2016) All the structural abnormality returned spontaneously to normal within a few days; however, scotomas

persisted in 30.3% of eyes with type 1, 56.3% of eyes with type 2, and 100% with type 3 maculopathy.

AMN lesions are characterized by hyporeflective parafoveal wedge shaped areas on near infrared imaging. Using SD-OCT classic AMN lesions can be assigned to the outer retina, presenting as hyper-reflectivity of the outer plexiform layer (OPL), Henle's layer and outer nuclear layer (ONL), which ultimately lead to localised disruption of the interdigitation zone (IZ), ellipsoid zone (EZ) and the external limiting membrane (ELM) (Figure 7B). Later in the disease course, subsequent thinning of the ONL ensues (Figure 7C-7E). The hyperreflection of AMN lesions on SD-OCT imaging attenuates fast within a 2-week follow-up interval. Although AMN is not found only in patients with dengue fever, Spectral-domain OCT applied before the attenuation of the lesions could facilitate the diagnosis of AMN in dengue maculopathy. A detailed morphological description of respective lesions can be found in chapter 4.4.

3.4 Cystoid macular edema and diffuse retinal thickening

Macular edema (ME) represents accumulation of fluid within the retina and is a common final pathway of many different ocular diseases (Daruich et al, 2018). It is characterized on OCT by either expanded areas of increased retinal thickness with reduced intraretinal reflectivity (so called diffuse ME) or accumulation of hyporeflective cystoid spaces (so called CME) (Hee et al, 1995). Visual acuity decrease due to macular edema is deemed to be induced by an impaired cell function relationship in the retina (Coscas et al, 2017). OCT is nowadays the most reliable way to detect and quantify ME and allows accurate assessment of the size,

extent and distribution of ME. Central macular thickness is the most utilized quantitative parameter on OCT to measure and follow ME, but unfortunately not the best indicator and predictor for visual function (Ou et al 2017). Rather the amount of preserved central retinal tissue on OCT seems a good marker for visual function (Pelosini et al 2011). Although ME is a nonspecific sign of various ocular diseases, the underlying contributing factors, which lead to the accumulation of fluid, differ leading to characteristic presentation of ME in respect to underlying disease (Munk et al, 2014; Munk et al 2015b; Daruich et al, 2018). Based on this characteristic presentation, uveitic versus diabetic ME might be differentiated in daily clinic but also automatically by using machine learning (Munk et al, 2014; Munk et al, 2015b; Hecht et al, 2018; Schlegl et al, 2018, Dysli et al, 2019). This generated classifier is also available as web-based tool (https://predictme.shinyapps.io/predictME/) and can be easily used in daily practice via computer or smartphone to help distinguish the different underlying causes (Hecht et al, 2019).

Uveitic cystoid macular edema is reported to be prevalent in about 20-30% of uveitic patients seen at tertiary referral clinics and is the primary cause of vision decrease; the majority of cases are a complication of intermediate, posterior or panuveitis, but also eyes with anterior uveitis may develop uveitic ME (Tomkins-Netzer et al, 2014; Fardeau et al, 2016; Agarwal et al, 2018b; Cunningham and Zierhut, 2018). The main underlying cause are a release of proinflammatory agents, mediators, and cytokines (such as TNF-α, IL-1, IL-6, TGF-β) with subsequent breakdown of the blood-retina barrier and an increase of vascular permeability (Lardenoye et al, 2006; Fardeau et al, 2016). However, uveitic macular edema may persist after the acute inflammation has worn off, mainly due to a persistently compromised blood retinal barrier (Ossewaarde-van Norel and Rothova, 2012). Formerly uveitic macular edema was differentiated into three different patterns, diffuse, CME and ME with serous retinal

detachment (Markomichelakis et al, 2004). But a post hoc analysis of the eyes with ME included in the MUST trial have shown no significant difference in terms of vision improvement or resolution of ME between diffuse vs cystoid ME (Tomkins-Netzer et al 2015). Morphologically uveitic ME has a distinct, characteristic presentation, which allows differentiation from ME of other underlying causes (Munk et al, 2014; Munk et al, 2015b; Hecht al, 2018). Usually uveitic ME presents as CME involving the central 1mm and the inner 3mm of the ETDRS grid (Munk et al, 2014). The horizontal and vertical B-scans show a central, concentric and symmetric CME, which is defined as cysts present foveally and parafoveally with homogenous extension of the horizontal OCT cross sectional scans (Munk et al, 2014). Also, the development and resolution of the uveitic ME follows a distinct pattern: characteristically, uveitic ME first emerges as small parafoveal inner nuclear layer (INL) cysts, which are followed by larger outer plexiform/outer nuclear layer (OPL/ONL) cysts. Finally, sub-retinal fluid (SRF) may develop, at least in around 65% of the cases (Munk et al, 2013a). The presence of SRF is associated with a favorable visual outcome and a shorter disease duration (Ossewaarde-van Norel et al, 2011). The resolution of ME in turn, starts in the OPL/ONL followed by the INL. SRF resolution lags behind (Munk et al, 2013b). Thus, eyes with uveitic CME all show cysts in the INL, and in the majority of cases these INL cysts are accompanied by OPL/ONL cyst. Up to 40% may also reveal cystic spaces in the ganglion cells layer (GCL) (Munk et al, 2014; Munk et al, 2015b). The reported prevalence of an epiretinal membrane (ERM) ranges between 30-45%, which is significantly higher than in other underlying causes of ME such as diabetes, Irvine Gass or vein occlusions (Munk et al, 2013a; Munk et al, 2013b; Munk et al, 2014). The presence of an ERM may alter the characteristic presentation of an uveitic ME and uveitic ME eyes may present with a hemi- or generalized ME pattern. The hemi ME is defined by cystoid spaces present foveally and parafoveally and

18

expanding either nasally or temporally. A generalized ME shows cystoid spaces distributed throughout the entire horizontal cross-sectional scans within the whole volume scan (Munk et al, 2014). Disorganization of the inner retinal layers (DRIL), which was first described in DME, may be present in a minority of eyes (around 18%) and correlates with worse visual function (Grewal et al, 2017). Given the high activity and interest in machine learning in the ophthalmology space, the automated detection as well as differentiation of CME will soon be no longer a pipe dream.

4. OUTER RETINAL OCT SIGNS IN POSTERIOR UVEITIS

4.1 Subretinal fluid (VKH)

Vogt-Koyanagi-Harada disease (VKH) is a multisystem autoimmune disease directed against melanocytes in the eye, auditory system, meninges, and skin. As such, it's characterized by bilateral uveitis and frequently accompanying extraocular manifestations such as meningismus, vitiligo, alopecia, poliosis and dysacusia. It has a genetic predisposition and primarily affects Asian, Middle Eastern, Hispanic and native American populations. The typical ophthalmological manifestation of VKH is a bilateral panuveitis with multifocal serous retinal detachments (Figure 8A, Figure 8C). Optical coherence tomography features in VKH disease have been extensively reported and include findings such as subretinal membranous structures, subretinal hyperreflective dots (which may represent clumps of inflammatory debris or macrophages engulfing shed outer segments), and intraretinal edema in the outer retinal layers, in addition to a thickened choroid in the acute stage, and potentially a thinned choroid in the chronic stage (da Silva et al, 2013).

19

The subretinal membranous structures appear to represent a portion of the outer photoreceptor segment layer that becomes separated from the inner segment layer by cystoid spaces (Figure 8B). Ishihara et al (2009) examined 20 eyes with VKH disease and found that in all eyes the floors of the cystoid spaces consisted of membranous structures of uniform thickness. These membranous structures appeared to include a highly reflective line, which was continuous with the line representing the ellipsoid band in regions with attached retina. Ishihara et al concluded that the membranous structures represented a portion of the outer segment of the photoreceptors that became separated from the inner segment by cystoid spaces.

The membranous structures separate the subretinal space into several compartments on the cross-sectional images of OCT (Figure 8B). There are arguments concerning the nature of these compartments. At first, it was assumed that the supra-membranous space is intra-retinal fluid (Maruyama and Kishi, 2004), intra-retinal edema (Parc et al, 2015), or cystoid space (Tsujikawa et al, 2005). OCT is not only valuable in providing morphological images, but also quantitative measurement of the optical intensity (also referred to as optical density, reflectivity) of normal and pathological tissue. In a study by Lin et al (2016), no significant difference in optical intensity was found between the sub-membranous space in VKH (Figure 8B, white asterisk) and the subretinal space in CSCR. The subretinal fluid of both VKH and CSCR are exudates from the choroidal vasculature through the breakdown of retinal pigment epithelium, and as such its composition in these two diseases might be similar. On the OCT image of VKH, the supra-membranous fluid (Figure 8B, yellow asterisk) is subjectively mildly reflective (Maruyama and Kishi, 2004) and its optical intensity is higher compared to that of the sub-membranous space, suggesting that there are more particles in supra-membranous fluid. This

finding supports the hypothesis that subretinal septa is splitting off of outer segments from the inner segments, resulting in cell debris increased in the supra-septa space. Nazari and Rao (2012) described in their study on 12 eyes with VKH disease the occurrence of RPE folds in 8 eyes (Figure 8D). In a retrospective clinical review of 57 Japanese patients, Kato et al (2013) examined the diagnostic usefulness of RPE folds for the diagnosis of VKH disease. They observed RPE folds in 30/42 (71%) of the eyes with VKH disease, but none in the other 72 eyes. The authors concluded that the detection of RPE folds was a simple and effective method for the diagnosis of VKH disease. Examining 61 eyes of 31 patients with acute VKH disease, Hashizume et al (2016) found some degree of RPE undulations or folds in 40 eyes. The patients with RPE folds or undulations in both eyes were significantly older, and the eyes with RPE undulations were more likely to develop recurrences and have worse vision at 12 months of follow up. In a study on 8 eyes of 4 patients with acute VKH disease, Gupta et al (2009) described undulations and bumps on the RPE surface in all eyes, whereas the retina from the inner limiting membrane to the external limiting membrane did not show any structural alteration. The undulations correspond to choroidal striations seen as hypofluorescent lines in the early phase on fluorescence angiograms, whereas the bumps over the undulations correspond to the pinpoint hyperfluorescent dots on the angiograms (unpublished data). In their study on 42 eyes of 22 patients undergoing glucocorticosteroid therapy for acute VKH and on 20 healthy eyes, Hosoda et al (2014) investigated the correlation between choroidal and retinal lesions in eyes with acute VKH disease and used the parameter of RPE undulation index, quantitatively describing choroidal deformations. The authors found that the eye with acute VKH disease showed an increased RPE undulation index in addition to an increased choroidal thickness. The increased RPE undulation index was significantly associated with increased choroidal thickness.

However, care should be taken in interpreting the RPE undulation index data, since tissue curvature on OCT may be artifactually modified.

Although the studies mentioned above described the occurrence of features such as RPE folds and a subretinal membranous structure, the diagnostic validity of these OCT characteristics for the diagnosis of acute VKH in the differentiation against other exudative maculopathies has only been assessed by Liu et al (2016). Liu et al reported that the presence of subretinal membranous structures, a high retinal detachment (minimal macular height >450 mm), subretinal hyperreflective dots, and RPE folds as single parameters had a rather high diagnostic value with respect to their sensitivity and specificity for the diagnosis of acute VKH disease. In particular, the combination of any two of these parameters in both eyes further increased the value as diagnostically predictive parameter.

Noteworthy seems also the fact that a VKH syndrome phenotype not discernible from a "classic" VKH syndrome can appear in patients with (metastatic) melanoma under MEK, BRAF and Checkpoint inhibitors. Onset of VKH like features have been also described under IFN therapy in hepatitis C (Moorthy et al, 2018). The underlying cause remains unknown, but it has been suggested that immune reactions toward melanocytes are triggered by respective drugs interacting with the immune system (Wong et al, 2012).

4.2 Neuroretinitis changes and star-shaped exudate

Recent onset neuroretinitis induces characteristic early OCT findings (Zatreanu et al, 2017; Abdelhakim and Rasool, 2018). Clustering of vitreous inflammatory cells adjacent to the optic nerve, so called "epipapillary infiltrates", in association with optic nerve head swelling were reported to be pathognomonic early OCT findings in

22

neuroretinitis (Zatreanu et al, 2017). They can be visualized as hyperreflective dots in the vitreous cavity contiguous to the optic nerve head. They are found in association with a thickening of the RNFL in the peripapillary OCT ring scan, retinal thickening visible on the retinal thickness maps on the optic nerve head of OCT volume scans and the presence of SRF and IRF adjacent to the optic nerve head (Figure 5C). Further a typical pattern of inner retinal folds due to mechanical forces of the macula edema can be seen. These inner retinal folds are described as outwardly expanding concentric rings from the optic nerve head extending into the fovea. These folds seem to be unique to neuroretinitis and differ compared to the pattern of retinal folds seen in other causes of disc edemas (Figure 8) (Zatreanu et al, 2017; Abdelhakim and Rasool 2018). OCT macular volume scans exhibit flattening of the foveal contour, the accumulation of SRF and thickening of the neurosensory retina (Figure 5C) (Habot-Wilner et al, 2011; Abdelhakim and Rasool 2018). SRF and IRF located in the OPL and ONL extending from the optic nerve head to the fovea points towards neuroretinitis (Habot-Wilner et al, 2011; Finger and Borruat 2014). After 7-10 days hard exudates develop (Figure 5A). These hyperreflective foci are mainly located in the OPL and often present in the characteristic macular star shaped pattern (Habot-Wilner et al, 2011; Finger and Borruat, 2014). Under treatment sub and intraretinal fluid resorbs rapidly, while the resolution of hard exudates lacks behind. They may be visible up to 2 months after onset of the disease (Finger and Borruat, 2014).

4.3 Acute retinal infiltrates of Behçet disease and post-acute RNFL defects

Behçet disease is a chronic multisystem inflammatory disorder, first described as a distinct entity by Hulusi Behçet in 1937 and characterized by a perivascular inflammatory infiltration of the veins, capillaries, and arteries of all sizes and a

23

thrombotic vasculopathy. Posterior segment involvement has been reported in 50-93% of patients with ocular disease, and recurrent inflammatory attacks may lead to severe retinal damage and visual loss. Therefore, identification of posterior segment involvement has a very important prognostic value.

Among the OCT features that can be used as a diagnostic sign of Behçet disease are transient retinal infiltrates seen during exacerbations (Tugal-Tutkun et al, 2017). SD OCT sections through retinal infiltrates typically show focal retinal thickening, increased hyper-reflectivity with blurring, especially of inner retinal layers, and optical shadowing. There is no focal choroidal thickening beneath the retinal infiltrate and the RPE contour is not affected in Behçet uveitis, retinal infiltrates rapidly resolve without any apparent retinochoroidal scarring. However, SD OCT sections typically show inner retinal atrophy. The development of non-glaucomatous localized RNFL defects has been recently described as sequelae of superficial retinal infiltrates affecting the posterior pole in Behçet uveitis (Oray et al, 2015). These papillomacular or arcuate RNFL defects can be easily identified by OCT and may be associated with corresponding visual field loss. This finding is a helpful diagnostic clue and indicator of posterior pole involvement in early Behçet uveitis.

4.3 Retinal pigment epithelitis

Acute retinal pigment epitheliitis (ARPE) is a rare inflammatory episode of the RPE and outer retina complex which was first described by Krill and Deutman (1972). The findings can be unilateral or bilateral, transient and subtle in a young healthy adult population suggesting a possible viral etiology (Deutman, 1974). Prior to the advent of OCT it was diagnosed entirely by history of an acute central scotoma and the

appearance of multiple discrete small gray spots with a yellow halo in the macula area. These disappear and vision recovers with the spontaneous resolution seen over weeks to months (Luttrull et al. 1995).

OCT has started to shed light onto the pathophysiology of the disease as the overall resolution of the technology has improved. A review of 18 cases by Cho et al. (2014), using SD-OCT, has shown all 18 eyes had focal inflammation and disruption at the inner border of the RPE layer – the interdigitation zone between the RPE and cone outer segment interface. They suggest this is the site of primary pathology as then only 16 of 18 eyes had a corresponding, smaller area of change in the EZ anterior. In the most severe cases there is further high signal anterior change to this in the ONL with swelling, disruption of the external limiting membrane (ELM) and a dome shaped appearance. (Figure 9A) These changes are confirmed in a case series by Lu et al. (2017) who also suggested a sequence of recovery and reconstitution where this dome shaped ONL lesion decreases in height then disappears, the ELM restores then the ellipsoid zone and finally the interdigitation zone reconstitute. (Figure 9B)

As well as making the diagnosis and tracking recovery, OCT can also aid in ruling out the differential diagnoses. Differential diagnose include AMN and APMPPE, but AMN as described in the sections below does not include the RPE layer changes and APMPPE has more widespread multifocal changes with choriocapillary changes visible on OCT (Figure 10C and 10D) (Hsu et al. 2007).

4.4 Acute macular neuroretinopathy lesions

Acute macular neuroretinopathy was initially described in 1975 (Bos and Deutman, 1975). Patients usually experience sudden paracentral scotoma or blurred vision (Bhavsar et al, 2016). Although the etiology of AMN remains a matter of debate, the

current weight of evidence is that AMN is associated with ischemia of the deep retinal circulation (Fawzi et al, 2012; Munk et al, 2016; Munk et al, 2017; Chu et al, 2018; Kulikov et al, 2018). While paracentral acute middle maculopathy (PAMM) seems to involve the DCP as well as the mid capillary plexus (MCP) and occasionally the superficial capillary plexus (SCP) (Chu et al, 2018; Pichi et al, 2018), AMN seems restricted to the retinal DCP (Figure 7E) (Chu et al, 2018; Nemiroff et al, 2018), although some studies have postulated an involvement of the choriocapillaris as well (Lee et al, 2017; Casalino et al, 2018). The postulated underlying risk factors are diverse and include an association with unspecific flu-like symptoms and fever, the use of epinephrine, cocaine, shock, flu vaccination, oral contraceptive intake, trauma, Dengue fever, caffeine, ADHD medication and SUSAC syndrome, all suggestive for an implication of immune processes and/or vasoconstriction (Bhavsar et al, 2016; Munk et al, 2016; Yang et al, 2018). Despite the uncertainty in terms of the underlying pathophysiology, the morphologic presentation on OCT and near infrared is pathognomonic and reflects the involvement of the DCP (Figure 7E). A case report of a patient with AMN and symptoms for no longer than 3 hours was able to capture for the first time the concurrent development of an AMN lesion on OCT (Baumuller and Holz, 2012). The lesions evolve at the posterior border of the OPL. Consecutively hyperreflectivity of the Henle layer, thinning of the ONL and attenuation of the EZ and IZ is visible (Baumuller and Holz, 2012), suggesting that the changes of the inner retina predate the involvement of the outer retina, which would be consistent with the proposed mechanism (Baumuller and Holz, 2012; Fawzi et al, 2012). The complete clinical picture of AMN reveals localized hyperreflectivity of the OPL, Henle layer and ONL on OCT, as well as localized disruption of the EZ and IZ (Figure 7B). Usually the ELM is attenuated but still appreciable (Baumuller and Holz, 2012; Fawzi et al, 2012; Munk et al, 2017). On near infrared, hyporeflective

parafoveal wedge-or petaloid shaped lesions are visible, which may appear uni-or bilateral and last for several weeks up to months. The lesion visible on near infrared corresponds best with the attenuation and thinning of the photoreceptor layers (Fawzi al, 2012; Munk et al, 2017), while the changes found in the ONL and OPL may exceed near infrared lesions and attenuation at the level of the photoreceptors (Munk et al, 2017). Funduscopically these lesions are sometimes hard to distinguish and usually appear either reddish-brown, or whitish grey (Figure 7A) (Fawzi et al, 2012; Bhavsar et al, 2016). Over time these lesions fade and the intensity of EZ and IZ improve, but usually attenuation of the EZ and often complete absence of the IZ remains (Fawzi et al, 2012; Munk et al, 2017). This corresponds to an improvement but nonetheless persistence of the paracentral scotoma. Although the presentation on OCT and near infrared is pathognomonic for AMN, the quantification is challenging. Due to the Stiles-Crawford effect, the lesions show a strong directional variability (Bottin et al, 2018). Depending on the entry points of the light of the scanning laser ophthalmoscopy, parts of the lesion present hypo-to iso-reflective on OCT as well as on near infrared (Bottin et al, 2018), which exacerbates a correct quantification and measurement of the lesion.

4.5 Ellipsoid layer inflammation, restoration and "true loss"

A pathognomonic, though, non-specific sign of posterior uveitis is attenuation and loss of the EZ and IZ. These changes may be found in various white dots syndromes, and in each individual disease they exhibit a characteristic presentation. In APMPPE (Figure 10C and 10D), the disruption of the EZ and IZ is accompanied by overlying hyperreflectivity of the outer retinal layers on OCT (Figure 10D). Sometimes subretinal fluid may be present (Figure 10C) (Cohen et al, 2015; Heiferman et al,

2017; Scarinci et al, 2017; Roberts et al, 2018). In the majority of cases the ELM is disrupted (Scarinci et al, 2017). Small areas of hypertransmission of the RPE and RPE proliferation can be found as well (Figure 10). Over the course of the disease, one can appreciate incomplete to complete restoration of respective layers, which goes along with the resolution of the overlying hyperreflectivity of the ONL. The small areas of RPE proliferation at initial presentation later correspond to areas of pigmentation and pigment migration visible on color fundus photographs and infrared (Goldenberg et al, 2012; Cohen et al, 2015; Heiferman et al, 2017; Roberts et al, 2018). The restoration of the photoreceptor volume strongly correlates with the improvement of intact ELM/Bruch's membrane ratio (Scarinci et al, 2017). Despite the favorable course of the disease, attenuation of the EZ, IZ and ELM and irregularities of the RPE may remain (Figure 10) (Goldenberg et al, 2012). Correspondingly, improvement but no complete recovery of the choroidal flow void in the affected areas is seen on OCT-angiography (Heiferman et al 2017; Mangeon et al, 2018; Pichi et al, 2017a).

Inflammation of the outer retina in punctate inner choroidopathy (PIC) and multifocal choroiditis (MFC) presents differently (Figure 10G and 10H). The typical course includes only localized and persistent disruption of the ELM, IZ and EZ, induced by lesions evolving from the choroid (Figure 10F) (Spaide et al, 2013; Zhang et al, 2013; Munk et al, 2015a). These chorioretinal lesions show a characteristic morphologic evolution on OCT and can be staged based on their presentation (Vance et al, 2011a; Zhang et al, 2013). Stage I is characterized by a subtle irregularity of the ONL, while stage II appears as focal elevation of the RPE with corresponding disruption of the IZ and EZ with still intact ELM. Stage III is characterized by a break of the Bruch's membrane and a burst of the RPE accompanied with a hyperreflective hump-shaped hyperreflective chorioretinal nodule with complete disruption of the

28

ELM, EZ and IZ (Figure 10G, Figure 10H). The regression of the lesions happens in a retrograde manner with subsequent loss and atrophy of the former involved tissue and layers defining Stage IV. The final stage V shows complete loss of the RPE and EZ layers with subsiding and sagging of the OPL and inner retina. During this period, proliferation of the RPE or RPE-ish material leads to a restoration of the RPE break (Zhang et al, 2013). Thus, new acute chorioretinal PIC and MFC lesions are usually conical and show RPE elevations due to iso-hyperreflective material. Some seem to have a ruptured appearance with hyperreflective material pushing anteriorly into the outer retina (Figure 10H) (Spaide et al, 2013; Tavallali and Yannuzzi, 2015).

In a minority of patients, who exhibit active, new evolving lesions, an acute, more widespread photoreceptor attenuation/loss can be observed (Munk et al, 2015a). Adjacent to the new evolving lesions, a widespread and extensive attenuation/loss of the EZ, IZ and ELM is seen on OCT, which corresponds to hyper-autofluorescent (AF) lesions on fundus autofluorescence (FAF) and hypo reflective lesions on near infrared. A corresponding hypo-fluorescent area on ICG may be seen as well (Figure 10F). The area of photoreceptors loss corresponds to visual field defects, and substantial vision decrease up to hand motion can occur if the fovea is involved. Recovery and regeneration of respective layers with consecutive recovery of visual fields defects and vision varies widely and the role of treatment in these cases is uncertain (Munk et al, 2015a). Complete recovery of the hyperreflective outer retinal layers, incomplete recovery with persistent irregularity of the EZ and IZ as well as persistent and complete loss of the EZ, IZ and ELM with significant ONL thinning/loss may all be observed (Chen and Hwang, 2013; Jung et al, 2013; Kramer and Priel, 2013; Munk et al, 2015a; Slakter et al, 1997; Volpe et al, 2001; Spaide et al, 2008; Freund et al, 2013). These changes were also deemed as a variant of the acute zonal occult outer retinopathy (AZOOR) complex in previous literature (Holz et al,

1994; Gass et al, 2002; Taira et al, 2006; Saito et al, 2007). However, the trizonal pattern, which is a pathognomonic sign for older AZOOR lesions (and which will be discussed in section 4.9) is missing in these cases (Tavallali and Yannuzzi 2015).

4.6 En face and B-scan "dots and spots" in multiple evanescent white dots syndrome

Multiple evanescent white dot syndrome (MEWDS), first reported by Jampol et al in 1984, is an acute-onset inflammatory syndrome characterized by multiple yellow-white spots, 100 to 200 um in size, that are deep to the retina (Figure 11A). This prevalently unilateral disorder (Veronese et al, 2018) is also associated with a unique foveal granularity (Figure 11E) and typically affects young healthy women in the second to fifth decades. Most patients have spontaneous improvement in vision with resolution of all lesions within weeks.

Although the clinical features of MEWDS are well described, the etiology is still unknown. MEWDS was termed "a chorioretinopathy with varying degrees of choroidal and retinal involvement" (Thomas et al, 2013). The acute decline in the amplitude of the a-wave with ERG analysis (Chen et al, 2002) and speckled hyper-fluorescence of the white spots in a wreath-like pattern of dots (Shahalee et al, 2015; Cheng et al, 2009) on FA, suggest that the location of the disease process resides in the outer retina and/or the RPE. At the same time, ICGA of MEWDS shows multiple hypo-fluorescent nummular lesions (Figure 11B) which has been suggested to be the result of choroidal nonperfusion (Hashimoto et al, 2015; Sikorsky et al, 2008).

With the integration of SD-OCT and *en face* OCT in the multimodal imaging assessment of this disease, Pichi et al (2016) were able to elucidate the location and nature of MEWDS lesions.

In the acute MEWDS phase, B-scan SD-OCT through the fovea shows a disrupted or irregular inner segment ellipsoid zone band of varied severity and a disappearance of the "COST line" (cone outer segment tip line between the IS/OS line and the retinal pigment epithelium, nowadays also described as interdigitation zone [IZ]) (Figure 11D). During the early recovery follow-up, the disruption of the ellipsoid zone gradually improves from diffuse to focal and from loss to irregularity, and at the late recovery stage the ellipsoid band is continuous in all affected eyes. Foveal granularity detected ophthalmoscopically seems to persist long after the OCT-restoration of the outer bands (Casalino et al, 2017) and it is thus an important sign of the condition during the recovery phase.

A discontinuity or disruption of the ellipsoid zone on SD-OCT can also be detected outside the fovea, correlating to numerous round hypo-reflective lesions on *en face* scans at the level of the ellipsoid zone (Figure 11C). These hyporeflective "spots" correspond to the classical yellow-white lesions identified with fundus photography.

These ellipsoid lesions match the hyper-autofluorescent lesions in the posterior pole and in the midperiphery with FAF. This correspondence between SD-OCT ellipsoid loss and hyper-autofuorescence reconciles the alternative mechanism proposed by Joseph et al (2013) in which photoreceptor loss causes unmasking of normal underlying RPE autofluorescence. Therefore, the hyporeflective "spots" seen with *en face* OCT may be due to primary inflammation of the photoreceptors, which become misaligned (as seen on SD-OCT) and attenuated, leading to an unmasking of the normal underlying RPE autofluorescence (hyper-autofluorescent lesions).

The hypo-fluorescent "spots" seen on ICGA precisely correlate with the confluent hyporeflective lesions located at the level of the inner segment ellipsoid (Figure 11B compared to Figure 11C) and very well defined with *en face* OCT. Chang et al (2005) studied the ICG absorption characteristics of the RPE and noted that the RPE

normally absorbs ICG causing physiological background hyperfluorescence. ICG uptake however may be disrupted in certain retinal RPE disorders, such as MEWDS, and may explain the late hypo-fluorescent lesions that co-localize with the associated areas of ellipsoid loss, as documented in this study.

Resolution of the hypo-reflective "spots" can also be observed in follow-up *en face* OCT (Figure 11), thus demonstrating a progressive and complete recovery of the outer bands.

A second feature highlighted in MEWDS cases by SD-OCT (Pichi et al, 2016) is the finding of hyper-reflective fine spicules coalescing into denser, more discrete, oval dots in the ONL (Figure 11H). These hyper-reflective punctate foci are not limited to the foveal area but can also be detected around the nerve and along the arcades. Of interest, the ELM underlying these oval SD-OCT lesions is intact in most cases. *En face* OCT scans at the level of the ONL shows an array of small, round hyper-reflective punctate dots (Figure 11G) corresponding to the oval and punctate hyper-reflective material seen in the ONL on B-scan OCT. These *en face* "dots" match the smaller cluster of speckled hyper-fluorescent "dots" seen with FA. The "dots" may represent photoreceptor debris shed and accumulated in the outer retina.

Based on these OCT patterns of ellipsoid "spots" and ONL "dots", Pichi et al (2016) have concluded that MEWDS seems to be primarily the result of inflammation at the RPE and outer photoreceptor level leading to a "photoreceptoritis" and causing loss of the inner and outer segments. The smaller "dots" may represent disrupted and shed photoreceptor segments and/or associated Muller cell disruption. Because of the very finite size of these punctate (and linear) lesions, they may be undetectable with fundus photography and examination. The structural B scan and enface OCT

detection of these ONL punctate and linear lesions in the fovea and around the optic nerve is very characteristic and may provide an additional important clue to the diagnosis of this sometimes elusive disorder.

Its evanescent nature suggests that the photoreceptor cell bodies remain intact ensuring complete recovery of the photoreceptor inner and outer segments in most cases, compatible with the clinical course of spontaneous resolution of white spots and dots and visual function recovery in almost every patient.

4.7 RPE nodularities and "OCT loss" of ellipsoid in placoid syphilis

Eye involvement is believed to occur most often during the secondary and tertiary stages of syphilis, although ocular manifestations have been reported at all stages of the disease (Kiss et al, 2005). Although syphilis may affect the eye in a number of ways, posterior uveitis is the most common complication, with the most frequent posterior segment manifestation being retinochoroiditis (Samson et al, 2001) in the confluent or in the placoid form.

Although de Souza et al (1988) first reported three cases of an unusual central chorioretinitis as a presenting manifestation of early secondary syphilis, Gass et al (1990) introduced the term acute syphilitic posterior placoid chorioretinitis (ASPPC) to describe this distinctive ocular manifestation of systemic syphilis infection, which they observed in six patients. ASPPC is an uncommon expression of syphilis represented by the presence of a unique or several yellowish and placoid-like lesions at the level of the RPE within the posterior pole (Figure 3D) (Morgan et al, 1984; Gass et al, 1990, Meira Freitas et al, 2009). It can present in immunocompetent and immunocompromised patients and the pathogenesis remains unknown.

Since the first description, more than 100 additional case have appeared in the literature (Eandi et al, 2012).

FA and ICGA findings in ASPPC have been described in detail, (Meira-Freitas et al, 2009; Eandi et al, 2012) but SD-OCT characteristics are quite distinctive and pathognomonic, suggesting a primary inflammation at the level of the choriocapillaris-retinal pigment epithelium complex.

Joseph et al (2007) reported two cases with ASPPC in whom time domain OCT imaging, a lower-resolution predecessor to SD-OCT, taken at presentation of symptoms demonstrated the presence of SRF with thickening of the neurosensory retina and RPE–choriocapillaris complex. Other authors have reported thickening at the level of the RPE–choriocapillaris complex without signs of serous retinal detachment (Meira-Freitas et al, 2009; Chen et al, 2008). Eandi et al (2012) described time domain OCT findings in eight eyes with ASPPC and saw a flat contour of the retina without neurosensory retinal or pigment epithelial detachment. However, in their review of the literature, Eandi et al (2012) reported an overall prevalence of SRF in hyper-acute ASPPC in 11 of 93 eyes (11.8%). The case series by Pichi et al (2014) of SD-OCT findings in this disease reports transient SRF, which resolved before treatment, in patients who had imaging done within the first 2 days of presentation (43.3%) (Figure 3E). This was accompanied by an intact ELM, disruption of the EZ, and thickening and granular hyperreflectivity of the RPE but without nodular elevations (Pichi et al, 2014). Although the incidence of SRF in Pichi's series was somewhat higher than that reported in Eandi's review, it seems plausible that earlier studies might have failed to identify small amounts of SRF present acutely after infection due either to the use of lower resolution time domain OCT units or to the later timing of OCT imaging.

The acute hyperreflectivity and thickening of the subfoveal RPE-choriocapillaris complex in ASPPC evolves at ~1 week after presentation in an irregular hyperreflectivity with prominent nodular elevations at the junction of the photoreceptors and the RPE associated with segmental loss of the ellipsoid band but no evidence of new or persistent fluid under the fovea (Figure 3F).

Brito et al (2011) described an acute loss of choroidal vascular detail. In the series by Pichi et al (2014) 30.8% of the eyes had hyperreflective spots in the choroid at days 1 to 2 and showed persistence of these spots at days 7 to 9; in addition, at this time point, scattered hyperreflective dots were noted in the choroid of 10 additional eyes.

Initiation of systemic penicillin therapy leads to prompt normalization of vision and restoration of outer retinal and choroidal anatomy. At 1-month follow-up, SD-OCT following antibiotic treatment demonstrated complete restoration of the EZ band with normalization of the RPE, and disappearance of the hyperreflective dots in the choroid (Figure 3G) This anatomical resolution is accompanied by improvement in vision.

Since patients with ASPPC usually receive prompt antimicrobial treatment after simple serologic investigation, the reports on the natural course of the disease are scarce. In 2014, Armstrong et al reported on the evolution of ASPPC to chorioretinitis. In their case, panuveitis developed 6 weeks after the initial diagnosis of ASPPC, without spontaneous resolution of the lesion. This suggests that ASPPC could be an early manifestation of posterior uveitis. Franco et al (2016) observed complete spontaneous recovery of the outer retina changes on SD-OCT after 2 weeks and the patient was free of any sign of inflammation for 2 months. Baek et al

(2016) reported a similar patient with untreated ASPPC that resolved spontaneously, with the macular placoid lesion disappearing in both eyes and SD-OCT showing only some granular hyperreflectivities on the RPE level. However, the longer follow-up compared to Franco et al (2016) demonstrated a progression to posterior uveitis 9 months later. A case of spontaneous resolution of ASPPC has been also reported by Aranda et al (2015). This sequential pattern with complete spontaneous resolution of inflammation reflects an adequate response of the immune system to this infection, being able to control it locally. Syphilis is characterized by episodes of active disease that are interrupted by periods of latency. Spontaneous resolution of initial ASPPC can be explained as the disease entering prolonged latency because of the host's cellular immune response.

Although the pathophysiology of ASPPC is not completely understood, we postulate the sequence of disease events based on the timing and characteristics of SD-OCT findings. Possibly, the choroidal hyperreflective pinpoint lesions seen on SD-OCT are consistent with inflammatory foci in the choroid vasculature as the circulating T. pallidum organisms enter the outer retina through the choroidal circulation.

The presence of treponemes in the choroid could result in the development of antibodies. Brito et al (2011) reported an increased level of anti-beta2 glycoprotein I antibody in a patient with ASPPC, an apolipoprotein that binds to cardiolipin. These antibodies could cause focal choroidal thrombosis and altered retinal pigment epithelium metabolism, causing disorganization of the RPE structure represented by the hyperreflective nodularity (SD-OCT). This results in impaired photoreceptor function expressed by disruption/loss. The acute infection of the outer retina leads to hyper-acute disruption of the outer blood ocular barrier producing variable amounts of SRF.

The reports of spontaneous resolution of ASPPC with late-onset posterior uveitis (Franco et al, 2016) question the role the immune system as a modulator of the clinical features of syphilis. Chorioretinitis or posterior uveitis in such cases presented at different stages and the same clinical course was observed: onset-aggravation-resolution. This may suggest that ASPPC could have its own clinical course, independent of steroid use.

4.8 AZOOR Trizonal changes

Characteristic EZ, IZ and ELM loss leading to persistent scotomas and vision loss can occur in a variety of diseases such as autoimmune retinopathy (AIR), toxic and drug induced retinopathies as well as in cancer associated retinopathy (CAR). However, the distribution and morphological appearance of the changes induced by AZOOR are pathognomonic. While CAR, AIR and drug related retinopathy present bilaterally and spare the fovea until very late, AZOOR presents with peripapillary loss of the EZ, IZ and ELM, is often unilateral and shows a characteristic trizonal pattern (Gass et al, 2002; Vance et al, 2011b; Wang et al, 2017). It was initially described by Gass as a disease with one or more zones of loss of outer retinal function (Gass, 2003). AZOOR may be self-limiting but may also respond to treatment (Barnes et al, 2018). The location, pattern, size and the number of AZOOR lesions vary. While the peripapillary region is most frequently involved (Figure 10I), the fovea is usually spared (Gass et al, 2002; Mrejen et al, 2014). The most common patterns are enlarged blind spots with corresponding peripapillary loss of the outer retinal hyperreflective bands and large areas of outer retinal loss connected to the blind spot and optic nerve head (Gass et al, 2002; Qian et al, 2017). Also, cases with peripapillary lesions continuously growing in a centripetal and centrifugal manner

leaving only a small area of unaffected normal retina have been described (Shifera et al, 2017; Tan et al, 2017). Morphological presentation may vary depending on disease stage (Shifera et al, 2017). Even if the fovea is not affected, the diseased eye will show a decreased thickness of the photoreceptors layer compared to healthy control eyes at respective location. The attenuation of the IZ, EZ and ELM goes along with thinning or complete loss of the ONL, while the inner retina and the choroid exhibit more or less no significant thickness changes (Figure 10K, Figure 10L) (Fujiwara et al, 2010). In areas of absent or severely thinned ONL, lengthy hyporeflective bands may be seen within the GCL (Fujiwara et al, 2010). The ONL thickness resembling the amount of surviving nuclear bodies of the photoreceptors may be a prognostic sign for potential improvement and restoration of the photoreceptors layers over the course of the disease.

Recent onset AZOOR lesions usually present with diffuse loss of the photoreceptors layers on OCT within the AZOOR lesion, which characteristically corresponds to a patchy hyperAF on FAF imaging (Figure 10J). During the subacute or chronic phase, the characteristic trizonal pattern is identifiable, which can be visualized on OCT, FAF and ICG. Zone 1 resembles the healthy retina, with intact RPE and photoreceptor layers. Zone 2 is the demarcation line, the transition zone between the healthy and the fully diseased retina, visible as attenuation of EZ and ELM, incipient thinning of the ONL, and the presence of hyperreflective, subretinal material. Zone 3 describes the fully diseased retina with complete loss of the photoreceptors layer, significant thinning or loss of the ONL and RPE and choroidal atrophy (Mrejen et al, 2014). Correspondingly, zone 1 has a normal appearance on FAF, a speckled hyperAF within zone 2 and is hypoAF in zone 3. The mean quantitative FAF of the AZOOR line is 60 times higher than the quantitative autofluorescence in healthy controls (Boudreault et al, 2017).

4.9 Secondary inflammatory choroidal neovascularisation

End stage punched out chorioretinal lesions are characteristic signs of posterior and pan-uveitis and the morphological development of respective lesions have been extensively described in the chapter above. A secondary, inflammatory CNV in this condition has a reported incidence of over 50%. On OCT-A the prevalence of a secondary, inflammatory CNV is even higher: Up to 83% of MFC/PIC lesions show a flow signal, which is consistent with neovascularization (Zahid et al, 2017; Levison et al 2017; Astroz et al, 2018). These CNV lesion have a distinct presentation on OCT compared to other causes of secondary CNV.

Inflammatory CNV usually develops subretinal, between the RPE and the neurosensory retina, resembling a Type 2 CNV (Wu et al, 2016; Agarwal, et al. 2018a).

An increase of subretinal, hyperreflective material including some roundish, hyporeflective structures (which probably resemble vascular subretinal elements) and adjacent subretinal fluid can be appreciated on OCT. In a minority of eyes an occult, subRPE type 1 component may accompany the main subretinal, type 2 neovascularization. This Type 1 component will present as undulating flat RPE detachment with mixed reflectivity (Roy et al, 2017). Sometimes no definite subretinal fluid may be visible and activity is associated with finger-like hyperreflective projections which extend from the CNV area into the outer retinal layers (Hoang et al, 2013; Spaide et al, 2013; Munk et al, 2015). This distinct presentation has been called "pitchfork sign" and helps to differentiate this Type 2 CNV from Type 2 CNVs of other underlying etiologies (Hoang et al, 2013). After treatment, a circumscribed

solid, subretinal, homogeneously medium-hyperreflective material can be appreciated, which resembles fibrosis.

4.10 Sub-Retinal material in primary vitreoretinal lymphoma

Primary vitreoretinal lymphoma (PVRL) is a rare malignant condition, usually of B-lymphocyte origin, that is considered as a subtype of the diffuse large B cell lymphomas of the central nervous system (Grimm et al, 2007). Primary vitreoretinal lymphoma has protean clinical manifestations and it is often characterized by inflammatory changes involving the posterior structures of the eye. For these reasons it is commonly misdiagnosed as an autoimmune uveitis and it is known as one of the masquerading syndromes (Chan and Sen, 2013).

Given the various clinical pictures characterizing PVRL, many OCT signs have been described in this condition, many of them non-specific. Cellular infiltration is thought to be responsible for many of the SD-OCT signs identified in eyes with PVRL. Vitreous cells, retinal pigment epithelium detachments and subretinal fluid are examples of OCT findings reported in eyes with PVRL that are so common in other diseases that cannot be considered as suggestive for PVRL. By contrast, the absence of cystoid macular edema, a common finding in inflamed eyes, should rise the suspect of a possible malignancy (Carreras et al, 2017; Velez et al, 2002).

Despite the protean manifestations some peculiar OCT signs could suggest PVRL in eyes with presumed uveitis. A well-defined hyper-reflective nodularity of the outer retinal layers was reported in more than 90% of the eyes with PVRL (Mapelli et al, 2016). The authors suggest this alteration to represent lymphomatous infiltrations. Interesting the nodularity induces disruption of the outer retinal bands between the

40

ONL and the RPE without affecting Bruch's membrane. The same material was further characterized in a following paper where the authors classified its distribution as "isolated nodules" or "confluent band" claiming the latter to be strongly suggestive for PVRL in patients with compatible clinical features Figure 12A) (Barry et al, 2018).

Malignant cells infiltrate the retina in PVRL eyes. These cellular elements are visible on OCT images as focal hyper-reflective alterations within the retinal layers (Mapelli et al, 2016). A recent paper described vertical hyper-reflective lesions deepening through the retinal layers in eyes with PVRL (Deak et al, 2018). The authors proposed these to represent infiltrating cells migrating from second-order and third order retinal vessels through the retina into the subretinal space. The identification of focal hyper/mid-reflective elements within the retina changing in position and size within weeks should suggest a highly active cellular turnover and a possible PVRL (Figure 12B, Figure 12C).

The presence of one or more of these OCT signs can suggest a possible PVRL etiology when accompanied by a compatible clinical picture. Eyes with these features should always be investigated searching for malignant cells on ocular samples to confirm the diagnosis of PVRL.

4.11 OCT differences in necrotizing retinitis (ARN, CMV and Toxo)

Necrotizing retinitis may occur due to different inflammatory or infectious uveitis including toxoplasmosis (Butler et al, 2013), herpetic viruses (Lau et al, 2007; Pearce et al, 2016) and Behçet disease (Tugal-Tutkun et al, 2013) among others. The necrotic retina typically appears hyper-reflective on SD-OCT scans with disruption of the physiological architecture regardless the causative agent (Kurup et al, 2014).

However, infective agents spread differently through ocular tissues, thus OCT findings may vary according to the causative infective agent (Invernizzi et al, 2018a).

Cytomegalovirus (CMV) is known to cause a necrotizing retinitis in immunocompromised patients. The virus can penetrate the eye through the choroid or the retinal vasculature. It can infect RPE cells, Muller cells and inner retinal layers neurons. By contrast it seems to spare photoreceptors (Zhang et al, 2005). This peculiar tropism could explain the presence of hyperreflective vertical lines on OCT connecting the RPE to the inner retinal layers crossing the outer nuclear layer (Figure 13A and 13B) (Invernizzi et al, 2017b). The authors that described this finding suggested these lines to be infected Mullers cells used by the virus to cross the photoreceptors layers to reach the neurons of the inner retina. In a paper comparing OCT findings in different necrotizing retinitis this sign was significantly more frequent in viral retinitis compared to those of toxoplasmic etiology (Invernizzi et al, 2018a).

Toxoplasmosis infection is responsible for the development of necrotizing lesions involving both the retina and the choroid (Butler et al, 2013). Differently from herpetic viruses, toxoplasma parasites preferentially infect glial cells and have been found within the choroid and the retina without sparing of any layer (Furtado et al, 2013). Toxoplasmic retinochoroiditis appears on SD-OCT scans as an area of thickened hyper-reflective homogeneously disrupted retina, overlaying a thickened and hypo-reflective choroid (Figure 2D) (Goldenberg et al, 2013). Subretinal fluid has been reported in about half of patients with active toxoplamic retinochoroiditis (Figure 2H) (Ouyang et al, 2015). The presence of fluid underneath the retina in association with an area of necrotizing retinitis could hence suggest the toxoplasmic etiology. A thickening and melting of the RPE has been reported virtually in all patients affected by acute toxoplasmic retinochoroiditis. However, a similar appearance has also been

noted in a certain percentage of viral necrotizing retinitis. Similarly, the presence of intraretinal fluid has been reported both in toxoplasmic retinochoroiditis (Ouyang et al, 2014) and in viral retinitis (Invernizzi et al, 2018a).

4.12 End-stage changes – thinning

Some inflammatory changes of the retina, such as the presence of cystoid macular edema or subretinal fluid, usually regress without scarring. However, occlusive retinal vasculitis, choriocapillaris infarcts and necrotizing retinitis almost invariably result in a persistent damage of the retina with loss of cells and thinning of the involved retinal layers (Invernizzi et al, 2019).

Both toxoplasmic and viral infections of the retina are full thickness necrotizing processes that leave a thinned hyper-reflective tissue in the area of the scar. Toxoplasmic lesions typically evolve in thinned areas of retina overlaying a thinned and disrupted choroid (Figure 2F) (Goldenberg et al, 2013). Viral retinitis by contrast, do not affect the choroid, usually scarring with a thin disrupted retina overlaying a normal looking choroid. CMV retinitis may lead to a scar formation when the RPE is involved in the necrotizing process or evolve in the formation of outer retinal lacunae and retinal detachment when the RPE and choroid are spared (Figure 13C) (Invernizzi et al, 2017b).

Focal infarcts of the retinal nerve fiber layer are common findings in many retinal diseases characterized by occlusive microangiopathy including uveitis associated with HIV or Behçet disease (Tugal-Tutkun, 2012). These lesions, visible on OCT scans as hyper-reflective thickening of the inner retina, disappear with time and leave a focal thinning of the inner retinal layers (Gomez et al., 2009). A similar but more

extensive thinning of the retina with loss of inner layers is seen on OCT in the late stages of occlusive vasculitis (Invernizzi et al, 2019). The thinning of the inner retina is not pathognomonic of any uveitic entity but this finding invariably suggests that the damage derives from a previous occlusive event involving the retinal vasculature.

The outer retinal layers and the RPE are mainly supplied by the choriocapillaris. Mechanical or inflammatory impairment of the choroidal/choriocapillaris blood flow may consequently result in outer retinal ischemia ultimately leading to loss of cells and thinning.

Focal round-shaped areas of RPE and outer retinal layers thinning are found in late stage uveitis characterized by choriocapillaris hypo-perfusion such as APMPPE (Invernizzi et al, 2016) or VKH disease (Aggarwal et al, 2018). An amoeboid pattern of scarring is more suggestive for serpiginous choroidopathy or serpiginous-like tuberculosis (Nazari Khanamiri and Rao, 2013).

Loss of outer retinal layers integrity has been associated with functional damage in many diseases including uveitis. A diffuse thinning of the outer retinal layers has been reported in long standing birdshot chorioretinopathy (Figure 6A) (Symes et al, 2015). Similarly, diffuse loss of the outer retinal structures associated with RPE changes has been reported in autoimmune retinopathies (Sepah et al, 2015). Although not pathognomonic of any specific disease, diffuse alterations of the outer retinal layers along with a compatible clinical picture should rise the suspect of one of these rare entities.

5. CHOROIDAL OCT SIGNS IN POSTERIOR UVEITIS

44

5.1 Choriocapillaris inflammatory changes

APMPPE is characterized in its active stage by the presence of multiple areas of choriocapillaris non perfusion. These foci are visible on indocyanine green angiography as areas of decreased fluorescence (Figure 10) (Invernizzi et al, 2016). Similar alterations of the choriocapillaris perfusion characterize the active edges of serpiginous choroiditis lesions, active serpiginous like tubercular lesions (Nazari Khanamiri and Rao, 2013) and sometimes active VKH disease (Aggarwal et al, 2018).

Inflamed, hypo-perfused choriocapillaris appears on enhanced depth imaging optical coherence tomography (EDI-OCT) as an area of decreased reflectivity just underneath the RPE, with thickening and loss of the physiological dotted pattern (Figure 10C) (Invernizzi et al, 2016). These lesions may resolve without scarring or lead to choriocapillaris loss accompanied by RPE and outer retinal atrophy. A normal looking outer retina overlying the affected choriocapillaris during the active stage predicts a good outcome without scarring, while the presence of hyper-reflective changes disrupting the outer retinal layers are a negative prognostic sign that often precedes the atrophic evolution (Figure 9D) (Invernizzi et al, 2016).

While the differential diagnosis between APMPPE, serpiginous choroiditis, VKH and serpiginous-like choroiditis requires a multimodal imaging approach and some systemic work-up, OCT findings allow to identify the choriocapillaris involvement, to follow the lesions overtime and most importantly to predict their evolution.

5.2 Choroidal thickening

5.2.1 Diffuse

As discussed in section 4.1 VKH is a condition characterized by choroidal granulomatous infiltration with secondary retinal effects. The choroidal thickening associated with the disease has been well reported with reports of mean choroidal thickness between 424 microns up to 805 microns (Herbort et al, 2007, Maruko et al, 2011). SD-OCT has allowed us to characterize the nature of this thickening secondary to massive infiltration of the choroidal space with inflammatory cells (Figure 8B) (Gupta et al, 2009). So thickened, in fact, that the RPE above is pushed into undulations (Figure 8D) on top of which are the small dots of compromised RPE through which fluid can leak into the sub-retinal space.

Fong et al (2011) have proposed that the tissue pressure from acute infiltration of inflammatory cells and granuloma is enough to compress the pre-capillary arterioles and venules in Sattler's layer. This is visible on OCT as a loss of the small hyper-reflective dots of the inner choroid, as these vessels become non-perfused. These dots are then observed to return in the convalescent phase but to be now fewer in number due to possible choroidal stromal scarring and overall thinning. The thinning of the choroid on OCT is a good diagnostic sign of recovery under treatment but may take months to occur fully (Jaisankar et al, 2017).

5.2.2 Localized

Some choroidal inflammatory conditions, such as serpiginous choroiditis, produce much more localized changes in the choroid. This is a rare, usually bilateral chronic inflammatory disease which is recurrent, poorly responsive to treatment and commonly complicated by choroidal neovascular membrane formation (Laatikainen

and Erkkila, 1974; Laatikainen and Erkkila, 1981). It classically starts in the peri-papillary region with greyish areas of chorioretinitis spreading centrifugally in a pseudopodal fashion. There are variants now known to be restricted to the macular, to spread like APMPPE (ampiginous) or to be related to tuberculosis (Lim et al, 2005).

Although the mainstay of diagnosis remains angiography, OCT has proven to show an interesting finding of localized choroidal thickening and elevation of the RPE in the area under an active lesion (Moorthy et al, 2016, Rifkin et al, 2014). When seen, this could act as a further contributing sign of the acute nature of any flare and should prompt treatment adjustment.

5.3 Choroidal granulomas

Choroidal granulomas are nodular collections of immune cells formed within the choroid to confine pathogens and inflammatory agents that cannot be eliminated. They can be found in few infectious and autoimmune uveitis either secondary to a systemic granulomatous disease or to a pathologic condition primarily affecting the eye (Invernizzi et al, 2015b).

Choroidal granulomas appear on OCT scans as round-shaped hypo-reflective structures contained within the choroidal stroma. Their size may vary with some lesions occupying the thickness of the choroid and the smaller ones almost invariably located in the inner choroid. Regardless their size, shape, margins an internal pattern, choroidal granulomas always generate an increased transmission effect on the OCT signal that allows a better visualization of the tissues underneath the lesion

(Figure 14) This feature allows to distinguish the granulomas from other choroidal structures with a similar appearance like large choroidal vessels (Invernizzi et al, 2015b).

The identification of choroidal granulomas allows to limit the differentials to a small number of diseases mainly including ocular tuberculosis (Gupta et al, 2007), non-tubercular mycobacteriosis (Invernizzi et al, 2018c), sarcoid (Bonfioli and Orefice, 2005) and VKH disease (Damico et al, 2005). Choroidal granulomas show common features regardless the underlying disease that allow to distinguish them from other choroidal lesions. Granulomas with lobulated margins and non-homogenous content seem to suggest tubercular etiology (Invernizzi et al, 2015b).

Optical coherence tomography allows the clinician to follow the granulomas over time and to demonstrate their response to treatment (Invernizzi et al, 2015a; Invernizzi et al, 2018c). In a study comparing different imaging modalities in the follow-up of choroidal granulomas, EDI-OCT resulted more sensitive in detecting early decrease in size of the lesions in response to treatment compared to indocyanine green angiography (Invernizzi et al, 2017a).

5.4 Choroidal changes in Toxoplasmosis

Toxoplasma gondii infection of the posterior segment of the eye consists of a retinochoroiditis (Butler et al, 2013). The parasites actively attack both the retina and the choroid at the same time and choroidal foci can be found either combined or far away from the areas or retinitis (Atmaca et al, 2006). During the active stages of the disease the choroid shows focal thickening and loss of the physiological architecture,

becoming homogeneously hypo-reflective (Figure 2D, Figure 2H) (Goldenberg et al, 2013). These feature allow to distinguish the toxoplasmic foci of necrotizing retinitis from those with a viral etiology that show a normal looking choroid (Figure 13A and 13B) (Invernizzi et al, 2018a). The focal thickening is also a peculiar feature that characterizes the toxoplasmic etiology and allows to differentiate it from other diseases that show a diffuse thickening and disruption of the choroidal architecture such as acute VKH disease (Figure 8B) (Nakayama et al, 2012).

The choroidal thickening progressively disappears with treatment and thickness changes can be used to monitor the progression of the disease. When the acute inflammation is resolved and the disease has been controlled the affected areas turn into a chorioretinal scar with a disrupted and thinner choroid overlaid by a thin hyperreflective retina (Goldenberg et al, 2013).

5.5 Birdshot lesions

Birdshot chorioretinopathy reveals typical findings on OCT. A symmetric central CME, an ERM and a chorioretinal atrophy visible as thinning of the choroid and retina with concomitant loss of the outer retinal hyperreflective bands is characteristic on OCT (Cunningham et al, 2017; Pohlmann et al, 2017). The fovea is usually spared until very late in the course of the disease. Conventional OCT will follow later stage changes such as retinal and choroidal thinning, CME formation and ERM. Choroidal thickness continuously decreases over the course of the disease and is significantly thinner in insufficiently treated late stage birdshot patients, compared to adequately treated patients (Skvortsova et al., 2017). It can be therefore used as long term follow up parameter in conjunction with other parameters such as visual field loss and

ERG. But also, earlier changes attributed to birdshot chorioretinopathy may be captured using OCT. Optic nerve head swelling and periphlebitis may be visualized using the retinal thickness maps of OCT volume scans placed on the ONH and the vascular arcades. Perivascular and ONH retinal thickening will be appreciable, which corresponds to vascular leakage on FA as discussed previously (Figure 6B and 6C) (Knickelbein et al, 2018; Tian et al, 2018). Although conventional B-scans are unable to illustrate the characteristic Birdshot lesions, OCT-angiography and, in particular, swept source (SS) wide field OCT-angiography is suited to illustrate and follow respective birdshot lesions (Pepple et al 2018). These imaging modalities give more insight into disease progression and disease stage than conventional imaging with ICG and CF. Birdshot lesions will present as attenuated (flow) signal in the choroidal OCT-A wide field slabs, corresponding to the hypofluorescent lesions visible on ICG (Figure 6E and 6F). They are located adjacent to the large vessels of the Haller layer. In acute onset patients these lesions of flow voids can be found in the deep choroidal slabs, however there will be very little attenuated flow signal in the choriocapillaris (Figure 6G), illustrating the acute onset of the disease with involvement of the deeper choroid but sparing of the choriocapillaris (Pepple et al, 2018). In chronic disease full thickness choroidal flow attenuation can be seen. Treatment response may be followed as well. In case of acute onset disease and adequate treatment, choroidal flow void will regress, while in chronic stages treatment initiation will not induce a decrease of flow void on the SS-OCT-A wide field scans (Pepple et al, 2018). Beside these characteristic changes on choroidal wide field SS-OCT-A, retinal OCT-A demonstrates chronic changes such as capillary loops more frequently in the DCP than in the SCP, telangiectasia, sparse capillaries and reduced vessel density of the SCP and DCP (Pohlmann et al, 2017; Roberts et al, 2018).

50

5.6 Suprachoroidal fluid

Previous papers described an association between suprachoroidal fluid, visible as hyporeflective suprachoroidal line on EDI OCTs and disease activity in birdshot patients (Keane et al, 2013; Birnbaum et al, 2014). However, a subsequent paper by Yiu et al (2014) found 44.6% of the evaluated healthy eyes exhibited such a layer, with an association suggested to hyperopic refractive error not inflammation. Further this line of supra-choroidal fluid may be more frequently visible in the presence of chorioretinal atrophy and is no longer considered an indication of disease activity in birdshot chorioretinopathy.

Future Directions

The field of medical imaging and, in particular, ocular retinal imaging is undergoing a revolution due to the advent of artificial intelligence (AI) and deep learning algorithms (Ting et al, 2019). The current focus is on the most common retinal disorders of diabetic retinopathy and age-related macular degeneration (Schmidt-Erfurth et al, 2019). However, OCT as shown herein, has the potential to identify imaging diagnostic signs of uveitic disease and, with increased ubiquity of OCT technology, may allow patients to be monitored for their uveitis burden in 'virtual' clinics or even at home.

By accurately recording and characterizing such diagnostic signs now it may be possible to apply deep learning AI algorithms to uveitis patients, even those with rare diseases where a large initial training data set is not available. Another way the rather limited number of available training data sets can be addressed in the future, may be

generative adversarial networks. These generative networks can synthesize new, artificial images, which cannot be differentiated from real images of diseased patients.

De Fauw et al (2018) successfully showed a two-step process with separate segmentation and classification algorithms to delineate ten medical retina, non-uveitic, pathological features such as drusen or macula holes. When this automatic segmentation of the OCT data improves to the point of easily distinguishing the choriocapillaris, ellipsoid zone, ELM and other layers then it may be possible to look for the characteristic pattern associated with, e.g. APMPPE as described above. Anticipating such improvements means a future focus on reviewing the rarer signs in neoplastic, vascular, degenerative and genetic retinal conditions. Finally, the field of retinal imaging advances constantly so there is a need to review what these newest techniques and modalities can instruct us about the uveitic entities described herein.

53

Acknowledgements

References

• Abdelhakim, A., Rasoo, I.N., 2018. Neuroretinitis: a review. Curr. Opin. Ophthalmol. 29, 514-519. doi: 10.1097/ICU.0000000000000527.

• Abu El-Asrar, A.M., Herbort, C.P., Tabbara, K.F., 2005. Retinal vasculitis. Ocul. Immunol. Inflamm. 13, 415-433. https://doi.org/10.1080/09273940591003828

• Adam, C.R., Sigler, E.J., 2014. Multimodal imaging findings in endogenous Aspergillus endophthalmitis. Retina. 34, 1914-1915. doi:10.1097/IAE.0000000000000135.

• Agarwal, A., Invernizzi, A., Singh, R.B., Foulsham, W., Aggarwal, K., Handa, S., Agrawal, R., Pavesio, C., Gupta, V., 2018a. An update on inflammatory choroidal neovascularization: epidemiology, multimodal imaging, and management. J. Ophthalmic Inflamm. Infect. 8, 13. doi: 10.1186/s12348-018-0155-6.

• Agarwal, A., Pichi, F., Invernizzi, A., Gupta, V., 2018b. Disease of the year: differential diagnosis of uveitic macular edema. Ocul. Immunol. Inflamm. 27, 72-88. doi: 10.1080/09273948.2018.1523437.

• Aggarwal, K., Agarwal, A., Katoch, D., Sharma, M., Gupta, V., 2017. Optical coherence tomography angiography features of acute macular neuroretinopathy in dengue fever. Indian J. Ophthalmol. 65, 1235-1238. doi:10.4103/ijo.IJO_485_17.

• Aggarwal, K., Agarwal, A., Mahajan, S., Invernizzi, A., Mandadi, S.K.R., Singh, R., Bansal, R., Dogra, M.R., Gupta, V., OCTA Study Group,. 2018. The role of optical coherence tomography angiography in the diagnosis and management of acute Vogt-Koyanagi-Harada disease. Ocul. Immunol. Inflamm. 26, 142-153. doi:

10.1080/09273948.2016.1195001.

• Akanda, M., Gangaputra, S., Kodati, S., Melamud, A., Sen, H.N., 2018. Multimodal imaging in dengue-fever-associated maculopathy. Ocul. Immunol. Inflamm. 26, 671-676. doi: 10.1080/09273948.2017.1351571.

• Arai, R., Kimura, I., Imamura, Y., Shinoda, K., Matsumoto, C.S., Seki, K., Ishida, M., Murakami, A., Mizota, A., 2014. Photoreceptor inner and outer segment layer thickness in multiple evanescent white dot syndrome. Graefes Arch. Clin. Exp. Ophthalmol. 252, 1645-1651. doi: 10.1007/s00417-014-2747-7.

• Aranda, S., Amer, R., 2015. Sequential spontaneous resolution of acute syphilitic posterior placoid chorioretinitis. Eur. J. Ophthalmol. 25, 263–265. doi: 10.5301/ejo.5000530

• Armstrong, B.K., Pitcher, J., Shah, R., Brady, C., Perlmutter, D., Garg, S.J., 2014. The evolution of untreated acute syphilitic posterior placoid chorioretinitis captured by multimodal retinal imaging. Ophthalmic Surg. Lasers Imaging Retina. 45, 606–609. doi: 10.3928/23258160-20141008-02.

• Astroz, P., Miere, A., Mrejen, S., Sekfali, R., Souied, E.H., Jung, C., Nghiem-Buffet, S., Cohen, S.Y., 2018. Optical coherence tomography angiography to distinguish choroidal neovascularization from macular inflammatory lesions in multifocal choroiditis. Retina. 38, 299-309. doi: 10.1097/IAE.0000000000001617

• Atmaca, L.S., Simsek, T., Atmaca Sonmez, P., Sonmez, K., 2006. Fluorescein and indocyanine green angiography in ocular toxoplasmosis. Graefes Arch. Clin. Exp. Ophthalmol. 244, 1688-1691. https://doi.org/10.1007/s00417-006-0345-z

• Baek, J., Kim, K.S., Lee, W.K., 2016. Natural course of untreated acute syphilitic posterior placoid chorioretinitis. Clin. Exp. Ophthalmol. 44, 431-433. doi:

10.1111/ceo.12679

• Baek, J., Park, Y.H., 2015. Optical density ratio in the subretinal fluid: differentiating chronic central serous chorioretinopathy and polypoidal choroidal vasculopathy. Am. J. Ophthalmol. 159, 386–392. doi:10.1016/j.ajo.2014.11.011

• Barnes, A.C., Lowder, C.Y., Bessette, A.P., Baynes, K., Srivastava, S.K.

, 2018. Treatment of acute zonal occult outer retinopathy with intravitreal steroids. Ophthalmic Surg. Lasers Imaging Retina. 49, 504-509. doi:10.3928/23258160-20180628-06

• Barry, R.J., Tasiopoulou, A., Murray, P.I., Patel, P.J., Sagoo, M.S., Denniston, A.K., Keane, P.A., 2018. Characteristic optical coherence tomography findings in patients with primary vitreoretinal lymphoma: a novel aid to early diagnosis. Br. J. Ophthalmol. 102, 1362-1366. doi: 10.1136/bjophthalmol-2017-311612

• Baumuller, S., Holz, F.G., 2012. Early spectral-domain optical coherence tomography findings in acute macular neuroretinopathy. Retina. 32, 409-410. doi:

10.1097/IAE.0b013e31822f573a

• Bhavsar, K.V., Lin, S., Rahimy, E., Joseph, A., Freund, K.B., Sarraf, D., Cunningham, E.T. Jr., 2016. Acute macular neuroretinopathy: A comprehensive review of the literature. Surv. Ophthalmol. 61, 538-565. doi: 10.1016/j.survophthal.2016.03.003

• Birnbaum, A.D., Fawzi, A.A., Rademaker, A., Goldstein, D.A., 2014. Correlation between clinical signs and optical coherence tomography with enhanced depth imaging findings in patients with birdshot chorioretinopathy. JAMA. Ophthalmol. 132, 929-935. doi: 10.1001/jamaophthalmol.2014.877.

• Blain, J.G., Riley, W., Logothetis, J., 1965. Optic nerve manifestations of sarcoidosis. Arch. Neurol. 13, 307-309. https://doi.org/10.1001/archneur.1965.00470030087008

• Bonfioli, A.A., Orefice, F., 2005. Sarcoidosis. Semin. Ophthalmol. 20, 177-182. https://doi.org/10.1080/08820530500231938

• Bos, P. J., Deutman A.F., 1975. Acute macular neuroretinopathy. Am. J. Ophthalmol. 80, 573-584. PMID: 1180301

• Bottin, C., Grieve, K., Rossant, F., Pedinielli, A., Mrejen, S., Paques, M., 2018. Directional variability of fundus reflectance in acute macular neuroretinopathy: Evidence for a contribution of the Stiles-Crawford effect. Retin. Cases Brief Rep. 12, Suppl 1, S19-S24. doi: 10.1097/ICB.0000000000000701.

• Boudreault K.A., Schuerch, K., Zhao, J., Lee, W., Cabral, T., Yannuzzi, L.A., Tsang, S.H., Sparrow, J.R., 2017. Quantitative autofluorescence intensities in acute zonal occult outer retinopathy vs healthy eyes. JAMA. Ophthalmol. 135, 1330-1338. doi:

10.1001/jamaophthalmol.2017.4499.

• Brinkman, C.J., Rothova, A., 1993. Fundus pathology in neurosarcoidosis. Int. Ophthalmol. 17, 23-26. https://doi.org/10.1007/BF00918863

• Brito, P., Penas, S., Carneiro, A., Palmares, J., Reis, F.F., 2011. Spectral-domain optical coherence tomography features of acute syphilitic posterior placoid chorioretinitis: the role of autoimmune response in pathogenesis. Case Rep. Ophthalmol. 2, 39–44. doi: 10.1159/000324086

• Butler, N.J., Furtado, J.M., Winthrop, K.L., Smith, J.R., 2013. Ocular toxoplasmosis II: clinical features, pathology and management. Clin. Exp Ophthalmol. 41, 95-108. doi: 10.1111/j.1442-9071.2012.02838.x.

• Carreras, E., Salomão, D.R., Nadal, J., Amin, S.R., Raja, H., Grube, T.J., Geraets, R.L., Johnston, P.B., O'Neill, B.P., Pulido, J.S., 2017. Macular edema is a rare finding in untreated vitreoretinal lymphoma: small case series and review of the literature. Int. J. Retina Vitreous. 24, 15. doi:10.1186/s40942-017-0067-x.

• Casalino, G., Arrigo, A., Romano, F., Munk, M.R., Bandello, F., Parodi, M.B., 2018. Acute macular neuroretinopathy: pathogenetic insights from optical coherence tomography angiography. Br. J. Ophthalmol. 103, 410-414. doi:

10.1136/bjophthalmol-2018-312197.

• Castellano, C.G., 2009. Retinal thickening in iridocyclitis. Am. J. Ophthalmol. 148, 341-349. https://doi.org/10.1016/j.ajo.2009.03.034

• Chan, C.C., Sen, H.N., 2013. Current concepts in diagnosing and managing primary vitreoretinal (intraocular) lymphoma. Discov. Med. 15, 93-100.

• Chang, A.A., Zhu, M., Billson, F., 2005. The interaction of indocyanine green with human retinal pigment epithelium. Invest. Ophthalmol. Vis. Sci. 46, 1463-1467

• Chen, D., Martidis, A., Baumal, C.R., 2002. Transient multifocal electroretinogram dysfunction in multiple evanescent white dot syndrome. Ophthalmic Surg. Lasers. 33, 246-249.

• Chen, J, Lee, L., 2008. Posterior placoid chorioretinitis: an unusual ocular manifestation of syphilis. Clin. Ophthalmol. 2, 669–673.

• Chen, S. N., Hwang, J.F., 2013. Ocular coherence tomographic and clinical characteristics in patients of punctuate inner choroidopathy associated with zonal outer retinopathy. Ocul. Immunol. Inflamm. 22, 263-269. doi:10.3109/09273948.2013.844264.

• Chen, S.N., Hwang, J.F., 2009. The outer and inner retinal function in patients with multiple evanescent white dot syndrome. Clin. Exp. Ophthalmol. 37, 478-484. doi:10.3109/09273948.2013.844264.

• Cho, H., Pillai, P., Nicholson, L., Sobrin, L., 2016. Inflammatory papillitis in uveitis: response to treatment and use of optic nerve optical coherence tomography for monitoring. Ocul. Immunol. Inflamm. 24, 194-206. https://doi.org/10.3109/09273948.2014.991041

• Cho, H.J., Han, S.Y., Cho, S.W., Lee, D.W., Lee, T.G., Kim, C.G., Kim, J.W., 2014. Acute retinal pigment epitheliitis: spectral-domain optical coherence tomography findings in 18 cases. Invest. Ophthalmol. Vis. Sci. 55, 3314-3319. https://doi.org/10.1167/iovs.14-14324

• Chu, C.J., Herrmann, P., Carvalho, L.S., Liyanage, S.E., Bainbridge, J.W., Ali, R.R., Dick, A.D., Luhmann, U.F., 2013. Assessment and in vivo scoring of murine experimental autoimmune uveoretinitis using optical coherence tomography. PLoS. One. 8, :e63002. https://doi.org/10.1371/journal.pone.0063002

• Chu, S., Nesper, P.L., Soetikno, B.T., Bakri, S.J., Fawzi, A.A., 2018. Projection-resolved OCT angiography of microvascular changes in paracentral acute middle maculopathy and acute macular neuroretinopathy. Invest. Ophthalmol. Vis. Sci. 59, 2913-2922. doi: 10.1167/iovs.18-24112.

• Cohen, L.M., Munk, M.R., Goldstein, D.A., Jampol, L.M. 2015. Acute, posterior multifocal placoid pigment epitheliopathy: a case of 11 recurrences over 15 years. Retin. Cases Brief Rep. 9, 226-230. doi: 10.1097/ICB.0000000000000145.

• Coscas, G., Cunha-Vaz, J., Soubrane, G., 2017. Macular edema: definition and basic Concepts. Dev. Ophthalmol. 58, 1-10. doi: 10.1159/000455264.

• Cunningham, E.T., Eandi, C.M., Pichi, F., 2014. Syphilitic uveitis. Ocul. Immunol. Inflamm. 22, 2-3. doi: 10.3109/09273948.2014.883236.

• Cunningham, E.T., Zierhut, M., 2018. Uveitic macular edema. Ocul. Immunol. Inflamm. 26, 987-990.

• Cunningham, E.T., Levinson, R.D., Denniston, A.K., Brézin, A.P., Zierhut, M., 2017. Birdshot chorioretinopathy. Ocul. Immunol. Inflamm. 25, 589-593. doi:10.1080/09273948.2017.1400800.

• da Silva, F.T., Sakata, V.M., Nakashima, A., Hirata, C.E., Olivalves, E., Takahashi, W.Y., Costa, R.A., Yamamoto, J.H., 2013. Enhanced depth imaging optical coherence tomography in long-standing Vogt-Koyanagi-Harada disease. Br. J. Ophthalmol. 97, 70–74. doi: 10.1136/bjophthalmol-2012-302089.

• Damico, F.M., Kiss, S., Young, L.H., 2005. Vogt-Koyanagi-Harada disease. Semin. Ophthalmol. 20, 183-190.

• Daruich, A., Matet, A., Moulin, A., Kowalczuk, L., Nicolas, M., Sellam, A., Rothschild, P.R., Omri, S., Gélizé, E., Jonet, L., Delaunay, K., De Kozak, Y., Berdugo, M., Zhao, M., Crisanti, P., Behar-Cohen F., 2018. Mechanisms of macular edema: Beyond the surface. Prog. Retin. Eye Res. 63, 20-68. doi: 10.1016/j.preteyeres.2017.10.006.

• Davis, J.L., Madow, B., Cornett, J., Stratton, R., Hess, D., Porciatti, V., Feuer, W.J., 2010. Scale for photographic grading of vitreous haze in uveitis. Am. J. Ophthalmol. 150, 637-641. https://doi.org/10.1016/j.ajo.2010.05.036

• De Fauw, J., Ledsam, J.R., Romera-Paredes, B., Nikolov, S., Tomasev, N., Blackwell, S., Askham, H., Glorot, X., O'Donoghue, B., Visentin, D., van den Driessche, G., Lakshminarayanan, B., Meyer, C., Mackinder, F., Bouton, S., Ayoub, K., Chopra, R., King, D., Karthikesalingam, A., Hughes, C.O., Raine, R., Hughes, J., Sim, D.A., Egan, C., Tufail, A., Montgomery, H., Hassabis, D., Rees, G., Back, T., Khaw, P.T., Suleyman, M., Cornebise, J., Keane, P.A., Ronneberger, O., 2018. Clinically applicable deep learning for diagnosis and referral in retinal disease. Nat. Med. 24, 1342-1350. https://doi.org/10.1038/s41591-018-0107-6

• de Souza, E.C., Jalkh, A.E., Trempe, C.L., Cunha, S., Schepens, C.L., 1988. Unusual central chorioretinitis as the first manifestation of early secondary syphilis. Am. J. Ophthalmol. 105, 271–276.

• Deák, G.G., Goldstein, D.A., Zhou, M., Fawzi, A.A., Jampol, L.M., 2018. Vertical hyperreflective lesions on optical coherence tomography in vitreoretinal lymphoma. JAMA. Ophthalmol. 137, 194-198. doi:10.1001/jamaophthalmol.2018.5835

• Denniston, A.K., Keane, P.A., 2015. Paravascular pathways in the eye: is there an 'ocular glymphatic system'? Invest. Ophthalmol. Vis. Sci. 56, 3955-3956. https://doi.org/10.1167/iovs.15-17243

• Denniston, A.K., Dick, A.D., 2013. Systemic therapies for inflammatory eye disease: past, present and future. BMC. Ophthalmol. 13, 18. https://doi.org/10.1186/1471-2415-13-18

• Deutman, A.F., 1974. Acute retinal pigment epitheliitis. Am. J. Ophthalmol. 78, 571-578. https://doi.org/10.1016/S0002-9394(14)76292-0

• Din, N.M., Taylor, S.R., Isa, H., Tomkins-Netzer, O., Bar, A., Talat, L., Lightman, S., 2014. Evaluation of retinal nerve fiber layer thickness in eyes with hypertensive uveitis. JAMA. Ophthalmol. 132, 859-865. https://doi.org/10.1001/jamaophthalmol.2014.404

• Dolz-Marco, R., Abreu-González, R., Alonso-Plasencia, M., Gallego-Pinazo, R., 2014. Treatment decisions in diabetic macular edema based on optical coherence tomography retinal thickness map: LET classification. Graefes Arch. Clin.. Exp. Ophthalmol. 252, 1687-1688. https://doi.org/10.1007/s00417-014-2699-y

• Eandi, C.M., Neri, P., Adelman, R.A., Yannuzzi, L.A., Cunningham, E.T. Jr; International Syphilis Study Group, 2012. Acute syphilitic posterior placoid chorioretinitis: report of a case series and comprehensive review of the literature. Retina. 32, 1915–1941.

• Eckstein, C., Saidha, S., Sotirchos, E.S., Byraiah, G., Seigo, M., Stankiewicz, A., Syc, S.B., Ford, E., Sharma, S., Calabresi, P.A., Pardo, C.A., 2012. Detection of clinical and subclinical retinal abnormalities in neurosarcoidosis with optical coherence tomography. J. Neurol. 259, 1390-1398. https://doi.org/10.1007/s00415-011-6363-8

• Errera, M.H., Coisy, S., Fardeau, C., Sahel, J.A., Kallel, S., Westcott, M., Bodaghi, B., Paques, M., 2014. Retinal vasculitis imaging by adaptive optics. Ophthalmology. 121, 1311-1312. https://doi.org/10.1016/j.ophtha.2013.12.036

• Fardeau, C., Champion, E., Massamba, N., LeHoang, P., 2016. Uveitic macular edema. Eye. 30, 1277-1292. doi: 10.1016/j.jfo.2014.09.001.

• Fawzi, A.A., Pappuru, R.R., Sarraf, D., Le, P.P., McCannel, C.A., Sobrin, L., Goldstein, D.A., Honowitz, S., Walsh, A.C., Sadda, S.R., Jampol, L.M., Eliott, D., 2012. Acute macular neuroretinopathy: long-term insights revealed by multimodal imaging. Retina 32, 1500-1513.

• Finger, M. L., Borruat, F.X., 2014. Dynamics of intraretinal fluid accumulation evidenced by SD-OCT in a case of cat scratch neuroretinitis. Eye. 28, 770-771. doi: 10.1038/eye.2014.44.

• Fong, A.H., Li, K.K., Wong, D., 2011. Choroidal evaluation using enhanced depth imaging spectral-domain optical coherence tomography in Vogt-Koyanagi-Harada disease. Retina. 31, 502-509. https://doi.org/10.1097/IAE.0b013e3182083beb

• Forrester, J.V., 1991. Uveitis: pathogenesis. Lancet. 338, 1498-1501. https://doi.org/10.1016/0140-6736(91)92309-P

• Franco, M., Nogueira, V., 2016. Severe acute syphilitic posterior placoid chorioretinitis with complete spontaneous resolution: The natural course. GMS. Ophthalmol. Cases. 16, 6. doi: 10.3205/oc000039.

• Freund, K.B., Mrejen, S., Jung, J., Yannuzzi, L.A., Boon, C.J., 2013. Increased fundus autofluorescence related to outer retinal disruption. JAMA. Ophthalmol. 131, 1645-1649. doi: 10.1001/jamaophthalmol.2013.5030.

• Fujiwara, T., Imamura, Y., Giovinazzo, V.J., Spaide, R.F., 2010. Fundus autofluorescence and optical coherence tomographic findings in acute zonal occult outer retinopathy. Retina 30, 1206-1216. doi: 10.1097/IAE.0b013e3181e097f0.

• Furtado, J.M., Ashander, L.M., Mohs, K., Chipps, T.J., Appukuttan, B., Smith, J.R., 2013. Toxoplasma gondii migration within and infection of human retina. PloS. ONE. 8, e54358. doi: 10.1371/journal.pone.0054358.

• Gallagher, M.J., Yilmaz, T., Cervantes-Castañeda, R.A., Foster, C.S., 2007. The characteristic features of optical coherence tomography in posterior uveitis. Br. J. Ophthalmol. 91, 1680-1685.

• Gass, J.D., Braunstein, R.A., Chenoweth, R.G., 1990. Acute syphilitic posterior placoid chorioretinitis. Ophthalmology. 97,1288–1297.

• Gass, J.D., 1993. Acute zonal occult outer retinopathy: Donders Lecture: The Netherlands Ophthalmological Society, Maastricht, Holland, June 19, 1992. Retina. 23, 79-97.

• Gass, J.D., Agarwal, A., Scott, I.U., 2002. Acute zonal occult outer retinopathy: a long-term follow-up study. Am. J. Ophthalmol. 134, 329-339.

• Gass, J.D.M., Olson, C.L., 1976. Sarcoidosis with optic nerve and retinal involvement. Arch. Ophthalmol. 94, 945-950. https://doi.org/10.1001/archopht.1976.03910030475008

• Goldberg, N.R., Jabs, D.A., Busingye, J., 2016. Optical coherence tomography imaging of presumed sarcoid retinal and optic nerve nodules. Ocul. Immunol. Inflamm. 24, 293-296. https://doi.org/10.3109/09273948.2014.971972

• Goldenberg, D., Goldstein, M., Loewenstein, A., Habot-Wilner, Z., 2013. Vitreal, retinal, and choroidal findings in active and scarred toxoplasmosis lesions: a prospective

study by spectral-domain optical coherence tomography. Graefes Arch. Clin. Exp. Ophthalmol. 251, 2037-2045. doi: 10.1007/s00417-013-2334-3.

• Goldenberg, D., Habot-Wilner, Z., Loewenstein, A., Goldstein, M., 2012. Spectral domain optical coherence tomography classification of acute posterior multifocal placoid pigment epitheliopathy. Retina. 32, 1403-1410. doi:10.1097/IAE.0b013e318234cafc.

• Gomez, M.L., Mojana, F., Bartsch, D.U., Freeman, W.R., 2009. Imaging of long-term retinal damage after resolved cotton wool spots. Ophthalmology. 116, 2407-2414. doi: 10.1016/j.ophtha.2009.05.012.

• Grewal, D.S., O'Sullivan, M.L., Kron, M., Jaffe, G.J., 2017. Association of disorganization of retinal inner layers with visual acuity in eyes with uveitic cystoid macular edema. Am. J. Ophthalmol. 177, 116-125. doi: 10.1016/j.ajo.2017.02.017.

• Grimm, S.A., Pulido, J.S., Jahnke, K., Schiff, D., Hall, A.J., Shenkier, T.N., Siegal, T.,Doolittle, N.D., Batchelor, T., Herrlinger, U., Neuwelt, E.A., Laperriere, N., Chamberlain, M.C., Blay, J.Y., Ferreri, A.J., Omuro, A.M., Thiel, E., Abrey, L.E., 2007. Primary intraocular lymphoma: an International Primary Central Nervous System Lymphoma Collaborative Group Report. Ann. Oncol. 18, 1851-1855. https://doi.org/10.1093/annonc/mdm340

• Gross, N.E., Yannuzzi, L.A., Freund, K.B., Spaide, R.F., Amato, G.P., Sigal, R., 2006. Multiple evanescent white dot syndrome. Arch. Ophthalmol. 124, 493-500. https://doi.org/10.1001/archopht.124.4.493

• Guagnini, A.P., De Potter, P., Levecq, L., Kozyreff, A., 2007. Atypical spherical deposition on vitreoretinal interface associated with toxoplasmic chorioretinitis. Graefes Arch. Clin. Exp. Ophthalmol. 245, 158-60. https://doi.org/10.1007/s00417-006-0330-6

• Gupta, V., Gupta, A., Rao, N.A., 2007. Intraocular tuberculosis--an update. Surv Ophthalmol. 52, 561-87. https://doi.org/10.1016/j.survophthal.2007.08.015

• Gupta, V., Gupta, A., Gupta, P., Sharma, A., 2009. Spectral domain cirrus optical coherence tomography of choroidal striations seen in the acute stage of Vogt-Koyanagi-Harada disease. Int. Ophthalmol. 31, 9-13. https://doi.org/10.1016/j.ajo.2008.07.028

• Habot-Wilner, Z., Zur, D., Goldstein, M., Goldenberg, D., Shulman, S., Kesler, A., Giladi, M., Neudorfer, M., 2011. Macular findings on optical coherence tomography in cat-scratch disease neuroretinitis. Eye. 25, 1064-1068. https://doi.org/10.1038/eye.2011.125

• Hashimoto, H., Kishi, S., 2015. Ultra-wide-field fundus autofluorescence in multiple evanescent white dot syndrome. Am. J. Ophthalmol. 159, 698-706. doi:

10.1016/j.ajo.2015.01.015.

• Hashimoto, Y., Saito, W., Saito, M., Hirooka, K., Mori, S., Noda, K., Ishida, S., 2015. Decreased choroidal blood flow velocity in the pathogenesis of multiple evanescent white dot syndrome. Graefes Arch. Clin. Exp. Ophthalmol. 253, 1457-1464. doi:10.1007/s00417-014-2831-z.

• Hashizume, K., Imamura, Y., Fujiwara, T., Machida, S., Ishida, M., Kurosaka, D., 2016. Retinal pigment epithelium undulations in acute stage of Vogt-Koyanagi-Harada disease: biomarker for functional outcomes after high-dose steroid therapy. Retina. 36, 415–421. doi: 10.1097/IAE.0000000000000728.

• Hecht, I., Bar, A., Rokach, L., Noy Achiron, R., Munk, M.R., Huf, W., Burgansky-Eliash, Z., Achiron, A., 2018. Optical coherence tomography biomarkers to distinguish diabetic macular edema from pseudophakic cystoid macular edema using machine learning algorithms. Retina. Oct 3. doi: 10.1097/IAE.0000000000002342. [Epub ahead of print]

• Hee, M.R., Puliafito, C.A., Wong, C., Duker, J.S., Reichel, E., Rutledge, B., Schuman, J.S., Swanson, E.A., Fujimoto, J.G., 1995. Quantitative assessment of macular edema with optical coherence tomography. Arch. Ophthalmol. 113, 1019-1029.
doi:10.1001/archopht.1995.01100080071031

- Heiferman, M.J., Rahmani, S., Jampol, L.M., Nesper, P.L., Skondra, D., Kim, L.A., Fawzi, A.A., 2017. Acute posterior multifocal placoid pigment epitheliopathy on optical coherence tomography angiography. Retina. 37, 2084-2094. doi:10.1097/IAE.0000000000001487.

- Herbort, C.P., Mantovani, A., Bouchenaki, N., 2007. Indocyanine green angiography in Vogt-Koyanagi-Harada disease: angiographic signs and utility in patient follow-up. Int. Ophthalmol. 27, 173-182. https://doi.org/10.1007/s10792-007-9060-y

- Hickman, S.J., Quhill, F., Pepper, I.M., 2016. The evolution of an optic nerve head granuloma due to sarcoidosis. Neuroophthalmology. 40, 59-68. https://doi.org/10.3109/01658107.2015.1134587

- Hoang, Q.V., Cunningham, E.T. Jr, Sorenson, J.A., Freund, K.B., 2013. The "pitchfork sign" a distinctive optical coherence tomography finding in inflammatory choroidal neovascularization. Retina. 33, 1049-1055. doi:10.1097/IAE.0b013e31827e25b8.

- Holz, F.G., Kim, R.Y., Schwartz, S.D., Harper, C.A., Wroblewski, J., Arden, G.B., Bird, A.C., 1994. Acute zonal occult outer retinopathy (AZOOR) associated with multifocal choroidopathy. Eye. 8, 77-83.

- Hornbeak, D.M., Payal, A., Pistilli, M., Biswas, J., Ganesh, S.K., Gupta, V., Rathinam, S.R., Davis, J.L., Kempen, J.H., 2014. Interobserver agreement in clinical grading of vitreous haze using alternative grading scales. Ophthalmology. 121, 1643-1648. https://doi.org/10.1016/j.ophtha.2014.02.018

- Hosoda, Y., Uji, A., Hangai, M., Morooka, S., Nishijima, K., Yoshimura, N., 2014. Relationship between retinal lesions and inward choroidal bulging in Vogt-Koyanagi-Harada disease. Am. J. Ophthalmol. 157, 1056–1063. doi: 10.1016/j.ajo.2014.01.015.

• Hsu, J., Fineman, M.S., Kaiser, R.S., 2007. Optical coherence tomography findings in acute retinal pigment epitheliitis. Am. J. Ophthalmol. 143, 163-165. https://doi.org/10.1016/j.ajo.2006.07.052

• Ingestad, R., Sigmar, G., 1971. Sarcoidosis with ocular hypothalamic pituitary manifestations. Acta Ophthalmologica. 49, 1-10. https://doi.org/10.1111/j.1755-3768.1971.tb08227.x

• Invernizzi, A., Franzetti, F., Viola, F., Meroni, L., Staurenghi, G., 2015a. Optic nerve head tubercular granuloma successfully treated with anti-VEGF intravitreal injections in addition to systemic therapy. Eur. J. Ophthalmol. 25, 270-272. doi:10.5301/ejo.5000528.

• Invernizzi, A., Mapelli, C., Viola, F., Cigada, M., Cimino, L., Ratiglia, R., Staurenghi, G., Gupta, A., 2015b. Choroidal granulomas visualized by enhanced depth imaging optical coherence tomography. Retina. 35, 525-531. doi:10.1097/IAE.0000000000000312.

• Invernizzi, A., Agarwal, A., Cozzi, M., Viola, F., Nguyen, Q.D., Staurenghi, G., 2016. Enhanced depth imaging optical coherence tomography features in areas of choriocapillaris hypoperfusion. Retina. 36, 2013-2021. doi:10.1097/IAE.0000000000001031.

• Invernizzi, A., Agarwal, A., Mapelli, C., Nguyen, Q.D., Staurenghi, G., Viola, F., 2017a. Longitudinal follow-up of choroidal granulomas using enhanced depth imaging optical coherence tomography. Retina. 37, 144-153. doi:10.1097/IAE.0000000000001128.

• Invernizzi, A., Agarwal, A., Ravera, V., Oldani, M., Staurenghi, G., Viola, F., 2017b. Optical coherence tomography findings in cytomegalovirus retinitis: A longitudinal study. Retina. 38, 108-117. doi: 10.1097/IAE.0000000000001503.

• Invernizzi, A., Symes, R., Miserocchi, E., Cozzi, M., Cereda, M., Fogliato, G., Staurenghi, G., Cimino, L., McCluskey, P., 2017c. Spectral domain optical coherence

tomography findings in endogenous candida endophthalmitis and their clinical relevance. Retina. 38, 1011-1018. doi: 10.1097/IAE.0000000000001630.

• Invernizzi, A., Agarwal, A.K., Ravera, V., Mapelli, C., Riva, A., Staurenghi, G., McCluskey, P.J., Viola, F., 2018a. Comparing optical coherence tomography findings in different aetiologies of infectious necrotising retinitis. Br. J. Ophthalmol. 102, 433-437. doi: 10.1136/bjophthalmol-2017-310210.

• Invernizzi, A., Cozzi, M., Symes, R., Pellegrini, M., Staurenghi, G.,

2018b. Ocular neovascularization in endogenous candida endophthalmitis: Using multimodal imaging to understand different pathogenic pathways. Retina. 38, e17-e19. doi: 10.1097/IAE.0000000000001978.

• Invernizzi, A., Ricaboni, D., Franzetti, M., Staurenghi, G., McCluskey, P., Franzetti, F., 2018c. Bilateral choroiditis as the only sign of persistent Mycobacterium intracellulare infection following haematogenous spread in an immunocompromised patient. Infection. 46, 423-426. doi: 10.1007/s15010-017-1109-x.

• Invernizzi, A., Cozzi, M., Staurenghi, G., 2019. Optical coherence tomography and optical coherence tomography angiography in uveitis: A review. Clin. Exp. Ophthalmol. 47, 357-371. doi: 10.1111/ceo.13470. Epub 2019 Mar 3.

• Ishihara, K., Hangai, M., Kita, M., Yoshimura, N., 2009. Acute Vogt- Koyanagi-Harada disease in enhanced spectral-domain optical coherence tomography. Ophthalmology. 116, 1799-807. doi: 10.1016/j.ophtha.2009.04.002.

• Iu, L.P.L., Lee, R., Fan, M.C.Y., Lam, W.C., Chang, R.T., Wong, I.Y.H., 2017. Serial spectral-domain optical coherence tomography findings in acute retinal pigment epitheliitis and the correlation to visual acuity. Ophthalmology. 124, 903-909 https://doi.org/10.1016/j.ophtha.2017.01.043

• Jabs, D.A., Johns, C.J., 1986. Ocular involvement in chronic sarcoidosis. Am. J. Ophthalmol. 102, 297-301. https://doi.org/10.1016/0002-9394(86)90001-2

• Jabs, D.A., Nussenblatt, R.B., Rosenbaum, J.T., Standardization of Uveitis Nomenclature (SUN) Working Group., 2005. Standardization of uveitis nomenclature for reporting clinical data. Results of the First International Workshop. Am. J. Ophthalmol. 140, 509-516. https://doi.org/10.1016/j.ajo.2005.03.057

• Jaisankar, D., Raman, R., Sharma, H.R., Khandelwal, N., Bhende, M., Agrawal, R., Sridharan, S., Biswas, J., 2017. Choroidal and retinal anatomical responses following systemic corticosteroid therapy in Vogt-Koyanagi-Harada disease using swept-source optical coherence tomography. Ocul. Immunol. Inflamm. 12, 1-9. https://doi.org/10.1080/09273948.2017.1332231

• Jampol, L.M., Sieving, P.A., Pugh, D., Fishman, G.A., Gilbert, H., 1984. Multiple evanescent white dot syndrome. I. Clinical findings. Arch. Ophthalmol. 102, 671-674. doi:10.1001/archopht.1984.01040030527008

• Jones, N.P., 2013. The Manchester Uveitis Clinic: the first 3000 patients - epidemiology and casemix. Ocul. Immunol. Inflamm. 23, 118-126. https://doi.org/10.3109/09273948.2013.855799

• Joseph, A., Rogers, S., Browning, A., Hall, N., Barber, C., Lotery, A., Foley, E., Amoaku, W.M., 2007. Syphilitic acute posterior placoid chorioretinitis in nonimmuno-compromised patients. Eye. 21, 1114–1119. https://doi.org/10.1038/sj.eye.6702504

• Joseph, A., Rogers, S., Browning, A., Hall, N., Barber, C., Lotery, A., Foley, E., Amoaku, W.M., 2013. Fundus autofluorescence and photoreceptor bleaching in multiple evanescent white dot syndrome. Ophthalmic Surg. Lasers Imaging Retina. 44, 588-592. https://doi.org/10.3928/23258160-20131105-08

- Jung, J.J., Khan, S., Mrejen, S., Gallego-Pinazo, R., Cunningham, E.T. Jr, Freund, K.B., Jampol, L.M., Yannuzzi, L.A., 2013. Idiopathic multifocal choroiditis with outer retinal or chorioretinal atrophy. Retina. 34, 1439-1450. doi:10.1097/IAE.0000000000000079.

- Karampelas, M., Sim, D.A., Chu, C., Carreno, E., Keane, P.A., Zarranz-Ventura, J., Westcott, M., Lee, R.W., Pavesio, C.E., 2015. Quantitative analysis of peripheral vasculitis, ischemia, and vascular leakage in uveitis using ultra-widefield fluorescein angiography. Am. J. Ophthalmol. 159, 1161-1168. https://doi.org/10.1016/j.ajo.2015.02.009

- Kato, Y., Yamamoto, Y., Tabuchi, H., Fukushima, A., 2013. Retinal pigment epithelium folds as a diagnostic finding of Vogt-Koyanagi-Harada disease. Jpn. J. Ophthalmol. 57, 90-4. doi: 10.1007/s10384-012-0212-x.

- Keane, P.A., Allie, M., Turner, S.J., Southworth, H.S., Sadda, S.R., Murray, P.I., Denniston, A.K., 2013. Characterization of birdshot chorioretinopathy using extramacular enhanced depth optical coherence tomography. JAMA. Ophthalmol. 131, 341-350. doi:10.1001/jamaophthalmol.2013.1724.

- Keane, P.A., Karampelas, M., Sim, D.A., Sadda, S.R., Tufail, A., Sen, H.N., Nussenblatt, R.B., Dick, A.D., Lee, R.W., Murray, P.I., Pavesio, C.E., Denniston, A.K., 2014. Objective measurement of vitreous inflammation using optical coherence tomography. Ophthalmology. 121, 1706-1714. https://doi.org/10.1016/j.ophtha.2014.03.006

- Keane, P.A., Balaskas, K., Sim, D.A., Aman, K., Denniston, A.K., Aslam, T., For The Equator Study Group., 2015. Automated analysis of vitreous inflammation using spectral-domain optical coherence tomography. Trans. Vis. Sci. Technol. 4, 4. https://doi.org/10.1167/tvst.4.5.4

- Kempen, J.H., Van Natta, M.L., Altaweel, M.M., Dunn, J.P., Jabs, D.A., Lightman, S.L., Thorne, J.E., Holbrook, J.T., Multicenter Uveitis Steroid Treatment (MUST) Trial Research Group., 2015. Factors predicting visual acuity outcome in intermediate, posterior

and panuveitis: the Multicenter Uveitis Steroid Treatment (MUST) Trial. Am. J. Ophthalmol. 160, 1133-1141. https://doi.org/10.1016/j.ajo.2015.09.017

• Kimura, S.J., Thygeson, P., Hogan, M.J.,1959. Signs and symptoms of uveitis, II: classification of the posterior manifestations of uveitis. Am. J. Ophthalmol. 47, 171-176. https://doi.org/10.1016/S0002-9394(14)78240-6

• Kiss, S., Damico, F.M., Young, L.H., 2005. Ocular manifestations and treatment of syphilis. Semin. Ophthalmol. 20, 161–167.

• Knickelbein, J.E., Tucker, W., Kodati, S., Akanda, M., Sen, H.N., 2018. Non-invasive method of monitoring retinal vasculitis in patients with birdshot chorioretinopathy using optical coherence tomography. Br. J. Ophthalmol. 102, 815-820. doi:10.1136/bjophthalmol-2016-309837.

• Kramer, M., Priel, E., 2013. Fundus autofluorescence imaging in multifocal choroiditis: Beyond the spots. Ocul. Immunol. Inflamm. 22, 349-355. doi:10.3109/09273948.2013.855797.

• Krill, A.E., Deutman, A.F., 1972. Acute retinal pigment epitheliitis. Am. J. Ophthalmol. 74, 193-205. https://doi.org/10.1016/0002-9394(72)90535-1

• Kulikov, A.N., Maltsev, D.S., Leongardt, T.A., 2018. Retinal microvasculature alteration in paracentral acute middle maculopathy and acute macular neuroretinopathy: A quantitative optical coherence tomography angiography study. Retin. Cases Brief Rep. 13. doi: 10.1097/ICB.0000000000000709.

• Kurup, S.P., Khan, S., Gill, M.K., 2014. Spectral domain optical coherence tomography in the evaluation and management of infectious retinitis. Retina. 34, 2233-2241. doi: 10.1097/IAE.0000000000000218.

• Laatikainen, L., Erkkila, H., 1974. Serpiginous Choroiditis. Br. J. Ophthalmol. 58, 777-783. http://dx.doi.org/10.1136/bjo.58.9.77

• Laaitkainen, L., Erkkila, H., 1981. A follow-up study on serpiginous choroiditis. Acta Ophthalmol. 59, 707-718. https://doi.org/10.1111/j.1755-3768.1981.tb08737.x

• Lardenoye, C.W., van Kooij, B., Rothova, A., 2006. Impact of macular edema on visual acuity in uveitis. Ophthalmology. 113, 1446-1449.

• Lau, C.H., Missotten, T., Salzmann, J., Lightman, S.L., 2007. Acute retinal necrosis features, management, and outcomes. Ophthalmology. 114, 756-62

• Lee, S.Y., Cheng, J.L., Gehrs, K.M., Folk, J.C., Sohn, E.H., Russell, S.R., Guo, Z., Abràmoff, M.D., Han, I.C., 2017. Choroidal features of acute macular neuroretinopathy via optical coherence tomography angiography and correlation with serial multimodal imaging. JAMA. Ophthalmol. 135, 1177-1183. doi:10.1001/jamaophthalmol.2017.3790.

• Levison, A.L., Baynes, K.M., Lowder, C.Y., Kaiser, P.K., Srivastava, S.K., 2017. Choroidal neovascularisation on optical coherence tomography angiography in punctate inner choroidopathy and multifocal choroiditis. Br. J. Ophthalmol. 101, 616-622. doi: 10.1136/bjophthalmol-2016-308806.

• Li, M., Zhang, X., Ji, Y., Ye, B., Wen, F., 2015. Acute macular neuroretinopathy in dengue fever: Short-term prospectively followed up case series. JAMA. Ophthalmol. 133, 1329-1333. doi: 10.1001/jamaophthalmol.2015.2687.

• Lim, W.K., Buggage, R.R., Nussenblatt, R.B., 2005. Serpiginous choroiditis. Surv. Ophthalmol. 50, 231-244. https://doi.org/10.1016/j.survophthal.2005.02.010

• Lin, D., Luo, X., Meng, L., Zhang, G., Chen, W., Chen, H., 2016. Optical intensities of different compartments of subretinal fluid in acute Vogt-Koyanagi-Harada disease. PLoS. ONE. 11, e0149376. doi: 10.1371/journal.pone.0149376.

• Lingappan, A., Wykoff, C.C., Albini, T.A., Miller, D., Pathengay, A., Davis, J.L., Flynn, H.W. Jr,. 2012. Endogenous fungal endophthalmitis: causative organisms, management

strategies, and visual acuity outcomes. Am. J. Ophthalmol. 1153, 162-166.e1. doi: 10.1016/j.ajo.2011.06.020.

• Liu, X.Y., Peng, X.Y., Wang, S., You, Q..S, Li, Y.B., Xiao, Y.Y., Jonas, J.B.,

2016. Features of optical coherence tomography for the diagnosis of Vogt-Koyanagi-Harada disease. Retina. 36, 2116-2123. https://doi.org/10.1097/IAE.0000000000001076

• Lowder, C.Y., Belfort, R.Jr, Lightman, S., Foster, C.S., Robinson, M.R., Schiffman, R.M., Li, X.Y., Cui, H., Whitcup, S.M., Ozurdex HURON Study Group, 2011. Dexamethasone intravitreal implant for non-infectious intermediate or posterior uveitis. Arch. Ophthalmol. 129, 545-553. https://doi.org/10.1001/archophthalmol.2010.339

• Luttrull, J.K., Chittum, M.E., 1995. Acute retinal pigment epitheliitis. Am. J. Ophthalmol. 120, 389-391. https://doi.org/10.1016/S0002-9394(14)72171-3

• Mahendradas, P., Avadhani, K., Madhavarao, B., Vinekar, A., Sahana, K., Shetty, R., Shetty, B.K., 2013. High definition spectral domain optical coherence tomography of retinal pigment epithelial rip in a case of sympathetic ophthalmia. J. Ophthalmic Inflamm. Infect. 3, 19. doi: 10.1186/1869-5760-3-19.

• Mangeon, M., Zett, C., Amaral, C., Novais, E., Muccioli, C., Andrade, G., Nascimento, H., Belfort, R.Jr., 2018. Multimodal evaluation of patients with acute posterior multifocal placoid pigment epitheliopathy and serpiginous choroiditis. Ocul. Immunol. Inflamm. 26, 1212-1218. doi: 10.1080/09273948.2017.1335757.

• Mapelli, C., Invernizzi, A., Barteselli, G., Pellegrini, M., Tabacchi, E., Staurenghi, G., Viola, F., 2016. Multimodal imaging of vitreoretinal lymphoma. Ophthalmologica. 36, 166-174. https://doi.org/10.1159/000447412

• Markomichelakis, N.N., Halkiadakis, I., Pantelia, E., Peponis, V., Patelis, A.,

Theodossiadis, P., Theodossiadis, G., 2004. Patterns of macular edema in patients with uveitis: qualitative and quantitative assessment using optical coherence tomography. Ophthalmology. 111, 946-953. https://doi.org/10.1016/j.ophtha.2003.08.037

• Maruko, I., Iida, T., Sugano, Y., Oyamada, H., Sekiryu, T., Fujiwara, T., Spaide, R.F., 2011. Subfoveal choroidal thickness after treatment of Vogt-Koyanagi-Harada disease. Retina. 31, 510-517. https://doi.org/10.1097/IAE.0b013e3181eef053

• Maruyama, Y., Kishi, S., 2004. Tomographic features of serous retinal detachment in Vogt-Koyanagi-Harada syndrome. Ophthalmic Surg Lasers Imaging. 35(3):239–42. PMID: 15185793

• Matsui, Y., Matsubara, H., Ueno, S., Ito, Y., Terasaki, H., Kondo, M., 2014.

Changes in outer retinal microstructures during six month period in eyes with acute zonal occult outer retinopathy-complex. PLoS. ONE. 9, e110592. doi:10.1371/journal.pone.0110592.

• Mehkri, M., Jayadev, C., Dave, N., Vinekar, A., 2015. Spectral domain optical coherence tomography in the diagnosis and monitoring of dengue maculopathy. Indian J. Ophthalmol. 2015 63, 342-343. doi: 10.4103/0301-4738.158087.

• Meira-Freitas, D., Farah, M.E., Höfling-Lima, A.L., Aggio, F.B., 2009. Optical coherence tomography and indocyanine green angiography findings in acute syphilitic posterior placoid choroidopathy: case report. Arq. Bras. Oftalmol. 72, 832–835. http://dx.doi.org/10.1590/S0004-27492009000600019

• Moore, D.B., Jaffe, G.J., Asrani, S., 2015. Retinal nerve fiber layer thickness measurements: uveitis, a major confounding factor. Ophthalmology. 122, 511-517. https://doi.org/10.1016/j.ophtha.2014.09.008

- Moorthy, R.S., Zierhut, M., 2016. Serpiginous choroiditis, in: Zierhut, M., Pavesio, C., Ohno, S., Orefice, F., Rao, N.A., (Eds), Intraocular Inflammation. Springer-Verlag, Berlin Heidelberg. pp. 1021-1032.

- Moorthy, R.S., Moorthy, M.S., Cunningham, E.T. Jr, 2018. Drug-induced uveitis. Curr. Opin. Ophthalmol. 29, 588-603. doi: 10.1097/ICU.0000000000000530.

- Morgan, C.M., Webb, R.M., O'Connor, G.R., 1984. Atypical syphilitic chorioretinitis and vasculitis. Retina. 4, 225–231.

- Mrejen, S., Khan, S., Gallego-Pinazo, R., Jampol, L.M., Yannuzzi, L.A., 2014. Acute zonal occult outer retinopathy: a classification based on multimodal imaging. JAMA. Ophthalmol. 132, 1089-1098. doi: 10.1001/jamaophthalmol.2014.1683.

- Munk, M.R., Kiss, C.G., Steiner, I., Sulzbacher, F., Roberts, P., Kroh, M., Montuoro, A., Simader, C., Schmidt-Erfurth, U., 2013a. Systematic correlation of morphologic alterations and retinal function in eyes with uveitis-associated cystoid macular oedema during development, resolution and relapse. Br. J. Ophthalmol. 97, 1289-1296. doi: 10.1136/bjophthalmol-2012-303052.

- Munk, M.R., Bolz, M., Huf, W., Sulzbacher, F., Roberts, P., Simader, C., Rückert, R., Kiss, C.G., 2013b. Morphologic and functional evaluations during development, resolution, and relapse of uveitis-associated cystoid macular edema. Retina. 33, 1673-1683. doi: 10.1097/IAE.0b013e318285cc52.

- Munk, M.R., Sacu, S., Huf, W., Sulzbacher, F., Mittermüller, T.J., Eibenberger, K., Rezar, S., Bolz, M., Kiss, C.G., Simader, C., Schmidt-Erfurth, U., 2014. Differential diagnosis of macular edema of different pathophysiologic origins by spectral domain optical coherence tomography. Retina. 34, 2218-2232 .doi:10.1097/IAE.0000000000000228.

- Munk, M.R., Jung, J.J., Biggee, K., Tucker, W.R., Sen, H.N., Schmidt-Erfurth, U., Fawzi, A.A., Jampol, L.M., 2015a. Idiopathic multifocal choroiditis/punctate inner

choroidopathy with acute photoreceptor loss or dysfunction out of proportion to clinically visible lesions. Retina. 35, 334-343. doi: 10.1097/IAE.0000000000000370.

• Munk, M.R., Jampol, L.M., Simader, C., Huf, W., Mittermüller, T.J., Jaffe, G.J., Schmidt-Erfurth, U., 2015b. Differentiation of diabetic macular edema from pseudophakic cystoid macular edema by spectral-domain optical coherence tomography. Invest. Ophthalmol. Vis. Sci. 56, 6724-6733. doi: 10.1167/iovs.15-17042.

• Munk, M.R., Jampol, L.M., Cunha Souza, E., de Andrade, G.C., Esmaili, D.D., Sarraf, D., Fawzi, A.A., 2016. New associations of classic acute macular neuroretinopathy. Br. J. Ophthalmol. 100, 389-394. doi:10.1136/bjophthalmol-2015-306845.

• Munk, M.R., Beck, M., Kolb, S., Larsen, M., Hamann, S., Valmaggia, C., Zinkernagel, M.S., 2017. Quantification of retinal layer thickness changes in acute macular neuroretinopathy. Br. J. Ophthalmol. 101, 160-165. doi:10.1136/bjophthalmol-2016-308367.

• Nakao, K., Ohba, N., 1996. HTLV-I associated uveitis revisited: characteristic grey-white, granular deposits on retinal vessels. Br. J. Ophthalmol. 80, 719-722. https://doi.org/10.1136/bjo.80.8.719

• Nakao, K., Ohba, N., Uemura, A., Okubo, A., Sameshima, M., Hayami, K., 1998. Gray-white, spherical deposition on retinal vessel associated with acute retinal necrosis and diabetic retinopathy in HTLV-I carriers. Jpn. J. Ophthalmol. 42, 490-494.

• Nakayama, M., Keino, H., Okada, A.A., Watanabe, T., Taki, W., Inoue, M., Hirakata, A., 2012. Enhanced depth imaging optical coherence tomography of the choroid in Vogt-Koyanagi-Harada disease. Retina. 32, 2061-2069. doi:10.1097/IAE.0b013e318256205a.

• Nazari, H, Rao, NA, 2012. Resolution of subretinal fluid with systemic corticosteroid treatment in acute Vogt-Koyanagi-Harada disease. Br. J. Ophthalmol. 96, 1410–1414. https://doi.org/10.1136/bjophthalmol-2012-301857

• Nazari Khanamiri, H., Rao, N.A., 2013. Serpiginous choroiditis and infectious multifocal serpiginoid choroiditis. Surv. Ophthalmol. 58, 203-232. https://doi.org/10.1016/j.survophthal.2012.08.008

• Nemiroff, J., Sarraf, D., Davila, J.P., Rodger, D., 2018. Optical coherence tomography angiography of acute macular neuroretinopathy reveals deep capillary ischemia. Retin. Cases Brief Rep. 12, 1:S12-S15. doi:10.1097/ICB.0000000000000706.

• Niederer, R.L., Gilbert, R., Lightman, S.L., Tomkins-Netzer, O., 2018. Risk factors for developing choroidal neovascular membrane and visual loss in punctate inner choroidopathy. Ophthalmology. 125, 288-294. doi:10.1016/j.ophtha.2017.09.002.

• Nussenblatt, R.B., Palestine, A.G., Chan, C.C., Roberge, F., 1985. Standardization of vitreal inflammatory activity in intermediate and posterior uveitis. Ophthalmology. 92, 467-471. https://doi.org/10.1016/S0161-6420(85)34001-0

• Oray, M., Onal, S., Bayraktar, S., Izgi, B., Tugal-Tutkun, I., 2015. Nonglaucomatous localized retinal nerve fiber layer defects in Behçet uveitis. Am. J. Ophthalmol. 159, 475–481. doi: 10.1016/j.ajo.2014.11.029.

• Ossewaarde-van Norel, J., Berg, E.M., Sijssens, K.M., Rothova A., 2011. Subfoveal serous retinal detachment in patients with uveitic macular edema. Arch Ophthalmol 129(2): 158-162. doi: 10.1001/archophthalmol.2010.337.

• Ossewaarde-van Norel, A., Rothova, A., 2012. Imaging methods for inflammatory macular edema. Int. Ophthalmol. Clin. 52, 55-66. https://doi.org/10.1097/IIO.0b013e318266bf14

• Ou, W.C., Brown, D.M., Payne, J.F., Wykoff, C.C., 2017. Relationship between visual acuity and retinal thickness during anti-vascular endothelial growth factor therapy for retinal diseases. Am. J. Ophthalmol. 180, 8-17. doi:10.1016/j.ajo.2017.05.014.

77

• Ouyang, Y., Pleyer, U., Shao, Q., Keane, P.A., Stübiger, N., Joussen, A.M., Sadda, S.R., Heussen, F.M., 2014. Evaluation of cystoid change phenotypes in ocular toxoplasmosis using optical coherence tomography. PloS. ONE. 9, e86626. doi:10.1371/journal.pone.0086626.

• Ouyang, Y., Li, F., Shao, Q., Heussen, F.M., Keane, P.A., Stübiger, N., Sadda, S.R., Pleyer, U., 2015. Subretinal fluid in eyes with active ocular toxoplasmosis observed using spectral domain optical coherence tomography. PloS. ONE. 10, e0127683. doi:10.1371/journal.pone.0127683.

• Parc, C., Guenoun, J.M., Dhote, R., Brézin, A., 2005. Optical coherence tomography in the acute and chronic phases of Vogt-Koyanagi-Harada disease. Ocul. Immunol. Inflamm. 13, 225–227. https://doi.org/10.1080/09273940490912416

• Pearce, W.A., Yeh, S., Fine, H.F., 2016. Management of cytomegalovirus retinitis in HIV and non-HIV patients. Ophthalmic Surg. Lasers Imaging Retina. 47, 103-107. doi: 10.3928/23258160-20160126-01.

• Pelosini, L., Hull, C.C., Boyce, J.F., McHugh, D., Stanford, M.R., Marshall, J., 2011. Optical coherence tomography may be used to predict visual acuity in patients with macular edema. Invest. Ophthalmol. Vis. Sci. 52, 2741-2748. doi:10.1167/iovs.09-4493.

• Pepple, K.L., Chu, Z., Weinstein, J., Munk, M.R., Van Gelder, R.N., Wang, R.K., 2018. Use of en face swept-source optical coherence tomography angiography in identifying choroidal flow voids in 3 patients with birdshot chorioretinopathy. JAMA. Ophthalmol. 136, 1288-1292. doi: 10.1001/jamaophthalmol.2018.3474.

• Philiponnet, A., Vardanian, C., Malcles, A., Pochat, C., Sallit, R., Kodjikian, L., 2017. Detection of mild papilloedema in posterior uveitis using spectral domain optical coherence tomography. Br. J. Ophthalmol. 101, 401-405. https://doi.org/10.1136/bjophthalmol-2016-309155

• Pichi, F., Ciardella, A.P., Cunningham, E.T. Jr, Morara, M., Veronese, C., Jumper, J.M., Albini, T.A., Sarraf, D., McCannel, C., Voleti, V., Choudhry, N., Bertelli, E., Giuliari, G.P., Souied, E., Amer, R., Regine, F., Ricci, F., Neri, P., Nucci, P., 2014. Spectral domain optical coherence tomography findings in patients with acute syphilitic posterior placoid chorioretinopathy. Retina. 34, 373-384. doi:10.1097/IAE.0b013e3182993f11.

• Pichi, F., Srvivastava, S.K., Chexal, S., Lembo, A., Lima, L.H., Neri, P., Saitta, A., Chhablani, J., Albini, T.A., Nucci, P., Freund, K.B., Chung, H., Lowder, C.Y., Sarraf, D., 2016. En face optical coherence tomography and optical coherence tomography angiography of multiple evanescent white dot syndrome: New insights into Pathogenesis. Retina. 36, 1:S178-S188. doi: 10.1097/IAE.0000000000001255.

• Pichi, F., Sarraf, D., Morara, M., Mazumdar, S., Neri, P., Gupta, V., 2017a. Pearls and pitfalls of optical coherence tomography angiography in the multimodal evaluation of uveitis. J. Ophthalmic. Inflamm. Infect. 7, 20. doi:10.1186/s12348-017-0138-z.

• Pichi, F., Fragiotta, S., Freund, K.B., Au, A., Lembo, A., Nucci, P., Sebastiani, S., Gutierrez Hernandez, J.C., Interlandi, E., Pellegrini, F., Dolz-Marco, R., Gallego-Pinazo, R., Orellana-Rios, J., Adatia, F.A., Munro, M., Abboud, E.B., Ghazi, N., Cunha Souza, E., Amer, R., Neri, P., Sarraf, D., 2018b. Cilioretinal artery hypoperfusion and its association with paracentral acute middle maculopathy. Br. J. Ophthalmol. 2. pii: bjophthalmol-2018-312774. doi: 10.1136/bjophthalmol-2018-312774.

• Pohlmann, D., Macedo, S., Stübiger, N., Pleyer, U., Joussen, A.M., Winterhalter, S., 2017. Multimodal imaging in birdshot retinochoroiditis. Ocul. Immunol. Inflamm. 25, 621-632. doi: 10.1080/09273948.2017.1375532.

• Qian, C.X., Wang, A., DeMill, D.L., Jayasundera, T., Branham, K., Abalem, M.F., Khan, N., Heckenlively, J.R., 2017. Prevalence of antiretinal antibodies in acute zonal occult

outer retinopathy: A comprehensive review of 25 Cases. Am. J. Ophthalmol. 176, 210-218. doi: 10.1016/j.ajo.2016.12.001.

• Rao, N.A., Hidayat, A.A., 2001. Endogenous mycotic endophthalmitis: variations in clinical and histopathologic changes in candidiasis compared with aspergillosis. Am. J. Ophthalmol. 132, 244-251. https://doi.org/10.1016/S0002-9394(01)00968-0

• Reddy, S., Cunningham, E.T. Jr, Spaide, R.F., 2006. Syphilitic retinitis with focal inflammatory accumulations. Ophthalmic Surg. Lasers Imaging Retina. 37, 429 –431.

• Rifkin, L.M., Munk, M.R., Baddar, D., Goldstein, D.A., 2015. A new OCT finding in tuberculous serpiginous-like choroidopathy. Ocul. Immunol. Inflamm. 23, 53-58. https://doi.org/10.3109/09273948.2014.964421

• Roberts, P.K., Nesper, P.L., Onishi, A.C., Skondra, D., Jampol, L.M., Fawzi, A.A., 2018. Characterizing photoreceptor changes in acute posterior multifocal placoid pigment epitheliopathy using adaptive optics. Retina. 38, 39-48. doi: 10.1097/IAE.0000000000001520.

• Roberts, P.K., Nesper, P.L., Goldstein, D.A., Fawzi, A.A., 2018. Retinal capillary density in patients with birdshot chorioretinopathy. Retina. 38(2): 387-394. doi:10.1097/IAE.0000000000001543.

• Roy, R., Saurabh, K., Bansal, A., Kumar, A., Majumdar, A.K., Paul, S.S., 2017. Inflammatory choroidal neovascularization in Indian eyes: Etiology, clinical features, and outcomes to anti-vascular endothelial growth factor. Indian J. Ophthalmol. 65, 295-300. doi: 10.4103/ijo.IJO_262_16.

• Saito, A., Saito, W., Furudate, N., Ohno, S. 2007. Indocyanine green angiography in a case of punctate inner choroidopathy associated with acute zonal occult outer retinopathy. Jpn. J. Ophthalmol. 51, 295-300. https://doi.org/10.1007/s10384-007-0451-4

- Saito, M., Barbazetto, I.A., Spaide, R.F., 2013. Intravitreal cellular infiltrate imaged as punctate spots by spectral-domain optical coherence tomography in eyes with posterior segment inflammatory disease. Retina. 33, 559-565. https://doi.org/10.1097/IAE.0b013e31826710ea

- Sallam, A., Lynn, W., McCluskey, P., Lightman, S., 2006. Endogenous Candida endophthalmitis. Expert Rev. Anti. Infect. Ther. 4, 675-685. https://doi.org/10.1586/14787210.4.4.675

- Samson, C.M., Foster, C.S., 2001. Syphilis, in: Foster, C.S., Vitale, A.T., (Eds), Diagnosis and treatment of uveitis. WB Saunders, Philadelphia, PA: pp 237- 243

- Scarinci, F., Fawzi, A.A., Shaarawy, A., Simonett, J.M., Jampol, L.M., 2017. Longitudinal quantitative evaluation of outer retinal lesions in acute posterior multifocal placoid pigment epitheliopathy using optical coherence tomography. Retina. 37, 851-857. doi: 10.1097/IAE.0000000000001245.

- Schlegl, T., Waldstein, S.M., Bogunovic, H., Endstraßer, F., Sadeghipour, A., Philip, A.M., Podkowinski, D., Gerendas, B.S., Langs, G., Schmidt-Erfurth, U., 2018. Fully automated detection and quantification of macular fluid in OCT using deep learning. Ophthalmology 125, 549-558. doi: 10.1016/j.ophtha.2017.10.031.

- Schmidt-Erfurth, U., Sadeghipour, A., Gerendas, B.S., Waldstein, S.M., Bogunović, H., 2018. Artificial intelligence in retina. Prog. Retin. Eye Res. 67, 1-29. https://doi.org/10.1016/j.preteyeres.2018.07.004

- Sepah, Y.J., Sadiq, M.A., Hassan, M., Hanout, M., Soliman, M., Agarwal, A., Afridi, R., Coupland, S.G., Nguyen, Q.D., 2015. Assessment of retinal structural and functional characteristics in eyes with autoimmune retinopathy. Curr. Mol. Med. 15, 578-586. https://doi.org/10.2174/1566524015666150731104626

• Shahlaee, A., Hong, B., Sridhar, J., Mehta, S., 2015. Multimodal imaging in multiple evanescent white dot syndrome. Ophthalmology. 122, 1836. doi:10.1016/j.ophtha.2015.06.044.

• Shifera, A.S., Pennesi, M.E., Yang, P., Lin, P., 2017. Ultra-wide-field fundus autofluorescence findings in patients with acute zonal occult outer retinopathy. Retina. 37, 1104-1119. doi: 10.1097/IAE.0000000000001311.

• Sikorski, B.L., Wojtkowski, M., Kaluzny, J.J., Szkulmowski, M., Kowalczyk, A., 2008. Correlation of spectral optical coherence tomography with fluorescein and indocyanine green angiography in multiple evanescent white dot syndrome. Br. J. Ophthalmol. 92, 1552-1557. doi: 10.1136/bjo.2007.135863.

• Sivadasan, A., Alexander, M., Mathew, V., Mani, S., Patil, A.K., 2013. Radiological evolution and delayed resolution of an optic nerve tuberculoma: Challenges in diagnosis and treatment. Ann. Indian Acad. Neurol. 16, 114-117. https://doi.org/10.4103/0972-2327.107722

• Slakter, J.S., Giovannini, A., Yannuzzi, L.A., Scassellati-Sforzolini, B., Guyer, D.R., Sorenson, J.A., Spaide, R.F., Orlock, D., 1997. Indocyanine green angiography of multifocal choroiditis. Ophthalmology. 104, 1813-1819. https://doi.org/10.1016/S0161-6420(97)30022-0

• Smith, J.R., Cunningham, E.T. Jr, 2002. Atypical presentations of ocular toxoplasmosis. Curr. Opin. Ophthalmol. 13, 387-392. PMID: 12441842

• Spaide, R.F., Koizumi, H., Freund, K.B., 2008. Photoreceptor outer segment abnormalities as a cause of blind spot enlargement in acute zonal occult outer retinopathy-complex diseases. Am. J. Ophthalmol. 146, 111-120. doi:10.1016/j.ajo.2008.02.027.

• Spaide, R.F., Goldberg, N., Freund, K.B., 2013. Redefining multifocal choroiditis and panuveitis and punctate inner choroidopathy through multimodal imaging. Retina. 33, 1315-1324. doi: 10.1097/IAE.0b013e318286cc77.

• Symes, R., Young, M., Forooghian, F., 2015. Quantitative assessment of retinal degeneration in birdshot chorioretinopathy using optical coherence tomography. Ophthalmic Surg. Lasers Imaging Retina. 46, 1009-1012. doi:10.3928/23258160-20151027-04.

• Taira, K., Nakazawa, M., Takano, Y., Ota, T., 2006. Acute zonal occult outer retinopathy in the fellow eye 5 years after presentation of punctate inner choroidopathy. Graefes Arch. Clin. Exp. Ophthalmol. 244, 880-882. https://doi.org/10.1007/s00417-005-0172-7

• Tan, A.C., Sherman, J., Yannuzzi, L.A., 2017. Acute zonal occult outer retinopathy affecting the peripheral retina with centripetal progression. Retin. Cases Brief Rep. 11, 134-140.

• Tavallali, A., Yannuzzi, L.A., 2015. Acute zonal occult outer retinopathy; Revisited. J. Ophthalmic Vis. Res. 10, 211-213. doi: 10.4103/2008-322X.170344.

• Tavallali, A., Yannuzzi, L.A., 2016. Idiopathic multifocal choroiditis. J. Ophthalmic Vis. Res. 11, 429-432.

• Teoh, S.C., Chee, C.K., Laude, A., Goh, K.Y., Barkham, T., Ang, B.S.; Eye Institute Dengue-related Ophthalmic Complications Workgroup., 2010. Optical coherence tomography patterns as predictors of visual outcome in dengue-related maculopathy. Retina. 30, 390-398. doi: 10.1097/IAE.0b013e3181bd2fc6.

• Thomas, B.J., Albini, T.A., Flynn, H.W.Jr., 2013. Multiple evanescent white dot syndrome: multimodal imaging and correlation with proposed pathophysiology. Ophthalmic Surg. Lasers Imaging Retina. 44, 584-587. doi:10.3928/23258160-20131015-03.

• Tian, M., Tappeiner, C., Zinkernagel, M.S., Huf, W., Wolf, S., Munk, M.R., 2018. Evaluation of vascular changes in intermediate uveitis and retinal vasculitis using swept-source wide-field optical coherence tomography angiography. Br. J. Ophthalmol. pii: bjophthalmol-2018-313078. doi:10.1136/bjophthalmol-2018-313078.

• Ting, D.S.W., Pasquale, L.R., Peng, L., Campbell, J.P., Lee, A.Y., Raman, R., Tan, G.S.W., Schmetterer, L., Keane, P.A., Wong, T.Y., 2019. Artificial intelligence and deep learning in ophthalmology. Br. J. Ophthalmol. 103, 167-175. https://doi.org/10.1136/bjophthalmol-2018-313173

• Tomkins-Netzer, O., Talat, L., Bar, A., Lula, A., Taylor, S.R., Joshi, L., Lightman, S., 2014. Long-term clinical outcome and causes of vision loss in patients with uveitis. Ophthalmology. 121, 2387-2392. doi: 10.1016/j.ophtha.2014.07.007.

• Tomkins-Netzer, O., Lightman, S., Drye, L., Kempen, J., Holland, G.N., Rao, N.A., Stawell, R.J., Vitale, A., Jabs, D.A., 2015. Outcome of treatment of uveitic macular edema: The Multicenter Uveitis Steroid Treatment Trial 2-year results. Ophthalmology. 122, 2351-2359. doi: 10.1016/j.ophtha.2015.07.036.

• Tsujikawa, A., Yamashiro, K., Yamamoto, K., Nonaka, A., Fujihara M., Kurimoto, Y., 2005. Retinal cystoid spaces in acute Vogt-Koyanagi-Harada syndrome. Am. J. Ophthalmol.139, 670–677. https://doi.org/10.1016/j.ajo.2004.11.053

• Tugal-Tutkun, I., Ozdal, P.C., Oray, M., Onal, S., 2017. Review for diagnostics of the year: Multimodal imaging in Behçet uveitis. Ocul. Immunol. Inflamm. 25, 7-19. doi: 10.1080/09273948.2016.1205100.

• Tugal-Tutkun, I., 2012. Imaging in the diagnosis and management of Behcet disease. Int. Ophthalmol. Clin. 52, 183-190. doi:10.1097/IIO.0b013e318265d56a.

• Tugal-Tutkun, I., Gupta, V., Cunningham, E.T., 2013. Differential diagnosis of Behçet uveitis. Ocul. Immunol. Inflamm. 21, 337-350. doi:10.3109/09273948.2013.795228.

• Vance, S.K., Spaide, R.F., Freund, K.B., Wiznia, R., Cooney, M.J., 2011a. Outer retinal abnormalities in acute macular neuroretinopathy. Retina. 31, 441-445. doi: 10.1097/IAE.0b013e3181fe54fa.

• Vance, S.K., Khan, S., Klancnik, J.M., Freund, K.B., 2011b. Characteristic spectral-domain optical coherence tomography findings of multifocal choroiditis. Retina. 31, 717-723. doi: 10.1097/IAE.0b013e318203c1ef.

• Velez, G., Chan, C.C., Csaky, K.G., 2002. Fluorescein angiographic findings in primary intraocular lymphoma. Retina. 22, 37-43.

• Volpe, N.J., Rizzo, J.F.3rd, Lessell, S., 2001. Acute idiopathic blind spot enlargement syndrome: a review of 27 new cases. Arch. Ophthalmol. 119, 59-63.

• Wang, Q., Jiang, L., Yan, W., Wei, W., Lai, T.Y.Y., 2017. Fundus autofluorescence imaging in the assessment of acute zonal occult outer retinopathy. Ophthalmologica. 237, 153-158. doi: 10.1159/000456724.

• Wickremasinghe, S., Ling, C., Stawell, R., Yeoh, J., Hall, A., Zamir, E., 2009. Syphilitic punctate inner retinitis in immunocompetent gay men. Ophthalmology. 116, 1195-1200. doi: 10.1016/j.ophtha.2008.12.055.

• Wojtkowski, M., Srinivasan, V., Fujimoto, J.G., Ko, T., Schuman, J.S., Kowalczyk, A., Duker, J.S., 2005. Three-dimensional retinal imaging with high-speed ultrahigh-resolution optical coherence tomography. Ophthalmology. 112, 1734-1746. https://doi.org/10.1016/j.ophtha.2005.05.023

• Wong, R.K., Lee, J.K., Huang, J.J., 2012. Bilateral drug (ipilimumab)-induced vitritis, choroiditis, and serous retinal detachments suggestive of Vogt-Koyanagi-Harada syndrome. Retin. Cases Brief. Rep. 6, 423-426. doi: 10.1097/ICB.0b013e31824f7130.

• Wu, K., Zhang, X., Su, Y., Ji, Y., Zuo, C., Li, M., Wen, F., 2016. Clinical characteristics of inflammatory choroidal neovascularization in a Chinese population. Ocul. Immunol. Inflamm. 24, 261-267. doi: 10.3109/09273948.2015.1015741.

• Wykoff, C.C., Flynn, H.W.Jr., Miller, D., Scott, I.U., Alfonso, E.C., 2008. Exogenous fungal endophthalmitis: microbiology and clinical outcomes. Ophthalmology. 115, 1501-1507. doi: 10.1016/j.ophtha.2008.02.027.

• Yamamoto, Y., Fukushima, A., Nishino, K., Koura, Y., Komatsu, T., Ueno, H., 2007. Vogt-Koyanagi-Harada disease with onset in elderly patients aged 68 to 89 years. Jpn. J. Ophthalmol. 51, 60-63. https://doi.org/10.1007/s10384-006-0379-0

• Yamamoto, M., Nishijima, K., Nakamura, M., Yoshimura, N., 2011. Inner retinal changes in acute-phase Vogt-Koyanagi-Harada disease measured by enhanced spectral domain optical coherence tomography. Jpn. J. Ophthalmol. 55, 1-6. https://doi.org/10.1007/s10384-010-0900-3

• Yang, Y.S., Zhang, L., Asdaghi, N., Henry, C.R., Davis, J.L., 2018. Acute macular neuroretinopathy in Susac syndrome: A new association. Retin. Cases Brief Rep. 28. doi: 10.1097/ICB.0000000000000738.

• Yiu, G., Pecen, P., Sarin, N., Chiu, S.J., Farsiu, S., Mruthyunjaya, P., Toth, C.A., 2014. Characterization of the choroid-scleral junction and suprachoroidal layer in healthy individuals on enhanced-depth imaging optical coherence tomography. JAMA. Ophthalmol. 132, 174-181. doi: 10.1001/jamaophthalmol.2013.7288.

• Zahid, S., Chen, K.C., Jung, J.J., Balaratnasingam, C., Ghadiali, Q., Sorenson, J., Rofagha, S., Freund, K.B., Yannuzzi, L.A., 2017. Optical coherence tomography angiography of chorioretinal lesions due to idiopathic multifocal choroiditis. Retina. 37, 1451-1463. doi: 10.1097/IAE.0000000000001381.

• Zarei, M., Abdollahi, A., Darabeigi, S., Ebrahimiadib, N., Roohipoor, R., Ghassemi, H., Moghaddam, R.S., Fard, M.A., 2018. An investigation of optic nerve head involvement in Fuchs uveitis syndrome using optical coherence tomography and fluorescein angiography. Graefes Arch. Clin. Exp. Ophthalmol. 256, 2421-2427. doi: 10.1007/s00417-018-4125-3.

- Zatreanu, L., Sibony, P.A., Kupersmith, M.J., 2017. Optical coherence tomography in neuroretinitis: Epipapillary infiltrates and retinal folds. J. Neuroophthalmol. 37, 176-178. doi: 10.1097/WNO.0000000000000501.

- Zhang, M., Xin, H., Roon, P., Atherton, S.S., 2005. Infection of retinal neurons during murine cytomegalovirus retinitis. Invest Ophthalmol Vis Sci. 46, 2047-2055. https://doi.org/10.1167/iovs.05-0005

- Zhang, X., Zuo, C., Li, M., Chen, H., Huang, S., Wen, F., 2013. Spectral-domain optical coherence tomographic findings at each stage of punctate inner choroidopathy. Ophthalmology. 120, 2678-2683. doi: 10.1016/j.ophtha.2013.05.012.

FIGURES LEGEND

Figure 1.

Baseline SS-OCT macular scan (A) of a patient with a peripheral focus of toxoplasmosis shows punctate hyperreflective spots in the posterior vitreous (white arrowhead) that represent a collection of inflammatory material and multiple

87

inflammatory cells. Initiation of antibiotic and steroid therapy (B) is accompanied by a decrease in the number of vitreous cells, and the inflamed hyaloid progressively separates from the retina surface (C, asterisk).

Figure 2. *Hyper-reflective oval pre-retinal deposits and choroidal appearance in eyes with active and healed toxoplasmic chorioretinitis seen on SD-OCT and on enhanced depth imaging optical coherence tomography (EDI-OCT) scans.*

The deposits (white arrowheads) are often found on the retinal surface mainly along the retinal vessels (A). Similar deposits can be observed on the outer surface of the hyaloid when the posterior vitreous is detached (B). Deposits on the hyaloid and on the retinal surface are co-located in most cases, suggesting a possible splitting of the same formation consequent to the vitreous detachment.

Combined fundus photography (C) and EDI-OCT scan (D) show and active toxoplasmic lesion. The retina (black asterisk) appears hyper-reflective and disrupted on EDI-OCT, whie the underlayng choroid demonstrates a focal thickening (white caliper) underneath the area of retinitis accompanied by hypo-reflectivity and disruption of the choroidal architecture (white asterisk). The fundus photo (E) and EDI-OCT scan (F) at follow-up demonstrate a healed lesion. The retina (black asterisk) looks hyperreflective and thin on EDI-OCT white the choroid appears thinner and still disrupted (white asterisk).

Combined fundus photo (G) and enhanced depth imaging OCT (H) in a patient affected by toxoplasmic chorioretinitis. The hyper-reflective necrotic retina (black asterisk) is accompanied by an accumulation of sub-retinal fluid (white asterisk).

Underneath the lesion a focal thickening and disruption of the choroid (black arrowheads) suggests the toxoplasmic etiology.

Figure 3 *. SD-OCT diagnostic signs of the two forms of syphilitic retinochoroiditis, confluent (top row) and placoid (bottom row).*

Areas of confluent retinochoroiditis secondary to syphilis present as triangular lesions (A) with a "ground-glass appearance" (B) that differentiate them from the denser foci of herpetic necrotizing retinitis. They can be associated with superficial pre-retinal precipitates, detected clinically as creamy white dots (B), and on OCT as hyperreflective round foci on the surface of the retina that can migrate over inflamed retina (C).

The placoid form of syhphilitic retinochoroiditis presents with an active, nonelevated, placoid yellowish outer retinal lesion involving the macula (D). Spectral domain OCT images taken at presentation and at 1-week and 4-week follow-up in 3 representative patients. Treatment with intravenous penicillin was initiated within 2 days of diagnosis. Spectral domain OCT image taken at Days 1 (E) shows SRF, disruption of the EZ junction, and irregular or granular hyperreflectivity of the RPE but without elevation. Small clumps of photoreceptor and/or RPE debris are present within the detachment spaces. At Days 7 (F), there is no evidence of fluid on SD-OCT, but the scan shows an irregular thickening of the RPE layer with small nodular elevations, along with a loss of the EZ layer, and areas of punctate hyperreflectivity in the choroid. At Day 30 (G), after therapy for neurosyphilis was completed, the SD-OCT shows complete restoration of the EZ layer and normalization of the contour of the RPE layer.

Figure 4. *Fungal colonies in eyes with endogenous candida endophthalmitis visualized on SD-OCT scans.*

Candida spp. enter the eye ether from the choroidal or the retinal vasculature and then head towards the vitreous to grow. The colonies appear as whitish hyper-reflective round-shaped lesions with homogenous content (Black asterisks) laying on the retinal surface (A) or growing into the vitreous body (B). Their high reflectivity generates a shadow on the underlying structures (white arrowheads). The combination of the white lesions and the underlying shadow suggested the name of "raincloud sign".

Figure 5. *Optic nerve head involvement in posterior uveitis can be due to solid lesion (top row) or to inflammatory swelling (bottom row) during neuroretinitis.*

In patients with sarcoidosis, the involvement of the optic nerve head by granulomas leads to a raised disc with hemorrhages (A) and to a focal leakage on fluorescein angiography (B). The granulomatous tissue is highly reflective on OCT and is usually nodular.

The swelling of the optic nerve head secondary to inflammatory cytokines, or papillitis, is often accompanied by fluid tracking from the nerve to the fovea, leading to neuroretinitis (D). On fluorescein angiography the disc is "hot" with diffuse leakage (E). Presence of SRF and IRF adjacent to the optic nerve head on OCT is more common than in granulomatous infiltration of the disc. Further a typical pattern of inner retinal folds due to mechanical forces of the macula edema can be seen.

Figure 6. *En face OCT and OCTA in Birdshot chorioretinopathy respectively show perivascular thickening corresponding to vessels that are leaking on fluorescein angiography and birdshot lesions in the choroidal slab.*

A: "Blue Retina", a significant diffuse thinning of outer retinal layers in a long-term Birdshot patient visible on a 15x9 montage color coded retinal thickness map; significant phlebitis and optic nerve head swelling visible on 12x 12 color coded retinal thickness map (B) and corresponding to leakage on fluorescein angiography in a Birdshot patient. The bottom left panels show color photo (D) and indocyanine green angiography (E) of a patient with recently diagnosed Birdshot chorioretinopathy. Corresponding wide-field SS-OCTA shows characteristic Birdshot lesion visible on the OCT-A choroidal slabs (F) but exhibits sparing of the choriocapillaris visible on the OCTA choriocapillaris slabs (G).

Figure 7. *A typical presentation of Dengue uveitis is the "foveolitis" that has been recently identified as an acute macular neuroretinopathy lesion.*

The main fundus changes in Dengue uveitis are macula and retinal hemorrhages, that can sometimes be accompanied by a yellow orange characteristic lesion at the fovea that has been thus termed a "foveolitis" (A). Through the use of SD-OCT it has been shown that this foveolitis is an acute macular neuroretinopathy lesion, presenting as hyper-reflectivity of the outer plexiform layer, Henle's layer and outer nuclear layer (B), which ultimately lead to localized disruption of these layers (C). The lesions of AMN are typically localized to the outer retina due to capillary endothelial dysfunction or occlusion of precapillary arterioles due to immune complex causing

deep capillary plexus ischemia in dengue maculopathy (E) that are usually discernible by OCT angiography.

Figure 8. *Two distinctive OCT signs of Vogt-Koyanagi-Harada disease are subretinal membranous structures (top row) and retinal pigment epithelium folds (bottom row).*

The typical ophthalmological manifestation of VKH is a bilateral panuveitis with multifocal serous retinal detachments (A). Those serous retinal detachments are delineated on SD-OCT by subretinal membranous structures (B) that divide the subretinal fluid in 2 compartments. The sub-membranous space (white asterisk) is optically empty, thus representing exudates from the choroidal vasculature through the breakdown of retinal pigment epithelium. The supra-membranous fluid (yellow asterisk) is mildly reflective, suggesting that there are more particles floating in it. This supports the hypothesis that subretinal membranous structures represent a portion of the outer photoreceptor segment layer that becomes separated from the inner segment layer.

The detection of RPE folds or undulations on SD-OCT (D), corresponding to the choroidal infiltration (C) are a simple and effective biomarker of VKH.

Figure 9. *Clinical course of acute retinal pigment epitheliopathy highlighted through OCT.*

SD-OCT shows acute focal inflammation and disruption at the interdigitation zone between the RPE and cone outer segment interface with ONL swelling, disruption of the ELM and a dome shaped appearance (A). During the spontaneous recovery

phase, this dome shaped ONL lesion decreases in height then disappears, the ELM restores then the ellipsoid zone and finally the interdigitation zone reconstitute (B).

Figure 10. *Inflammation, restoration and "true loss" of the ellipsoid layer in white dots syndrome.*

APMPPE, MFC and AZOOR are all considered part of the white dots syndrome spectrum.

Acute multifocal placoid pigment epitheliopathy (APMPPE) is characterized by yellow-white placoid lesions (A) better highlighted with indocyanine green angiography (B) that shows patchy ischemia of the choriocapillaris underlying the lesions. In APMPPE, the disruption of the EZ and IZ is accompanied by overlying, hyperreflectivity of the outer retinal layers on OCT (D). Sometimes also SRF may be present (C). Small areas of RPE proliferation can be found as well.

Inflammation of the outer retina in multifocal choroiditis (MFC) presents differently. The multifocal lesions are of different age, with newer lesions whitish and older lesions pigmented (E). This is reflected in the hypofluorescent appearance of the lesions in ICGA (F). The younger MFC chorioretinal lesions are usually conical on OCT and show RPE elevations due to iso-hyperreflective material (G,H). As the lesions evolve, they seem to rupture the Bruchs membrane with hyperreflective material being outpoured in the outer retina and a complete disruption of the ELM, EZ and IZ.

The faint appearance of acute zonal occult outer retinopathy (AZOOR) on clinical exam and fundus photos (I) is compensated by the "trizonal pattern" visible on FAF (J) and OCT (K,L). Zone 1 resembles the healthy retina, with intact RPE and

photoreceptor layers. Zone 2 is the demarcation line, the transition zone between the healthy and the fully diseased retina, visible as attenuation of EZ and ELM, incipient thinning of the ONL, and the presence of hyperreflective, subretinal material. Zone 3 describes the fully diseased retina with complete loss of the photoreceptors layer, significant thinning or loss of the ONL and RPE and choroidal atrophy.

Figure 11. *Two OCT lesions can be detected on b scan and en face, "ellipsoid" spots due to photoreceptors attenuation, and outer nuclear layer "dots" corresponding to swollen photoreceptors bodies.*

The superior panel shows a patient with MEWDS with en face OCT imaging at the ellipsoid level and corresponding spectral domain OCT. The fundus photograph shows classical white spots (A). The en face OCT segmented at the level of the ellipsoid (C) shows hyporeflective "spots". SD-OCT through the "spots" shows attenuation of the ellipsoid band corresponding to the "spots" and hypertrophy of the underlying retinal pigment epithelium. Indocyanine green angiography shows hypofluorescent lesions (B) that colocalize with the hyporeflective "spots" detected with en face OCT segmentation of the ellipsoid. This precise colocalization suggests that choroidal ICG hypofluorescence may be the result of blockage form the RPE.

In the bottom row, en face scan segmented at the level of the ONL (G) shows multiple hyperreflective dots nasal to the nerve, lesions that could not be detected on fundus examination (E). Spectral domain optical coherence tomography scanning through these hyperreflective ONL "dots" (H) confirms their location in the ONL and shows how they tend to form linear extensions from the external limiting membrane to the outer plexiform layer.

MEWDS lesions seem hyperautofluorescent (F), and correspond perfectly to the hyporeflective "spots" identified with en face OCT segmentation of the ellipsoid. This multimodal correspondence of the "spots" seems to point toward an inflammation of the photoreceptors with primary or secondary hypertrophy of the RPE: this is detected at the level of the ellipsoid as hyporeflectivity, and unmasks the underlying physiological autofluorescence. The second lesion on en face OCT, the hyperreflective "dots," cannot be detected with FAF.

Figure 12. *Optical coherence tomography signs suggestive for primary vitreo-retinal lymphoma (PVRL).*

Subretinal mid/hyper-reflective material (white asterisk) is highly suggestive for PVRL when accompanied by a consistent clinical picture (A). Patients with PVRL often show hyper-reflective alterations within the retinal layers at the level of the outer retina (white arrowheads) and the middle/inner retina (black arrowhead) and a certain granularity of the junction between the photoreceptors and the retinal pigment epithelium (black arrows) (B). A recently described finding in eyes with PVRL consists of hyper-reflective vertical lines (white arrows) crossing the retina (C).

Figure 13*. Retinal features in necrotizing retinitis secondary to CMV.*

Optical coherence tomography scan in a patient affected by Cytomegalovirus retinitis (A). Hyper-reflective vertical lines within the outer nuclear layer (white arrowhead) are visible and better appreciated in magnified view (B). CMV retinitis may evolve in the formation of outer retinal lacunae and retinal detachment when the RPE and choroid are spared (C).

Figure 14. *Choroidal granulomas in a patient with ocular sarcoidosis.*

Two choroidal granulomas are visible on as hypo-fluorescent round-shaped lesions on indocyanine green (ICG) angiography (A). Both the lesions both encircled by a black and a white dotted line respectively appear hypo-reflective on combined enhanced depth imaging optical coherence tomography (EDI-OCT) scan (B-C). An increased transmission effect is clearly visible underneath both the lesions (white arrowheads). This feature helps in distinguishing choroidal granulomas from other similar looking choroidal structures.

	VITREOUS	PERIPAPILLARY	INNER RETINA	OUTER RETINA	CHORIOCAPILLARIS	CHOROID
SARCOIDOSIS		- swollen, hemorrhagic optic discs - peripapillary intraretinal, subretinal fluid	-perivascular thickening			- round-shaped hyporeflective granulomas - increased transmission effect
BEHCET			- RNFL thickening with subsequent defects	- transient retina infiltrates		
BIRDSHOT		- swollen	- perivascular thickening			- Choroidal thinning
VOGT-KOYANAGI-HARADA			- RNFL thickening	- subretinal membranous structures - supra-membranous fluid with increased reflectivity - RPE undulations	- decreased reflectivity with thickening and loss of the physiological dotted pattern	- diffuse thickening

RETINAL PIGMENT EPITHELITIS				- disruption at the inner border of the RPE layer - dome-shaped disruption of the ELM		
MEWDS				- focal disruption of EZ - RPE mottling - dense oval dots in the ONL		
APMPPE				- disruption of the EZ - overlying, hyperreflectivity of the outer retinal layers - disrupted ELM	- local decreased reflectivity	
MFC / PIC				- conical RPE elevations - rupture of Bruch - outpouring of inflammatory material in outer retina	- local decreased reflectivity	

AZOOR				- trizonal pattern - attenuation of EZ and ELM, incipient thinning of the ONL		
SERPIGINOU S CHOROIDITIS					- decreased reflectivity with thickening and loss of the physiological dotted pattern	- localized choroidal thickening
ACUTE RETINAL NECROSIS	- Hypereflectiv e hialoid oval deposits (over a dense white retinitis)					

CMV RETINITIS				- hyper reflective vertical lines connecting the RPE to the inner retinal layers - scarring with a disrupted retina and normal choroid OR outer retinal lacunae		
TOXOPLASMOSIS	- Hyperreflective hialoid oval deposits (over a dense white retinitis)			- area of thickened hyperreflective homogeneously disrupted retina - thickening and melting of the RPE		- focal thickening and loss of the architecture
SYPHILIS	- hyperreflective preretinal oval deposits (over a "ground" glass retina)			- RPE nodularity - EZ transient loss		- thickening with hyperreflective dots

DENGUE			- foveolitis - CME	- AMN		
TUBERCULOSIS		- swollen, hemorrhagic optic discs - peripapillary intraretinal, subretinal fluid				- round-shaped hyporeflective granulomas - increased transmission effect
CANDIDA	- Preretina hypereflect ive colonies - obscuratio n of the retina underneath					
VITREO-RETINAL LYMPHOMA			- absence of CME	- hypereflective nodularity of the outer retinal layers, disrupting the NOL and RPE with a normal Bruch's		

TABLE 1. *Optical coherence diagnostic signs of posterior uveitis syndromes.*
The table summarizes OCT signs at the various levels of the vitreous, retina and choroid, that may be diagnostic of particular uveitis enthities.
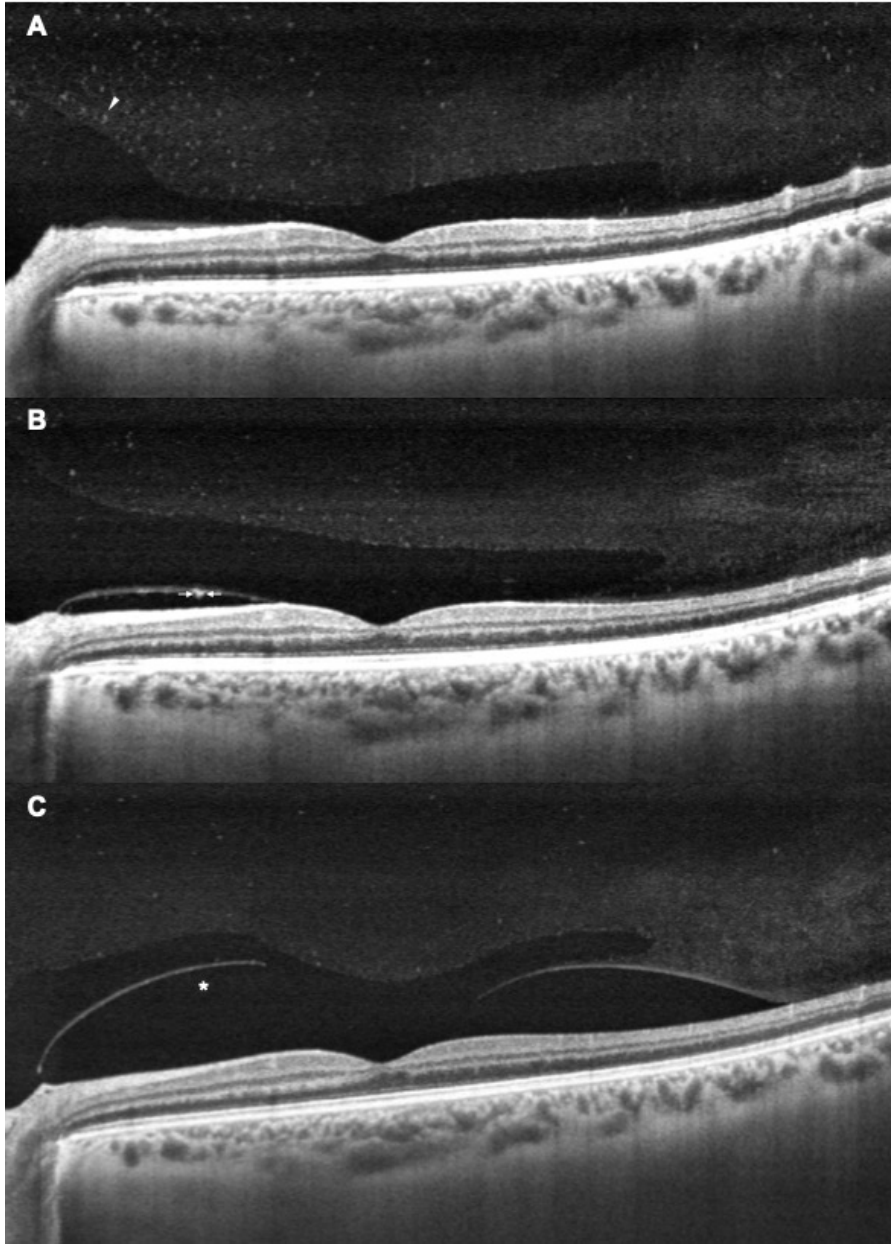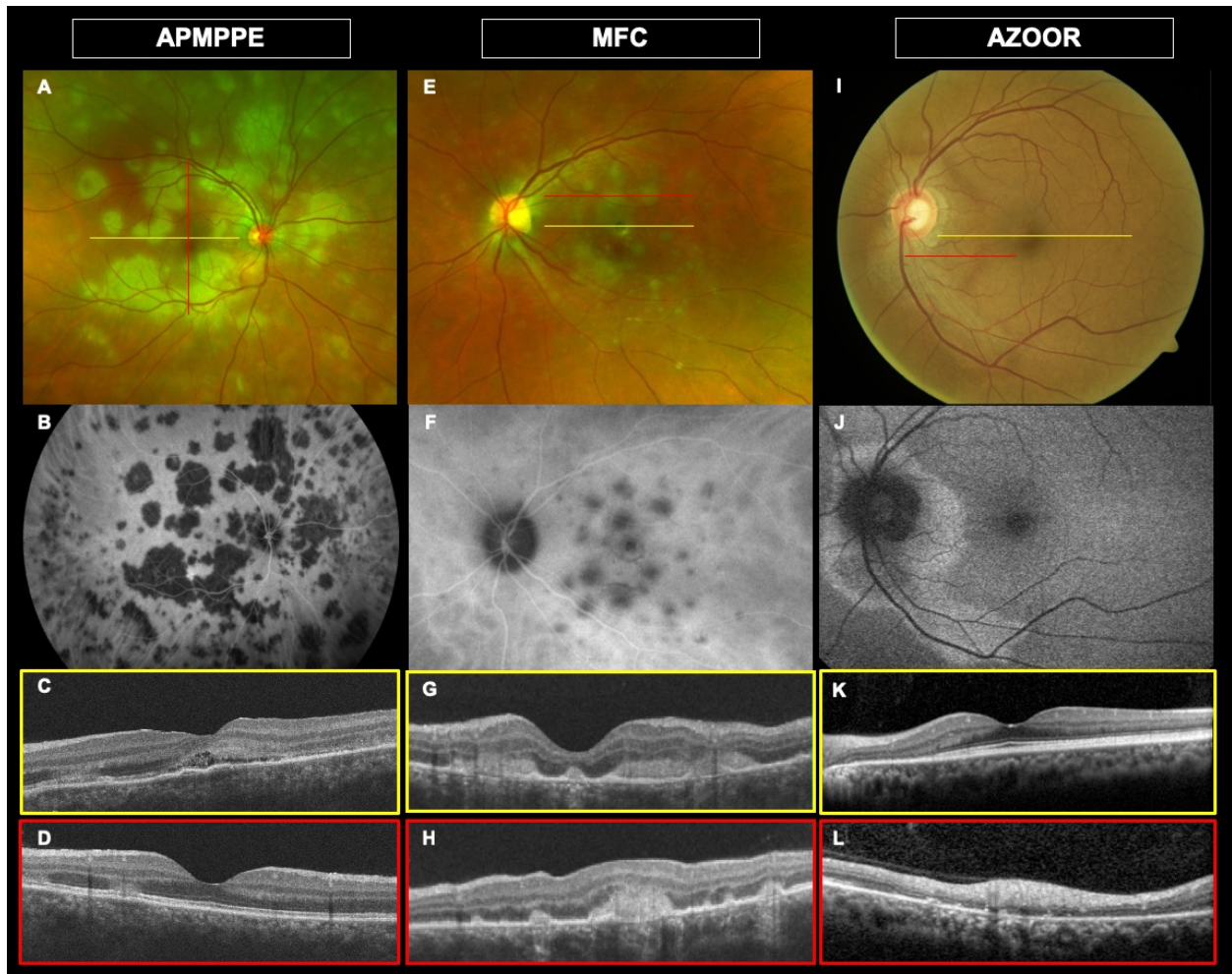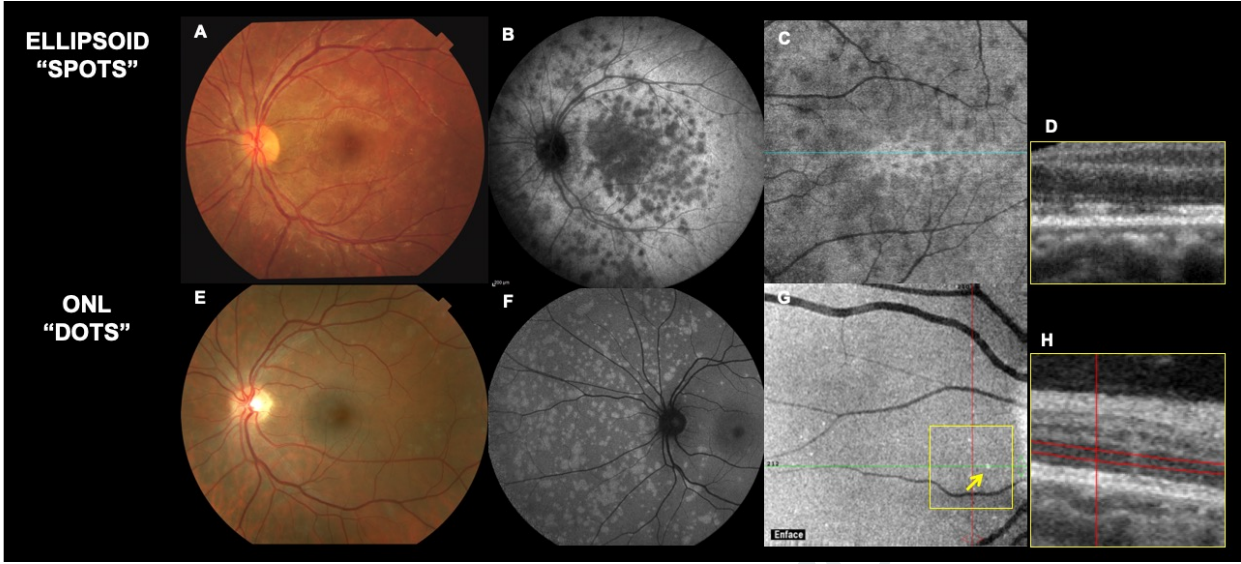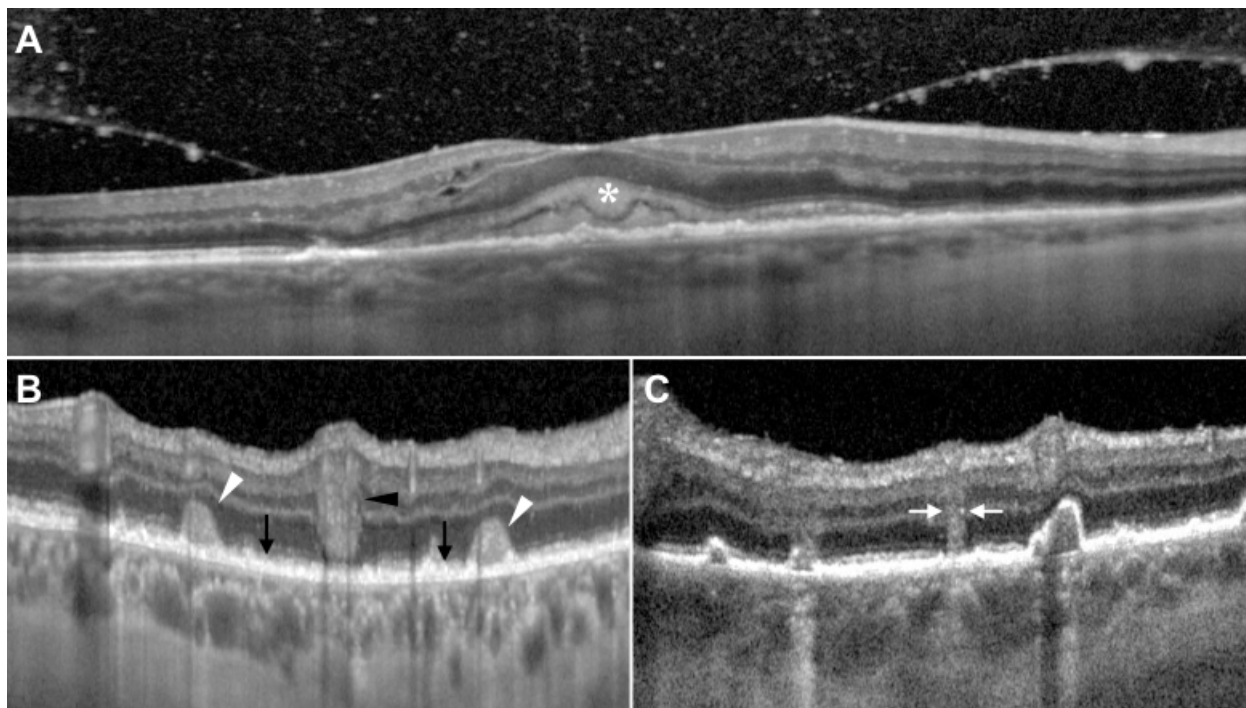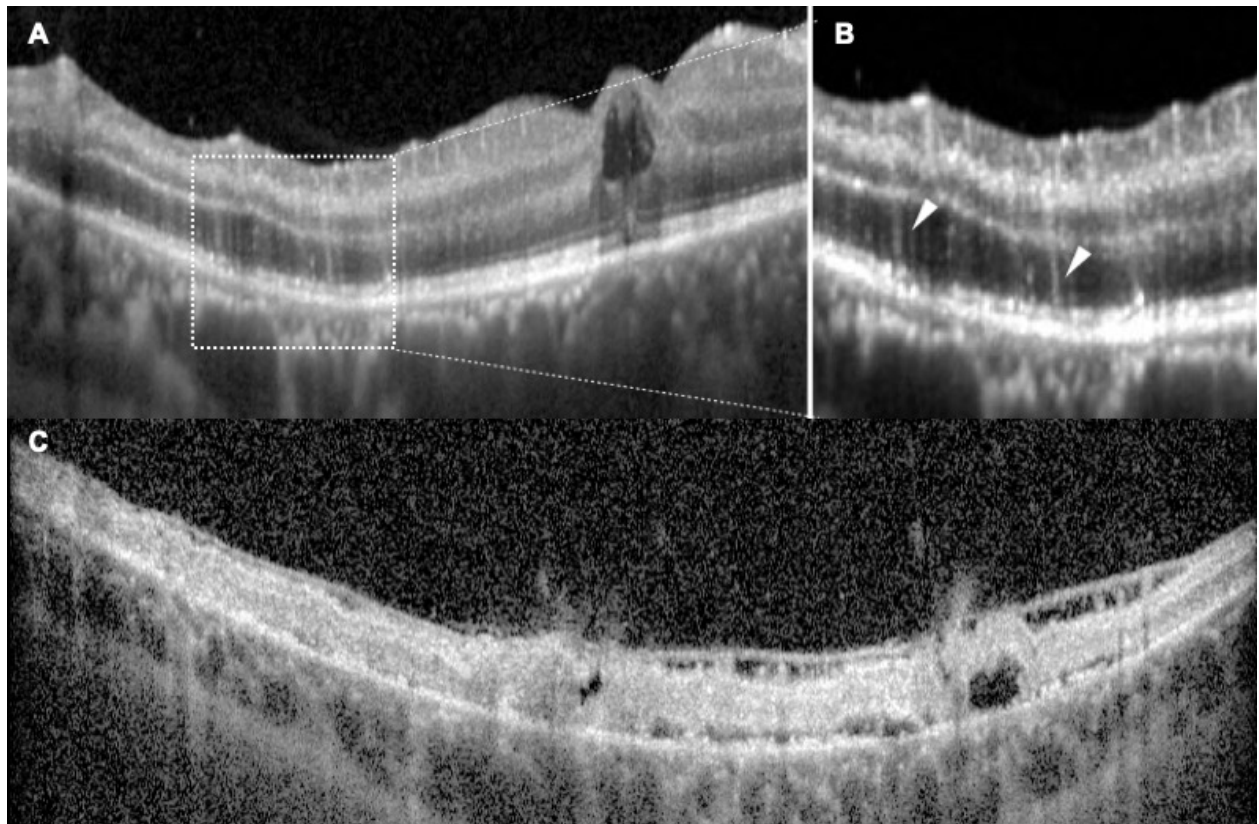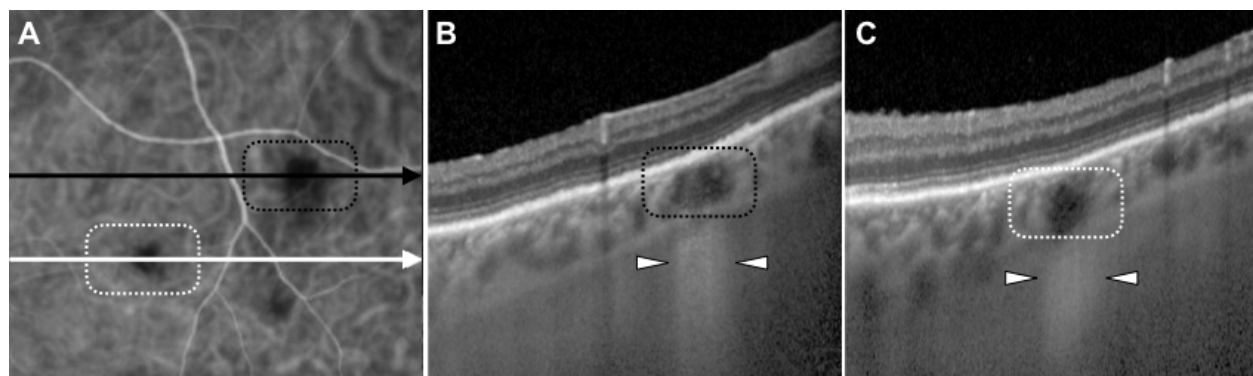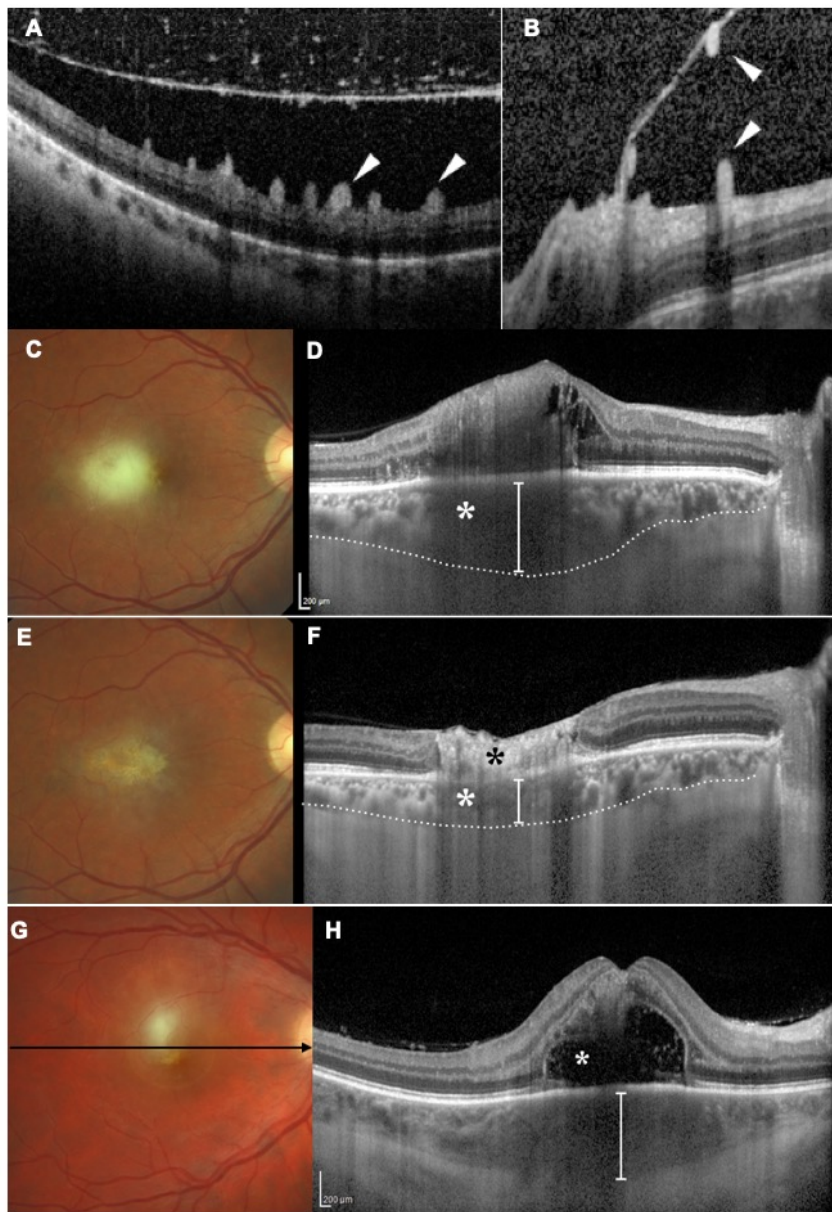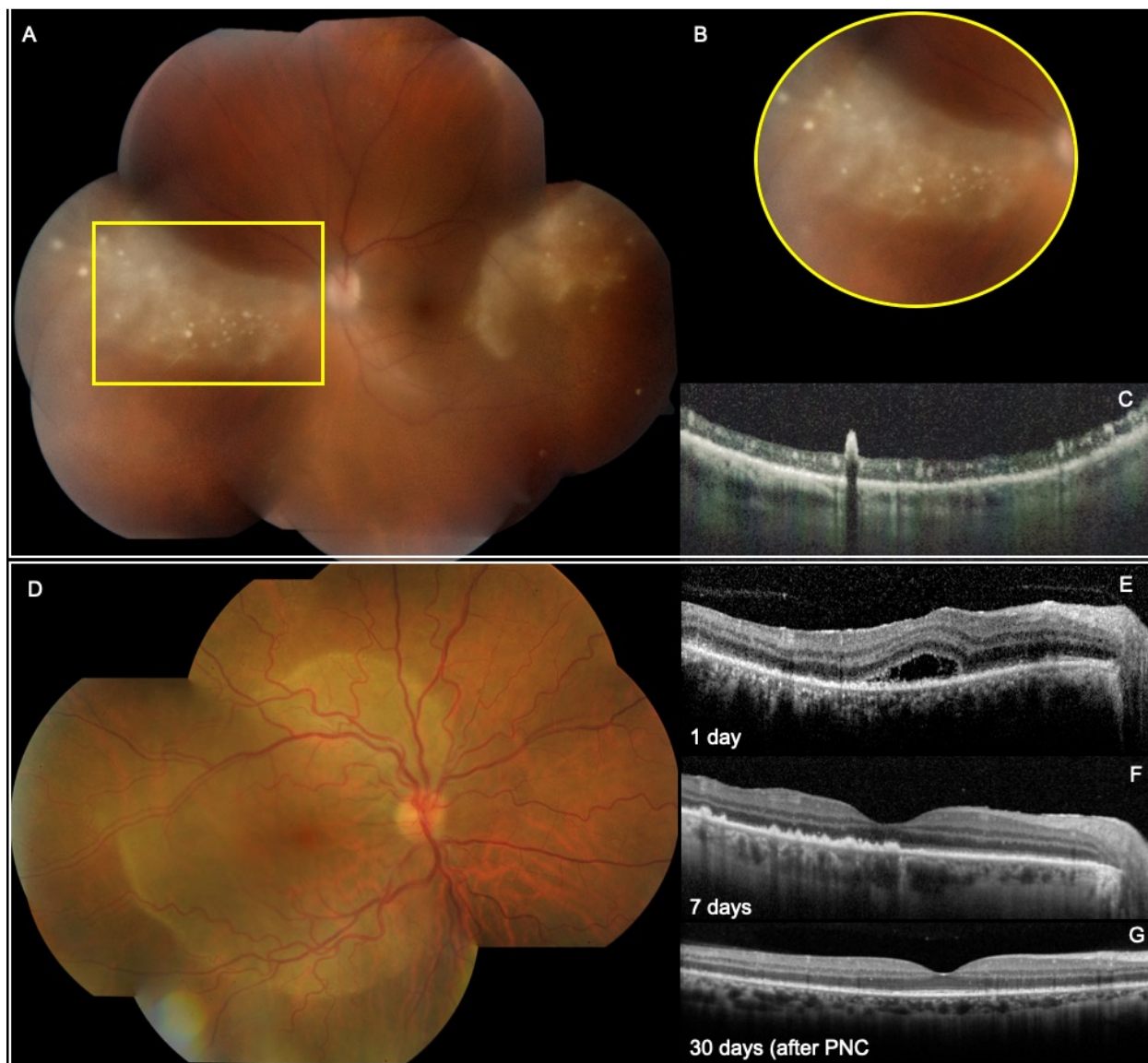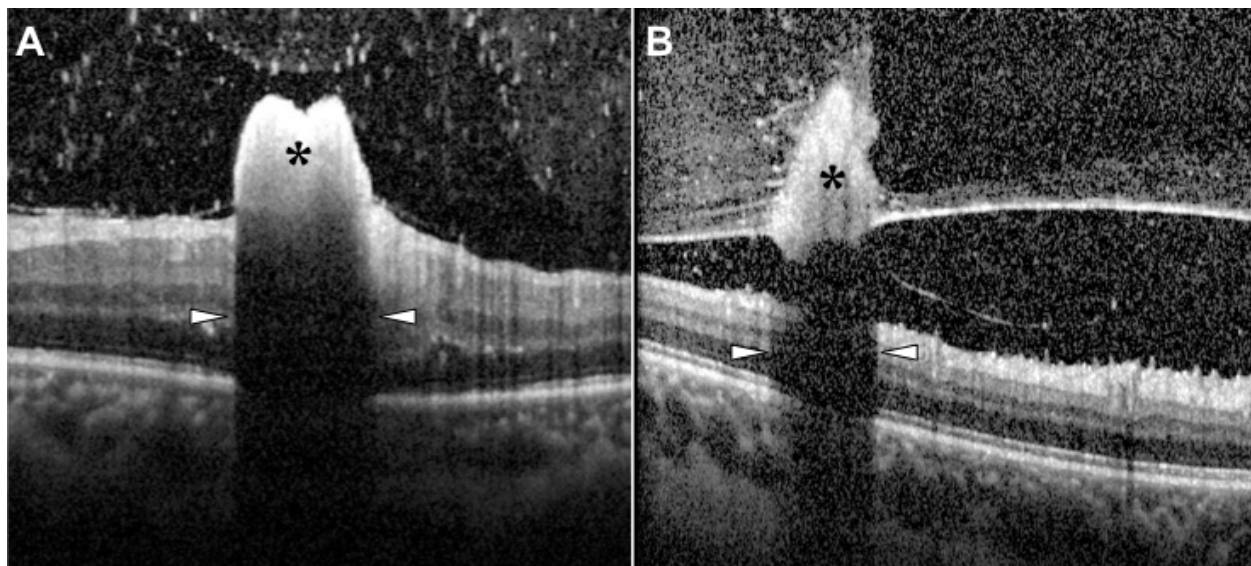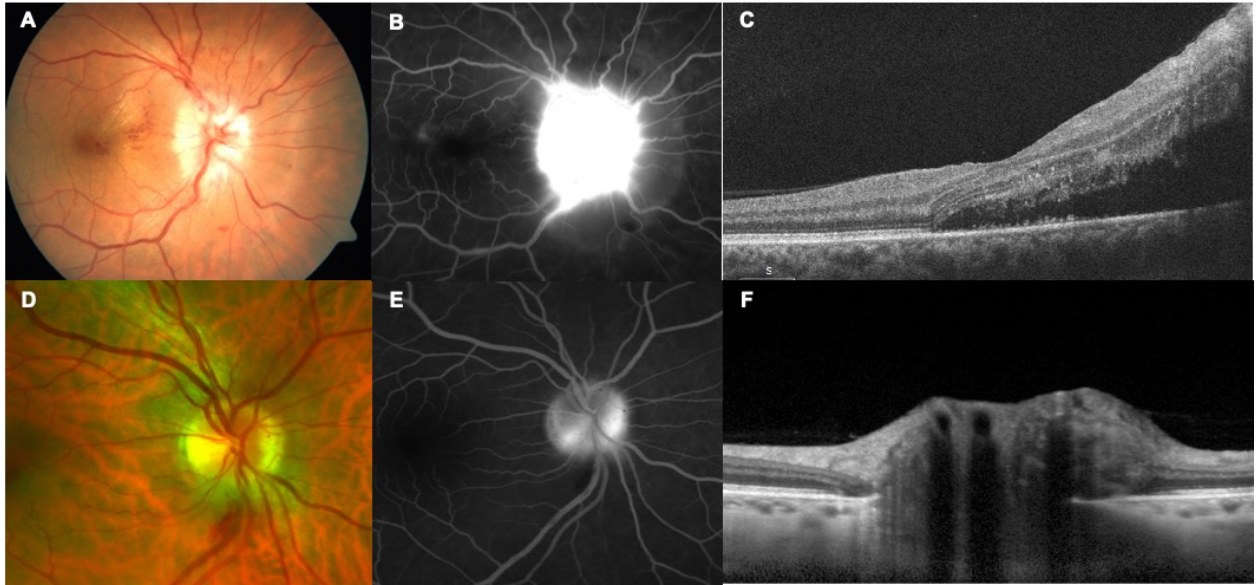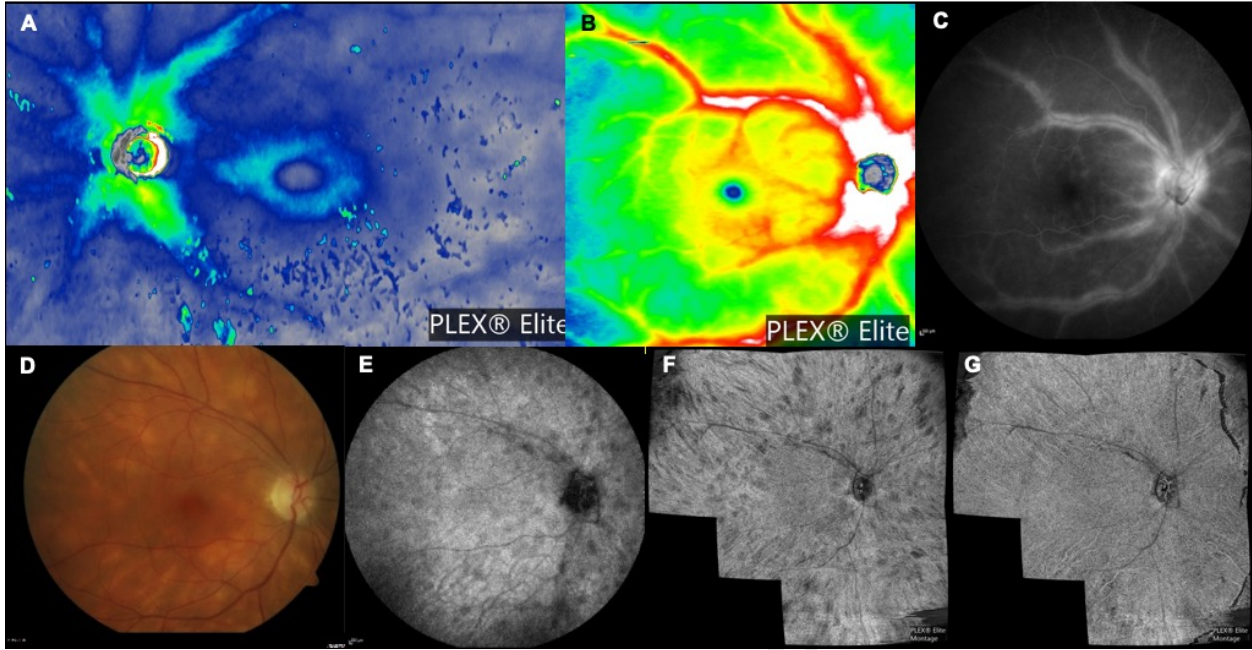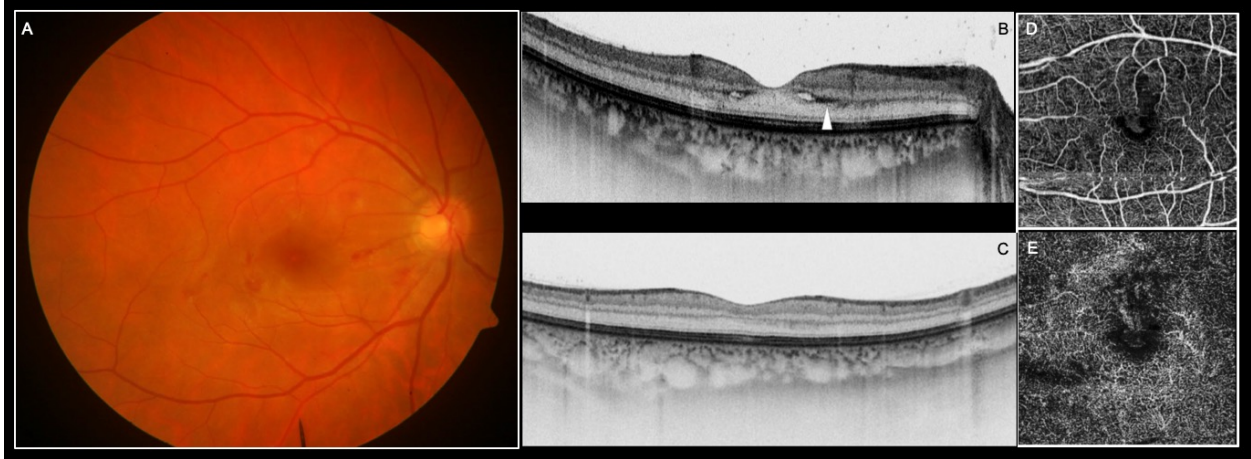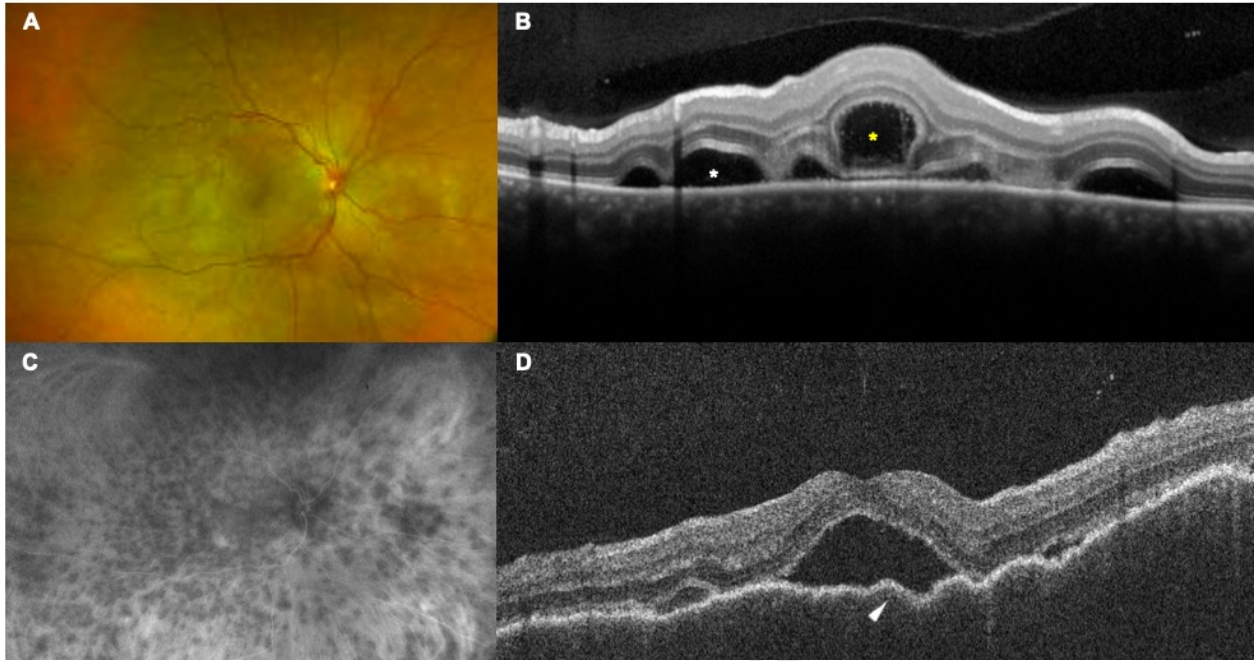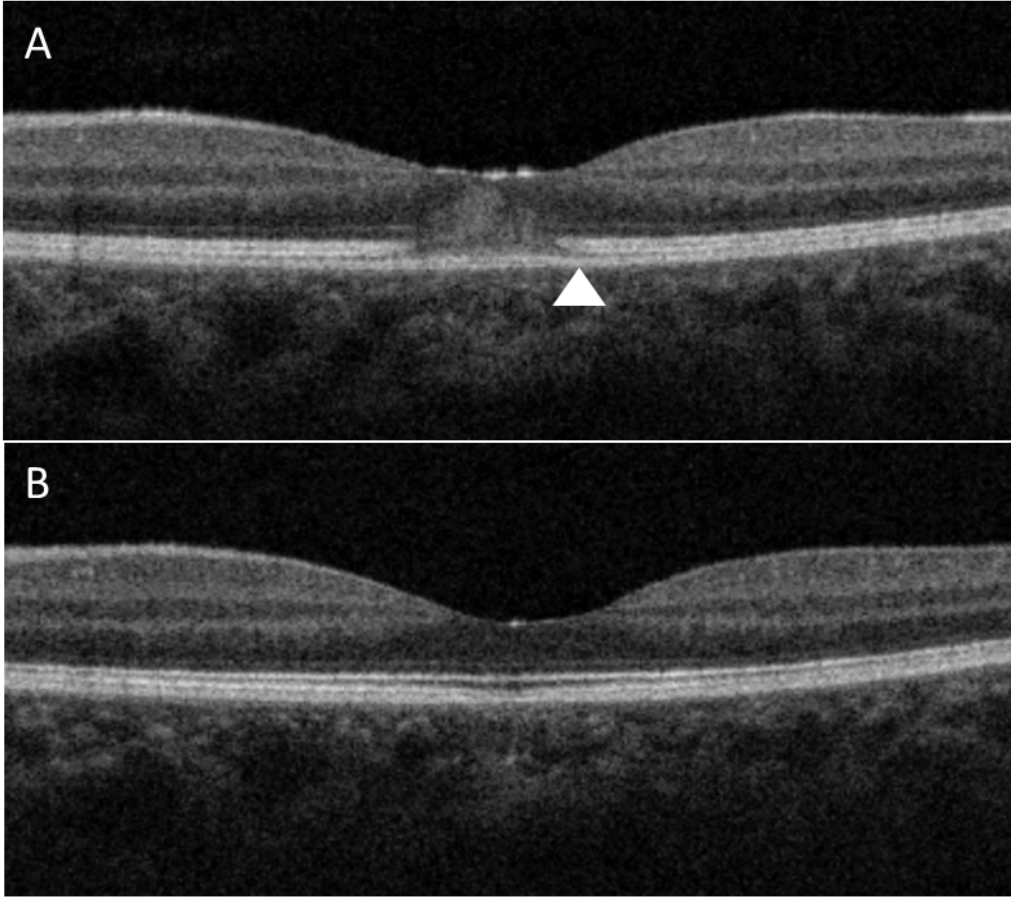
OPTICAL COHERENCE TOMOGRAPHY BIOMARKERS IN POSTERIOR UVEITIS

Article Highlights

- A biomarker is a measurable indicator of the presence of some disease state

- Optical coherence tomography biomarkers have many advantages for the uveitis patients

- OCT biomarkers in uveitis are usually noninvasive, and they produce intuitive, multidimensional results

- Yielding both qualitative and quantitative data, they are usually relatively comfortable for patients

- When combined with other sources of information, they can be very useful to clinicians seeking to make a diagnosis.

OPTICAL COHERENCE TOMOGRAPHY BIOMARKERS IN POSTERIOR UVEITIS

Authors contribution

Francesco Pichi 40% (ideation, literature review, manuscript preparation, approval of the final draft)

Alessandro Invernizzi 20% (literature review, drafts correction, approval of the final draft)

William Tucker 20% (literature review, drafts correction, approval of the final draft)

Marion Munk 20% (literature review, drafts correction, approval of the final draft)